Threshold dynamics in mathematical models for mosquito- and rodent-borne diseases with seasonality

Ph.D. Thesis

by

Mahmoud Abdalla Ali Ibrahim

Supervisor:
Dr. Attila Dénes
associate professor

Doctoral School of Mathematics and Computer Science
University of Szeged
Faculty of Science and Informatics
Bolyai Institute

Szeged
2022

Dedication

The dissertation is dedicate to my beloved mother, Hania Khalil, who passed away before I started my doctoral studies.

I had promised to make my mother proud by the achievement of this monumental academic goal, and I hope that I have fulfilled that promise. I wish that she is still alive today to share with me the celebration and success of my graduation with a Doctor of Philosophy degree.

Acknowledgments

I would like to start by expressing my deep appreciation to my supervisor, Dr. Attila Dénes, for directing my Ph.D. studies. I would also like to thank him for all the time he spent for me during the past four years, for his encouragement, expertise, immense knowledge, for having always given me useful suggestions to improve my work and pointing me in the right direction. Thank you for having given to me the opportunity to travel, meet and collaborate with other people in the field. Your tireless efforts and your guidance on execution of activities related to my Ph.D. study and related research will always be appreciated in my profession and personal life.

My sincere thanks also go to both Doctoral School of Mathematics and Computer Science and Bolyai Institute, University of Szeged for the opportunity to undertake my Ph.D. studies at the Department of Applied and Numerical Mathematics, and giving me access to all research facilities. It was a great pleasure to study here, learn from outstanding teachers, and meet wonderful colleagues, co-authors and friends.

I acknowledge a (Stipendium Hungaricum) scholarship from Tempus Public Foundation (TPS) and the support of the ÚNKP-20-3-New National Excellence Program of the Ministry for Innovation and Technology from the source of the National Research, Development, and Innovation Fund. I also acknowledge a scholarship from Egypt's Ministry of Higher Education and Scientific Research, and the support I have received from Egypt's office for cultural and Educational Relations in Vienna is greatly acknowledged.

My special thanks go to my wife AL-Shimaa, who has always believed in my success and supported my decisions. I would also like to express my sincere gratitude to my son Ibrahim, for allowing me to spend time away from you at the start of my Ph.D. studies. Last, but not least, I wish to thank my family, father and siblings for their constant love, patience and support in all my efforts.

Contents

List of Figures

List of Tables

Notations

Acronyms

G.A.S.	Globally asymptotically stable
L.A.S.	Locally asymptotically stable
LHF	Lassa haemorrhagic fever
MBD	Mosquito-borne diseases
PRCC	Partial Rank Correlation Coefficients
VBD	Vector-borne diseases
WHO	World health organization
ZIKV	Zika Virus

Symbols

$\mathbb{N}$	set of positive integers
$\mathbb{R}$	set of real numbers
$\mathbb{R}_+$	set of non-negative real numbers
$\mathbb{R}^n$	n-dimensional real vector space
$d(x, y)$	euclidean distance in $\mathbb{R}^n$
x'	derivative of the function x
C_ω	ordered Banach space from $\mathbb{R}$ to $\mathbb{R}^m$ with the maximum norm
C_ω^+	the positive cone defined as $C_\omega^+ \coloneqq \{\phi \in C_\omega : \phi(t) \geqslant 0,\ \forall t \in \mathbb{R}\}$
$C(\mathbb{R}_+^6, \mathbb{R}_+)$	the Banach space of continuous functions from $\mathbb{R}_+^6$ to $\mathbb{R}_+$ with the maximum norm
$\|x\|$	Euclidean norm of a vector $x \in \mathbb{R}^d,\ d \in \mathbb{N}$
$\mathcal{R}_0$	basic reproduction number of the non-autonomous model
$[\mathcal{R}_0]$	time-average basic reproduction number associated with the non-autonomous model
$\mathcal{R}_0^A$	basic reproduction number of the autonomous model
ρ	spectral radius
E_0	disease-free periodic solution

Chapter 1

Introduction

The study of how and why populations change in size and structure over time is known as population dynamics. Reproduction rates, death and migration are significant factors in population dynamics. Population dynamics is an important topic in mathematical biology, and the study of the long-term behaviour of modelling systems is a central problem. The majority of these systems are characterized by various evolutionary equations, such as difference, ordinary, functional, and partial differential equations. Interactive populations often live in a fluctuating environment. For instance, physical environmental conditions such as temperature and humidity, as well as the supply of food, water, and other resources, usually change over time, either seasonally or daily. For that reason, more realistic models should be non-autonomous systems, especially, if the data in a model are periodic functions of time with a commensurate period.

The basic reproduction number can be considered as the expected number of secondary infections generated by one infected individual in a population where all individuals are susceptible to infection. This quantity is an important threshold parameter for measuring the effort required to eradicate the infectious disease. For autonomous epidemic models, Diekmann et al. [37] and van den Driessche and Watmough [101] established general approaches for the calculation of basic reproduction numbers. For periodic epidemic compartmental models, Bacaër and Guernaoui [11] provided a definition of the basic reproduction number as the spectral radius of an integral operator acting on the space of continuous periodic functions. Later, Wang and Zhao [103] characterized the basic reproduction number for such models and proved that it serves as a threshold parameter regarding the local stability properties of the disease-free periodic solution. Rebelo et al. [90] studied persistence in epidemiological models in a seasonal environment. Bacaër and Ait Dads [10] gave a more biological explanation of the reproduction number for compartmental epidemic models with periodic parameters. Therefore, the dynamics of the system is characterized by the basic reproduction number ($\mathcal{R}_0$) of periodic compartmental models. One

can also show that the global dynamics is determined by this threshold parameter: if $\mathcal{R}_0 < 1$, then the disease-free periodic solution is globally asymptotically stable, while if $\mathcal{R}_0 > 1$, then the disease remains endemic in the population and there exists at least a positive ω-periodic solution.

My thesis is concerned with periodic mathematical models for the spread of two different mosquito-borne diseases and a rodent-borne disease. In particular, it presents compartmental population models for the transmission dynamics of malaria, Zika virus and Lassa virus diseases in a seasonal environment.

The main aim of the thesis was to investigate the impact of the periodicity of weather on the spread of the above mentioned diseases by applying non-autonomous mathematical models with time-dependent parameters. The basic reproduction number $\mathcal{R}_0$ is defined as the spectral radius of a linear integral operator and the global dynamics is determined by this threshold parameter. We show the global stability of the disease-free periodic solution and the extinction of the disease if $\mathcal{R}_0 < 1$, as well as the persistence of the disease in the population and there exist at least a positive ω-periodic solution when $\mathcal{R}_0 > 1$. Numerical simulations to illustrate and support the analytical results are given.

Chapter 2 provides a brief introduction to the modes of transmission and spread of mosquito- and rodent-borne diseases. In addition, the impact of weather seasonality on malaria, Zika fever and Lassa fever is also presented.

In Chapter 3, we briefly discuss some basic mathematical and epidemiological definitions, conditions, theorems and methods in the study of non-autonomous dynamical systems that are relevant to this thesis and required for the understanding of subsequent chapters.

A compartmental population model to describe malaria transmission in a seasonal environment with periodic mosquito birth, death and biting rates is presented in Chapter 4, dividing the human population into two classes: those who do not have any immunity and those who have a partial immunity due to an earlier malaria infection or due to their genetics. The global dynamics of the system is characterized by the basic reproduction number by using the general method established in Wang and Zhao [103]. The simulations suggest that mosquito-control is an important factor in malaria transmission and the time-average basic reproduction number provides an underestimation of the disease transmission risk. This chapter summarizes the results of Ibrahim and Dénes [53].

In Chapter 5, we present a non-autonomous mathematical model for the spread of Zika virus disease including sexual and vectorial transmission as well as asymptomatic carriers. The impact of the periodicity of weather on the Zika transmission is considered by including time-dependent mosquito birth, death and biting rates. Following the general theory for the extinction or persistence of infectious diseases given by Rebelo et al. [90], the basic reproduction number is used to show the global

stability of the disease free-solution and the persistence of the infective compartments. Using our model and taking Ecuador and Colombia as two examples, the fitted curves match the data very well. Based on the sensitivity analysis, we can assess that the most effective measures to reduce transmission are control of mosquito populations and protection against their bites. Numerical examples to study what kind of parameter changes might lead to a periodic recurrence of Zika are shown. The results of this chapter were published in Ibrahim and Dénes [54].

Finally in Chapter 6, we formulate and study a compartmental model for Lassa fever transmission dynamics considering human-to-human, rodent-to-human transmission and the vertical transmission of the virus in rodents. To incorporate the impact of periodicity of weather on the spread of Lassa, we introduce a non-autonomous model with time-dependent parameters for rodent birth rate and carrying capacity of the environment with respect to rodents. Again by using the theory presented in [103], it is demonstrated that the global dynamics is determined by the basic reproduction number. The fitted curve based on our model reflects the seasonal fluctuation and coincides rather well with the reported data concerning Lassa fever in Nigeria. Using numerical simulations, we observed that the human-to-human transmission rate has a substantial impact on the prevalence of the disease, but the most significant factors in Lassa's periodic recurrence are the rodent-related parameters. The results of this chapter have been published in Ibrahim and Dénes [52].

The thesis is based on three scientific articles of the author. These publications are the following.

[52] M. A. Ibrahim and A. Dénes. A mathematical model for Lassa fever transmission dynamics in a seasonal environment with a view to the 2017–20 epidemic in Nigeria. *Nonlinear Analysis: Real World Applications*, 60:103310, 2021. https://doi.org/10.1016/j.nonrwa.2021.103310.

[53] M. A. Ibrahim and A. Dénes. Threshold and stability results in a periodic model for malaria transmission with partial immunity in humans. *Applied Mathematics and Computation*, 392:125711, 2021. https://doi.org/10.1016/j.amc.2020.125711

[54] M. A. Ibrahim and A. Dénes. Threshold dynamics in a model for Zika virus disease with seasonality. *Bulletin of Mathematical Biology*, 83:27, 2021. https://doi.org/10.1007/s11538-020-00844-6

Chapter 2

Impact of weather seasonality on the spread of mosquito- and rodent-borne diseases

2.1 Vector-borne diseases

Vector-borne diseases (VBD) are illnesses that are transmitted by vectors, which include mosquitoes, ticks, and fleas. These vectors can carry infective pathogens such as parasites, viruses, bacteria, and protozoa, which can be transferred from one host (carrier) to another. VBDs are commonly found in tropical and subtropical regions and in places where access to safe drinking water and sanitation is problematic. According to WHO [111], vector-borne diseases account for more than 17% of all infectious diseases. Every year there are more than 700,000 deaths from diseases such as malaria, dengue, schistosomiasis, human African trypanosomiasis, leishmaniasis, Chagas disease, yellow fever, Japanese encephalitis and onchocerciasis. The most deadly vector-borne disease, malaria, caused an estimated 409,000 deaths in 2019, mostly children in the African region.

2.2 Mosquito-borne diseases

Mosquito-borne diseases (MBD) are those spread by the bite of an infected mosquito. Diseases transmitted to humans by mosquitoes include Zika virus, West Nile virus, chikungunya virus, dengue, and malaria [24].

Malaria is a life-threatening disease caused by Plasmodium parasites that are transmitted to humans through the bites of infected female *Anopheles* mosquitoes. People with malaria often suffer from fever, chills and flu-like symptoms. If left untreated, they can develop severe complications and die. In the United States, about

2,000 cases of malaria are diagnosed each year. The vast majority of cases in the United States occur in travelers and immigrants returning from countries where malaria transmission occurs, many from sub-Saharan Africa and South Asia [27, 109].

Zika virus disease is caused by the Zika virus (ZIKV) and is transmitted to humans primarily through the bite of an infected *Aedes* species mosquito. These mosquitoes bite most actively during the day, but also bite at night [25]. ZIKV is also spread via sexual contacts, mainly from men to women [67]. In many cases, there are no symptoms, but it can present similarly to dengue fever. Symptoms might include fever, red eyes, joint pain, headache, and a maculopapular rash. Women infected with ZIKV during pregnancy may give birth to children with severe health disorders, including microcephaly and Guillain–Barré syndrome, which can lead to lifelong disabilities [108]. There is currently no vaccine to prevent Zika infection.

2.3 Rodent-borne diseases

A zoonotic disease is an infectious disease that is transmitted between species from animal to human (or from human to animal). Rodents carry a variety of disease-causing organisms, including many types of bacteria, viruses, protozoa, and helminths (worms). Through their ectoparasites such as fleas, ticks, lice, and mites, they also act as vectors or reservoirs for many diseases as well as some diseases transmitted by mosquitoes [42].

Lassa fever is an animal-borne, or zoonotic, acute viral illness caused by Lassa virus, a member of the *arenavirus* family of viruses. Humans usually become infected with Lassa virus through exposure to food or household items contaminated with urine or faeces of infected *Mastomys* rats. Person-to-person infections and laboratory transmission can also occur. The disease is endemic in the rodent population in parts of West Africa including Sierra Leone, Liberia, Guinea and Nigeria. Neighboring countries are also at risk, as the animal vector for Lassa virus, the multimammate rat (*Mastomys natalensis*) is distributed throughout the region [110]. The overall case-fatality rate is 1%. Among patients who are hospitalized with severe clinical symptoms of Lassa fever, case-fatality is estimated to be about 15%. In some areas of Sierra Leone and Liberia, 10–16% of those admitted to hospitals annually are known to have Lassa fever, illustrating the severe impact of the disease on the region [26].

2.4 Weather seasonality and vector-borne diseases

Climate change is a reality that affects both our ecosystem and human health. The periodicity of weather is already affecting the transmission and spread of VBDs, and

the effects are likely to intensify. As climate change continues, we must increase our efforts to prevent and control VBDs. Of concern is whether these climatic changes will increase the incidence and geographic distribution of various vector-borne infectious diseases. The key factors that have a major influence on the distribution of VBD-producing pathogens are changing rainfall patterns, high temperatures and humidity [7].

Periodicity of weather and climate change are very important factors in the life cycle of the parasites and the mosquitoes transmitting them. Variations in climatic conditions, such as temperature, rainfall patterns and humidity, have a profound effect on mosquito longevity and on the development of malaria parasites in the mosquito and subsequently on malaria transmission [49]. Elementary modelling suggests that temperature increases MBD transmission rates and expands their geographic distribution [48], with increases in malaria in particular identified as a possible effect of weather seasonality [69]. While some studies have suggested an increase in the spread of the disease in current malaria endemic areas [86, 116], or a resurgence of the disease in areas that have controlled transmission or eliminated the disease in the past [14, 58].

Mosquitoes are cold-blooded and have no thermostatic mechanism. They need the appropriate temperature to survive and develop [112]. The emergence and reemergence of ZIKV is associated with high temperatures and shifts in precipitation patterns [68]. The *Aedes* mosquitoes that transmit ZIKV cannot tolerate temperatures below 10°C and above 35°C [7]. At temperatures below 10°C, the mosquito life cycle ceases, but if it is not much below that, there may be some mosquito survival during the colder winter months [60]. Larval development of mosquito vectors accelerates with increases in ambient temperature [112]. Larval stages mature more rapidly at warmer temperatures. Adult female mosquitoes responsible for transmission of ZIKV feed more frequently and digest blood more rapidly, increasing transmission. Global warming is changing the growth rate and population dynamics of the *Aedes* mosquitoes. As the world climate changes and global temperatures increase, the geographic distribution of diseases transmitted by *A. aegypti* is expected to increase. If climate change continues at the current rate, it will most likely promote the growth and spread of mosquito species to higher latitude regions [55]. Although a regular periodic recurrence of Zika has not been observed so far, it is expected that this might be altered by weather seasonality.

2.5 Weather seasonality and rodent-borne diseases

Rodent populations are affected by weather conditions. In particular, warm, wet winters and springs increase rodent populations, which has been observed in recent years. Under climate change scenarios, rodent populations are expected to in-

crease in temperate zones, leading to greater human-rodent interaction and higher risk of disease transmission, especially in urban areas. In some European countries, breakdowns in sanitation and inadequate hygiene contribute to serious rat infestations [96].

Future climate projections for West Africa include warmer temperatures and increased precipitation, which are expected to increase climatic suitability for *Mastomys natalensis* in much of the region [91]. Most land-use projections predict extensive expansion of cropland, for both subsistence and commercial export agriculture [4, 105]. This could lead to an increase in Lassa virus exposure in humans by expanding suitable habitat for *Mastomys natalensis*, facilitating the spread of Lassa virus between geographically separated rodent populations, or shifting ecological community composition toward higher densities of generalist small mammals (including Mastomys) on more intensively managed land (dilution effects) [19, 56].

In a recent study, a theoretical framework based on a generalization of Poisson processes was developed to jointly model zoonotic spread and human-to-human transmission to assess the impact of biological, environmental, and social parameters on transmission outcomes [64]. Modeling data from Kenema General Hospital LF as a case study again suggested that seasonal variation in infection risk may underpin the observed distribution of hospitalized cases. Another recent analysis developed a large-scale, spatially explicit compartmental model to assess the impact of future climate, land use, and socioeconomic scenarios on human Lassa virus infections [91]. Their results suggested that climate change and population growth could lead to a doubling of Lassa virus infections by 2070. Lassa fever appears in WHO's Blueprint list of diseases to be prioritized for research and development. Although rodent populations are affected by weather conditions, so far, no compartmental model with time-dependent parameters has been established.

Chapter 3

Non-autonomous epidemic systems

In mathematical biology, population dynamics is an important topic, and the study of the long-term behaviour of modelling systems is a central problem. The majority of these systems are characterized by various evolutionary equations, such as difference, ordinary, functional, and partial differential equations. Interactive populations, as we all know, often live in a fluctuating environment. For instance, physical environmental conditions such as temperature and humidity, as well as the supply of food, water, and other resources, usually change over time, either seasonally or daily. For that reason, more realistic models should be non-autonomous systems, especially, if the data in a model are periodic functions of time with a commensurate period.

For periodic epidemic compartmental models, Bacaër and Guernaoui [11] provided a definition of the basic reproduction number as the spectral radius of an integral operator acting on the space of continuous periodic functions. Later, Wang and Zhao [103] characterized the basic reproduction number for such models and proved that it serves as a threshold parameter regarding the local stability properties of the disease-free periodic solution. Rebelo et al. [90] studied persistence in epidemiological models in a seasonal environment. Bacaër and Ait Dads [10] gave a more biological explanation of the reproduction number for compartmental epidemic models with periodic parameters. Therefore, the dynamics of the system is characterized by the basic reproduction number ($\mathcal{R}_0$) of periodic compartmental models. One can also show that the global dynamics is determined by this threshold parameter: if $\mathcal{R}_0 < 1,$ then the disease-free periodic solution is globally asymptotically stable , while if $\mathcal{R}_0 > 1,$ then the disease remains endemic in the population and there exists at least a positive ω-periodic solution.

This is an introductory chapter and it is important to mention that most of the results here are from Wang and Zhao [103], Rebelo et al. [90], Zhang and Zhao [113], Smith and Waltman [97] and Zhao [115]. The remaining sections of this chapter present the theory of the basic reproduction number for periodic compartmental models and the threshold condition for the global persistence and extinction of diseases.

3.1 Periodic epidemic models

Let us consider a heterogeneous population whose individuals can be grouped into n ($n \geqslant 2$) homogeneous compartments. Let $x = (x^1, \ldots, x^n)^T \geqslant 0$, with each $x_i \geqslant 0$, be the state of individuals in each compartment. The compartments can be divided into two types: infected compartments, labeled by $i = 1, \ldots, m$ ($1 \leqslant m \leqslant n$), and uninfected compartments, labeled by $i = m+1, \ldots, n$. Define X_s to be the set of all disease-free states:

$$X_s \coloneqq \{x \geqslant 0 : x_i = 0,\ \forall i = 1, \ldots, m\}\,.$$

Let $\mathcal{F}_i(t,x)$ be the input rate of newly infected individuals in the ith compartment, $\mathcal{V}_i^+(t,x)$ be the input rate of individuals by other means, and $\mathcal{V}_i^-(t,x)$ be the rate of transfer of individuals out of compartment i. Thus, the disease transmission model is governed by a non-autonomous ordinary differential system:

$$x_i' = \mathcal{F}_i(t,x) - \mathcal{V}_i(t,x) \coloneqq f_i(t,x), \quad i = 1, \ldots, n, \tag{3.1}$$

where $\mathcal{V}_i = \mathcal{V}_i^- - \mathcal{V}_i^+$.

Following the setting of Rebelo et al. [90], we assume throughout the chapter the following conditions:

(A1) For each $1 \leqslant i \leqslant n$, the functions $\mathcal{F}_i, \mathcal{V}_i^+$ and $\mathcal{V}_i^-$ are nonnegative and continuous on $\mathbb{R} \times \mathbb{R}_+^n$ and continuously differential with respect to x.

(A2) There is a positive real number ω such that for each $1 \leqslant i \leqslant n$, the functions $\mathcal{F}_i, \mathcal{V}_i^+, \mathcal{V}_i^-$ are ω-periodic in t.

(A3) If $x_i = 0$ then $\mathcal{V}_i^- = 0$. In particular, if $x \in X_s$, then $\mathcal{V}_i^- = 0$ for $1 \leqslant i \leqslant m$.

(A4) $\mathcal{F}_i = 0$ if $i > m$.

(A5) If $x \in X_s$ then $\mathcal{F}_i = 0$ and $\mathcal{V}_i^+ = 0$ for $1 \leqslant i \leqslant m$.

(A6) System (3.1) has a unique disease-free ω-periodic solution

$$x^*(t) = \left(0, \ldots, x_{m+1}^*(t), \ldots, x_n^*(t)\right),$$

with $x_i^*(t) > 0\ \forall t$ for at least one index i with $m+1 \leqslant i \leqslant n$, which is linearly stable in the disease free subspace X_s. That is, if

$$z' = M(t)z, \quad M(t) = \left[\frac{\partial \mathcal{F}_i(t, x^*(t))}{\partial x_j}\right]_{m+1 \leq i,j \leq n}$$

is the ω-periodic linearisation of (3.1) around $x^*(t)$ in X_s, and if Φ_M is its monodromy matrix, then $\rho(\Phi_M) < 1$.

(A7) Setting

$$D_x\mathcal{F}(t,x^*(t)) = \begin{bmatrix} F(t) & 0 \\ 0 & 0 \end{bmatrix}, \qquad D_x\mathcal{V}(t,x^*(t)) = \begin{bmatrix} V(t) & 0 \\ J(t) & -M(t) \end{bmatrix},$$

where $F(t)$ and $V(t)$ are two ω-periodic $m \times m$ matrices defined by

$$F(t) = \left[\frac{\partial \mathcal{F}_i(t,x^*(t))}{\partial x_j}\right]_{1\le i,j\le m} \quad \text{and} \quad V(t) = \left[\frac{\partial \mathcal{V}_i(t,x^*(t))}{\partial x_j}\right]_{1\le i,j\le m},$$

and $J(t)$ is an $(n-m)\times m$ matrix. $F(t)$ is nonnegative, and $-V(t)$ is cooperative, that is the off-diagonal elements of $-V(t)$ are nonnegative.

Denote by $Y(t,s),\ t \geqslant s$ the evolution operator of equation

$$\frac{\mathrm{d}y}{\mathrm{d}t} = -V(t)y, \tag{3.2}$$

meaning that, for any $s \in \mathbb{R}$, the $m \times m$ matrix function $Y(t,s)$ fulfils

$$\frac{\mathrm{d}Y(t,s)}{\mathrm{d}t} = -V(t)Y(t,s), \quad \text{for all } t \geqslant s,\ Y(s,s) = I,$$

with I being the $m \times m$ unit matrix. From this, $\Phi_{-V}(t)$, the monodromy matrix of (3.2) is equal to $Y(t,0), t \geqslant 0$. We assume that $\rho(\Phi_{-V}) < 1$.

(A8) There exists a compact set $\mathcal{K} \subset \mathcal{E}$ which is positively invariant for the flow of system (3.1) and which is also an absorbing set for that flow. More formally, given $x_0 \in \mathcal{K}$ and $s_0 \in \mathbb{R}$ we have $x(t,(x_0,s_0)) \in \mathcal{K}$ for all $t \geq s_0$, and for any $x_0 \in \mathcal{E}$ and $s_0 \in \mathbb{R}$ there exists $t_1 \geq s_0$ such that for each $t \geq t_1$ we have $x(t,(x_0,s_0)) \in \mathcal{K}$.

3.2 The basic reproduction number

In epidemiology, the basic reproduction number can be considered as the expected number of secondary infections generated by one infected individual in a population where all individuals are susceptible to infection. This quantity is an important threshold parameter for measuring the effort required to eradicate the infectious disease. It is a usual condition that a disease dies out if the basic reproduction number is less than unity and the disease becomes endemic in the population if it is greater than unity. For autonomous epidemic models, Diekmann et al. [37] and van den Driessche and Watmough [101] established general approaches for the calculations of basic reproduction numbers. The basic reproduction numbers are computed for specific infectious diseases in several studies [43, 45, 50].

For periodic mathematical models, the basic reproduction number can be estimated as the spectral radius of a linear integral operator on a space of time dependent functions. Despite the fact that there is no analytical method to calculate the actual value of the basic reproduction number, there are methods to compute it numerically (see e.g. [72] for details). Furthermore, the time-average basic reproduction number of the associated periodic model provides interesting results. The formula for the time-average basic reproduction number can be obtained by setting the time-dependent parameters to constant. Unfortunately, the time-average basic reproduction number is applicable only in certain circumstances, and in many other cases it overestimates or underestimates the risk of infection. Later, Bacaër and Guernaoui [11] provided a general definition of the basic reproduction number in a periodic environment. Wang and Zhao [103] characterized the basic reproduction number for a large class of periodic compartmental epidemic models and proved that it serves as a threshold parameter regarding the local stability properties of the disease-free periodic solution.

Next, we follow the general technique introduced by Wang and Zhao [103] to define the basic reproduction number ($\mathcal{R}_0$) of system (3.1).

Assume that the initial distribution of infected is given by $\phi(s)$, which is ω-periodic in s. $F(s)\phi(s)$ gives the rate of new cases due to those infected who were introduced at time s. For $t \geqslant s$, the formula $Y(t,s)F(s)\phi(s)$ provides the distribution of the infectious individuals who were newly infected at time s and who are still infected at time t. From this we obtain that the distribution of cumulative new infections at t, generated by all infected $\phi(s)$ introduced at any time $s \leqslant t$ is

$$\psi(t) \coloneqq \int_{-\infty}^{t} Y(t,s)F(s)\phi(s)ds = \int_{0}^{\infty} Y(t,t-a)F(t-a)\phi(t-a)da.$$

Let us introduce the notation C_ω for the ordered Banach space

$$\{h\colon \mathbb{R} \to \mathbb{R}^m : h \text{ is } \omega\text{-periodic}\},$$

with the maximum norm $\|\cdot\|_\infty$. Consider the positive cone C_ω^+ defined as

$$C_\omega^+ \coloneqq \{\phi \in C_\omega : \phi(t) \geqslant 0,\ \forall t \in \mathbb{R}\}.$$

Following [103], we then define the linear operator $L\colon C_\omega \to C_\omega$ as

$$(L\phi)(t) = \int_{0}^{\infty} Y(t,t-a)F(t-a)\phi(t-a)da, \qquad \forall t \in \mathbb{R},\ \phi \in C_\omega, \tag{3.3}$$

called the next infection operator. The basic reproduction number of (3.1) is defined as $\mathcal{R}_0 := \rho(L)$, i.e. the spectral radius of the next infection operator L.

3.3 Numerical estimation of the basic reproduction number of non-autonomous models

For the periodic case, let $W(t,\lambda)$ denote the monodromy matrix of the ω-periodic linear equation

$$\frac{\mathrm{d}w(t)}{\mathrm{d}t} = \left(-V(t) + \frac{1}{\lambda}F(t)\right) w(t), \qquad \forall\, t \in \mathbb{R}, \tag{3.4}$$

where $\lambda \in (0,\infty)$ is a parameter. $F(t)$ being non-negative and $-V(t)$ being cooperative imply that $\rho(W(\omega,\lambda))$ is continuous and non-increasing in $\lambda \in (0,\infty)$ and $\lim_{\lambda\to\infty} \rho(W(\omega,\lambda)) < 1$.

We evoke the following theorem from [103] as we will need it for the numerical calculation of the basic reproduction number.

Theorem A (Wang and Zhao [103, Theorem 2.1]).

(i) *If $\rho(W(\omega,\lambda)) = 1$ has a solution $\lambda_0 > 0$, then λ_0 is an eigenvalue of $\mathcal{L}$, and thus $\mathcal{R}_0 > 0$.*

(ii) *If $\mathcal{R}_0 > 0$, then $\lambda = \mathcal{R}_0$ is the only solution of $\rho(W(\omega,\lambda)) = 1$.*

(iii) *$\mathcal{R}_0 = 0$ if and only if $\rho(W(\omega,\lambda)) < 1$ for all $\lambda > 0$.*

First we find the monodromy matrix Φ of (3.4) by finding m linearly independent solutions, most simply by taking the (linearly independent) unit vectors of $\mathbb{R}^m$ as initial values. Then we select an initial guess λ_0 and determine the spectral radius $\rho(\Phi(\lambda_0))$. If this ρ_0 is less than 1, then we set $\lambda_- = \lambda_0$ and increase our guess λ_0 to find an upper bound λ_+ with which $\rho(\Phi(\lambda_+))$ is larger than 1. If $\rho_0 > 1$, we proceed similarly, but the other way around. Then we keep choosing $\lambda_j \in (\lambda_-,\lambda_+)$ e.g. as $(\lambda_- + \lambda_+)/2$ and if $\rho(\Phi(\lambda_j)) < 1$, we set $\lambda_- = \lambda_j$, otherwise $\lambda_+ = \lambda_j$. We proceed until $\lambda_+ - \lambda_- < \varepsilon$ for some sufficiently small ε. For more details see e.g. [72].

3.4 Stability of disease-free solution

3.4.1 Local stability

From the above discussion, we obtain the following result for the local asymptotic stability of the disease-free periodic solution of system (3.1).

Theorem B (Wang and Zhao [103, Theorem 2.2]).

(i) *$\mathcal{R}_0 = 1$ is equivalent to $\rho(\Phi_{F-V}(\omega)) = 1$.*

(ii) $\mathcal{R}_0 > 1$ *is equivalent to* $\rho(\Phi_{F-V}(\omega)) > 1$.

(iii) $\mathcal{R}_0 < 1$ *is equivalent to* $\rho(\Phi_{F-V}(\omega)) < 1$.

Hence, the disease-free periodic solution is locally asymptotically stable if $\mathcal{R}_0 < 1$, and unstable if $\mathcal{R}_0 > 1$.

3.4.2 Global stability

In this subsection, our aim is to show the global stability of the disease-free periodic solution of system (3.1). Then we must prove the following theorem.

Theorem C. *If* $\mathcal{R}_0 < 1$*, then the disease-free periodic solution* $x^*(t)$ *of system* (3.1) *is globally asymptotically stable and if* $\mathcal{R}_0 > 1$*, then it is unstable.*

To do this, there are two different general methods described in Wang and Zhao [103] and Rebelo et al. [90].

(A) In the first method, one can prove the global stability of disease-free solution by using Theorem B and Part 1. of the following theorem.

Theorem D (Rebelo et al. [90, Theorem 2]). *Assume (A1) to (A7).*

1. *Assume that* $0 < \mathcal{R}_0 < 1$ *and that there exists* $\epsilon^* > 0$ *and* $\mu\colon (0, \epsilon^*) \to \mathbb{R}_+$ *such that*
   (i) $\lim_{\epsilon\to 0^+} \mu(\epsilon) = 1$,
   (ii) for all $\epsilon \in (0, \epsilon^*)$*, for any solution* $x(t) = (x^1(t), \dots, x^n(t))^T$ *of* (3.1) *with initial condition* $(x_0, s_0) \in \mathcal{E} \times \mathcal{R}$*, there exists* $t_0 \geq s_0$ *such that*

$$\frac{\mathrm{d}\tilde{x}(t)}{\mathrm{d}t} \leqslant \left(\frac{F(t)}{\mu(\epsilon)} - V(t)\right)\tilde{x}(t), \quad \forall t \geqslant t_0, \tag{3.5}$$

   where $\tilde{x}(t) = (x^1(t), \dots, x^m(t))^T$.

   Then the disease dies out: $\tilde{x}(t) \to 0$ *as* $t \to \infty$*. Moreover if* $x^*(t)$ *is globally asymptotically stable (G.A.S.) in* X_s *, it is G.A.S. in* $\mathcal{E}$.

2. *Assume* $\mathcal{R}_0 > 1$*, (A8), and that there exists* $\tau \in [0, \omega)$ *such that* $F(\tau) - V(\tau)$ *is irreducible. Fix* $j \in 1, \dots, m$*. Assume that there exists* $\epsilon^* > 0$ *and* $\lambda \in (0, \epsilon^*) \to \mathbb{R}_+$ *such that:*
   (i) $\lim_{\epsilon\to 0^+} \lambda(\epsilon) = 1$,
   (ii) for all $\epsilon \in (0, \epsilon^*)$*, for any solution* $x(t)$ *of* (3.1) *with initial condition* $(x_0, s_0) \in \mathcal{K} \times \mathcal{R}$*, there exists* $t_0 \geq s_0$ *such that such that* $x_j(t) \leq \epsilon$ *for each* $t \geq t_0$*, then there exists* $t_1 \geq t_0$ *such that*

$$\frac{\mathrm{d}\tilde{x}(t)}{\mathrm{d}t} \geq \left(\frac{F(t)}{\lambda(\epsilon)} - V(t)\right)\tilde{x}(t), \quad \forall t \geqslant t_1, \tag{3.6}$$

where $\tilde{x}(t) = (x^1(t), \ldots, x^m(t))^T$. *Then system* (3.1) *is uniformly persistent with respect to* x_j, *that is,* $\{x : x_j = 0\}$ *is a uniform repeller.*

(B) Firstly, we recall the next lemma from [113] and the the comparison principle Theorem from [97].

Lemma A (Zhang and Zhao [113, Lemma 2.1]). *Let* $\mu = \frac{1}{\omega} \ln \rho(\Phi_{A(\cdot)}(\omega))$. *Then there exists an* ω*-periodic positive function* $v(t)$ *such that* $e^{\mu t}v(t)$ *is a positive solution of* $x' = A(t)x$.

Theorem E (Smith and Waltman [97, Theorem B.1]). *Let* f *be continuous on* $\mathbb{R} \times D$ *and of type* K. *Let* $x(t)$ *be a solution of* $x' = f(t, x)$, *defined on* $[a, b]$. *If* $z(t)$ *is a continuous function on* $[a, b]$ *satisfying* $z' \leq f(t, z)$, *on* (a, b) *with* $z(a) \leq x(a)$, *then* $z(t) \leq x(t)$ *for all* t *in* $[a, b]$. *If* $y(t)$ *is continuous on* $[a, b]$ *satisfying* $y' \geq f(t, y)$, *on* (a, b) *with* $y(a) \geq x(a)$, *then* $y(t) \geq x(t)$ *for all* t *in* $[a, b]$.

In this method, it is enough to use Theorem B, Lemma A and the comparison principle Theorem E to prove that the disease-free solution of system (3.1) is globally asymptomatically stable.

The method **(A)** will be used to prove the global stability of the disease-free equilibrium in Chapter 5, while the method **(B)** will be used to prove the global stability of the disease-free equilibrium in Chapter 4 and Chapter 6.

Lemma A and Theorem E will be needed in proving the global stability of the disease-free periodic solution and the uniform persistence of the disease throughout the dissertation.

3.5 Persistence of the infectives and existence of positive periodic solutions

The following theorem shows the persistent of the infective compartments and the existence of positive periodic solutions of system (3.1) when the basic reproduction number $\mathcal{R}_0$ is larger than 1.

Theorem F. *If* $\mathcal{R}_0 > 1$. *Then*

(i) system (3.1) *is persistent with respect to the infective compartments;*

(ii) system (3.1) *admits at least one positive* ω*-periodic solution.*

To prove Theorem F, we can follow one of the following methods.

(C) In this method, we can use Part 2. of Theorem D or the following theorem to prove the persistent of the infective compartments.

Theorem G (Rebelo et al. [90, Theorem 4]). *Assume (A1) to (A7) and (A8). Assume that $\mathcal{R}_0 > 1$, that there exists $\tau \in [0,\omega]$ such that $F(\tau) - V(\tau)$ is irreducible, and that there exist $\epsilon^* > 0$ and $\lambda \in (0,\epsilon^*) \to \mathbb{R}_+$ satisfying:*

(i) $\lim_{\epsilon\to 0^+} \lambda(\epsilon) = 1$,

(ii) for all $\epsilon \in (0,\epsilon^*)$, for each solution $x(t)$ of (3.1) with initial condition $(x_0,s_0) \in \mathcal{K}\times\mathcal{R}$, if there is $t_0 \geq s_0$ such that $\|\tilde{x}(t)\| \leq \epsilon$ for each $t \geq t_0$, then there exists $t_1 \geq t_0$ such that $\tilde{x}'(t) \geq \left(\frac{F(t)}{\lambda(\epsilon)} - V(t)\right)\tilde{x}(t)$, for each $t \geqslant t_1$ with $\tilde{x}(t) = (x^1(t),\ldots,x^m(t))^T$.

Then the set

$$\rho = \left\{ x_0 \in \mathcal{K} \colon \sum_{j=1}^{m} (x_0)_j = 0 \right\},$$

is a uniform repeller.

We will use method **(C)** in Chapter 5 to prove the persistent of the infective compartments.

(D) To show the existence of positive ω-periodic solutions of system (3.1), let us introduce the notations

$$\begin{aligned} X &\coloneqq \left\{ \left(x^1(t),\ldots,x^n(t)\right) \in \mathbb{R}^n_+ \right\}, \\ X_0 &\coloneqq \left\{ \left(x^1(t),\ldots,x^n(t)\right) \in X \colon x_j > 0,\ j = 1,\ldots,m \right\}, \end{aligned}$$

and

$$\partial X_0 \coloneqq X \setminus X_0.$$

Note that ∂X_0 need not be the boundary of X_0 as the notation suggests.

Let $P\colon \mathbb{R}^n_+ \to \mathbb{R}^n_+$ be defined as the Poincaré map corresponding to (3.1), i.e. the map P is defined as

$$P(x^0) = u(\omega, x^0), \qquad x^0 \in \mathbb{R}^n_+,$$

with $u(t,x^0)$ being the single solution of (3.1) started from initial condition $x^0 \in \mathbb{R}^n_+$. Clearly,

$$P^m(x^0) = u(m\omega, x^0), \qquad \forall m \geqslant 0.$$

First, we prove the uniform persistence of P with respect to $(X_0, \partial X_0)$, as from this, we need to apply the comparison principle Theorem E and the following theorems.

Theorem H (Zhao [115, Theorem 3.1.1]). *Let $T(t)$ be an ω-periodic semiflow on X with $T(t)X_0 \subset X_0,\ \forall t \geq 0$, and $S = T(\omega)$. Assume that $S\colon X \to X$ is asymptotically smooth and has a global attractor. Then uniform persistence of S with respect to $(X_0, \partial X_0)$ implies that of $T(t)\colon X \to X$. More precisely, $S\colon X_0 \to X_0$ admits a global attractor $A_0 \subset X_0$, and the compact set $A_0^* = \bigcup_{0\leq t\leq\omega} T(t)A_0 \subset X_0$ attracts every point in X_0 for $T(t)$ in the sense that $\lim_{t\to\infty} d(T(t)x, A_0^*) = 0$ for any $x \in X_0$.*

Theorem I (Zhao [115, Theorem 1.3.1 (Strong repellers)]). *Assume that*

(C1) *$f(X_0) \subset X_0$ and f has a global attractor A,*

(C2) *The maximal compact invariant set $A_\partial = A \bigcap M_\partial$ of f in ∂X_0, possibly empty, admits a Morse decomposition $\{M_1, \ldots, M_k\}$ with the following properties:*

(a) *M_i is isolated in X,*

(b) *$W_s(M_i) \bigcap X_0 = \emptyset$ for each $1 \leq i \leq k$.*

Then there exists $\delta > 0$ such that for any compact internally chain transitive set L with $L \not\subset M_i$ for all $1 \leq i \leq k$, we have $\inf_{x\in L} d(x, \partial X_0) > \delta$.

Theorem J (Zhao [115, Theorem 1.3.6]). *Assume that f is asymptotically smooth and uniformly persistent with respect to $(X_0, \partial X_0)$, and that f has a global attractor A. Then $f\colon (X_0, d) \to (X_0, d)$ has a global attractor A_0. Moreover, if a subset B of X_0 has the property that $\gamma^+\big(f^k(B)\big)$ is strongly bounded for some $k \geq 0$, then A_0 attracts B for f.*

By Theorem J, P has a fixed point $\phi \in X_0$, and hence at least one periodic solution $u(t, \phi)$ of system (3.1) exists.

The method **(D)** will be used throughout the dissertation to prove the existence of positive ω-periodic solutions.

Chapter 4

Threshold and stability results in a periodic model for malaria spread with partial immunity in humans

In this chapter, we develop a periodic compartmental population model for the spread of malaria, dividing the human population into two classes: non-immune and semi-immune. The effect of seasonal changes in weather on the malaria transmission is considered by applying a non-autonomous model where mosquito birth, death and biting rates are time-dependent. We show that the global dynamics of the system is determined by the basic reproduction number, which we define as the spectral radius of a linear integral operator. For values of the basic reproduction number less than unity, the disease-free periodic solution is globally asymptotically stable, while if $\mathcal{R}_0 > 1$, then the disease remains endemic in the population. We show simulations in accordance with the analytic results. Finally, we show that the time-average reproduction rate gives an underestimation for malaria transmission risk.

The content of this chapter has been published in

[53] M. A. Ibrahim and A. Dénes. Threshold and stability results in a periodic model for malaria transmission with partial immunity in humans. *Applied Mathematics and Computation*, 392:125711, 2021. https://doi.org/10.1016/j.amc.2020.125711

4.1 Introduction

Malaria is an acute febrile illness caused by *Plasmodium* microorganisms spread to humans by female *Anopheles* mosquitoes. Out of the five *Plasmodium* species, most of the lethal malaria cases can be attributed to *P. falciparum*. The latest malaria report of WHO from December 2019 estimated around 230 million malaria cases and more

than 400,000 deaths in both of the preceding two years [109]. Figure 4.1 shows the malaria transmission cycle.

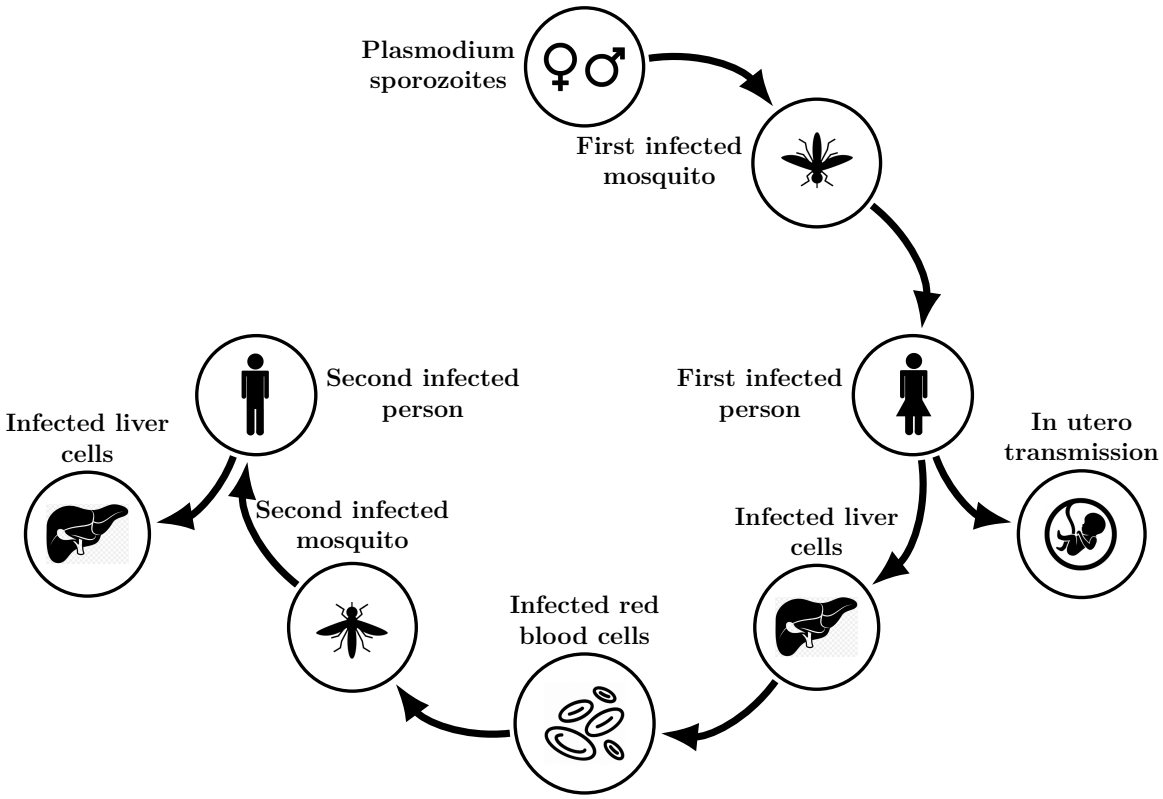

Figure 4.1: *Malaria transmission cycle.*

In a person without immunity, symptoms usually appear ten to fifteen days after infection. The symptoms of the disease, including fever, headache, and chills are often mild, making malaria difficult to recognize at early stages. *P. falciparum* malaria can develop to a serious, often lethal illness if not treated within one day. Children suffering from severe malaria often show severe anemia, respiratory distress or cerebral malaria [44, 109], while multi-organ failure is frequent in infected adults. In regions where the disease is endemic, several years of exposure may contribute to a partial immunity, making asymptomatic infections are possible. Partial immunity does not provide a complete protection, though it reduces the risk of a severe disease due to malaria infection. Hence, most malaria-related death cases in Africa affect young children, while in regions with lower transmission and immunity, every age group has an equal threat. It is important to note that heterozygotes for the sickle gene (AS) also have a partial protection against malaria [65].

Several sophisticated mathematical models of malaria transmission have been previously established, the first one by Ronald Ross [93], later extended by Macdonald [66]. Ducrot et al. [39] presented a deterministic model for malaria transmission

in which the population of humans is divided into two host types: non-immunes who are especially vulnerable to malaria and semi-immunes who are less vulnerable because of an earlier malaria infection providing partial immunity. Further works also (see e.g. [13, 57]) study the transmission of malaria with the human population divided into two types of hosts.

Periodicity of weather and climate change are very important factors in the life cycle of the parasites and the mosquitoes transmitting them. Hence, it is of crucial importance to understand how changes in weather affect the spread of malaria [38]. Mordecai et al. [73] formulated a nonlinear thermal-response model to explain the role of temperature changes in the spread of malaria. Other works [1, 2, 3, 13, 16, 31, 41, 59, 80, 82] have discussed the impacts of weather on mosquito populations and malaria transmission. In the case of a disease like malaria, which depends on the abundance of mosquitoes, which, in turn, is highly dependent on the periodically changing weather, it is especially important to include this seasonality in our models. Several papers [13, 33, 38, 79, 94, 102, 104] study the spread of malaria transmission with periodically changing mosquito birth, death and biting rates.

In our present work, motivated by [13, 39] we set up and study a compartmental population model for malaria transmission in a periodically changing environment: we extend the model given in [39] by including periodicity of the environment. Unlike [13], we consider periodic vital dynamics of mosquitoes by setting the mosquito birth rates and mosquito death rates as well as the biting rates to be periodic with one year as period, following the annual change of weather. We note, however, that the model given in [13] included a compartment for immature mosquitoes, which we do not consider. The total human population is divided into two major categories: non-immune and semi-immune. We determine the basic reproduction number $\mathcal{R}_0$ to characterize the dynamics of our model, and we show the global stability of the disease-free periodic solution or the endemicity of malaria as well as the existence of a positive ω-periodic solution, depending on the basic reproduction number. We show numerical simulations to illustrate and support the analytical results.

4.2 Mathematical model

In our model, human population is divided into two types based on their immunity level: the non-immune, i.e. those who have not developed any immunity against malaria, and the semi-immune, that is those who have some partial immunity due to their genetics or by contracting the disease earlier in their life. Semi-immune human, non-immune human and mosquito compartments are denoted by the lower indices m, n and v. Susceptible humans (S_m and S_n) can be infected by malaria. Following the infectious mosquito bite, susceptibles proceed to the exposed compartment (E_m, E_n). Individuals in these compartments have no symptoms yet. After

the incubation time, exposed individuals proceed to the infectious class (I_m, I_n). For semi-immune, there is an additional immune compartment (R_m). Humans in the class R_m are partially immune to the disease, but their blood stream still has a low level of parasites and they are still able to infect susceptible mosquitoes [30]. We have three compartments for the mosquitoes: susceptibles (S_v), exposed (E_v) and infected (I_v).

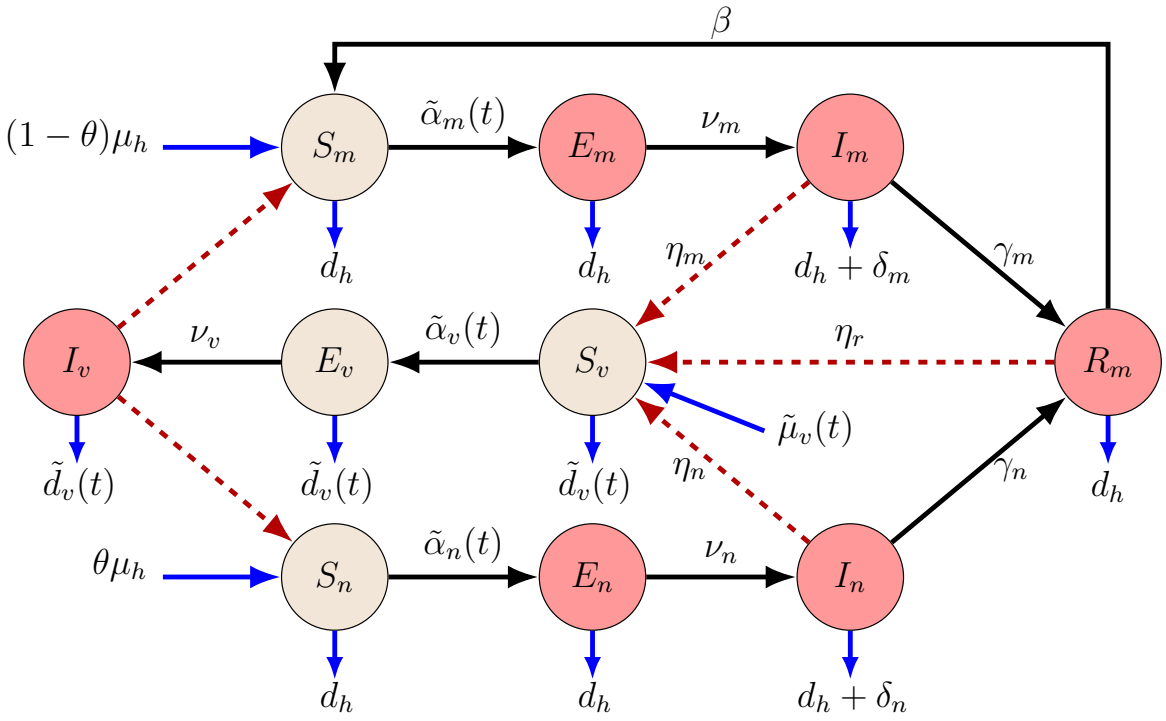

Figure 4.2: *Flow diagram of model* (4.1). *Human population are divided into two major types: the non-immune and the semi-immune. Red nodes are infectious and brown nodes are non-infectious. Black solid arrows show the progression of infection, while red dashed arrows show direction of transmission between humans and mosquitoes. Blue solid arrows show birth and death.*

We denote the total population of humans by $N_h(t)$ and total population of mosquitoes by $N_v(t)$, that is

$$N_h(t) = S_n(t) + E_n(t) + I_n(t) + S_m(t) + E_m(t) + I_m(t) + R_m(t),$$

and

$$N_v(t) = S_v(t) + E_v(t) + I_v(t).$$

The transmission dynamics is illustrated in Figure 4.2. With the above notations, our model equations can be written as

$$
\begin{aligned}
S_n^{'}(t) &= \theta\mu_h - \tilde{\alpha}_n(t)\frac{I_v(t)}{N_h(t)}S_n(t) - d_hS_n(t),\\
E_n^{'}(t) &= \tilde{\alpha}_n(t)\frac{I_v(t)}{N_h(t)}S_n(t) - \nu_nE_n(t) - d_hE_n(t),\\
I_n^{'}(t) &= \nu_nE_n(t) - \gamma_nI_n(t) - (d_h+\delta_n)I_n(t),\\
S_m^{'}(t) &= (1-\theta)\mu_h - \tilde{\alpha}_m(t)\frac{I_v(t)}{N_h(t)}S_m(t) - d_hS_m(t) + \beta R_m(t),\\
E_m^{'}(t) &= \tilde{\alpha}_m(t)\frac{I_v(t)}{N_h(t)}S_m(t) - \nu_mE_m(t) - d_hE_m(t),\\
I_m^{'}(t) &= \nu_mE_m(t) - \gamma_mI_m(t) - (d_h+\delta_m)I_m(t),\\
R_m^{'}(t) &= \gamma_nI_n(t) + \gamma_mI_m(t) - \beta R_m(t) - d_hR_m(t),\\
S_v^{'}(t) &= \tilde{\mu}_v(t) - \tilde{\alpha}_v(t)\frac{\eta_nI_n(t)+\eta_mI_m(t)+\eta_rR_m(t)}{N_h(t)}S_v(t) - \tilde{d}_v(t)S_v(t),\\
E_v^{'}(t) &= \tilde{\alpha}_v(t)\frac{\eta_nI_n(t)+\eta_mI_m(t)+\eta_rR_m(t)}{N_h(t)}S_v(t) - \nu_vE_v(t) - \tilde{d}_v(t)E_v(t),\\
I_v^{'}(t) &= \nu_vE_v(t) - \tilde{d}_v(t)I_v(t),
\end{aligned}
\tag{4.1}
$$

where $\tilde{\mu}_v(t)$, $\tilde{\alpha}_n(t)$, $\tilde{\alpha}_m(t)$, $\tilde{\alpha}_v(t)$ and $\tilde{d}_v(t)$ are the mosquito birth rate, the rate of transmission from an infected mosquito to a non-immune susceptible human, transmission rate from an infectious mosquito to susceptible semi-immune humans, the transmission rate from infected humans to susceptible mosquitoes and mosquito death rate, respectively. In our model we assumed $\tilde{\mu}_v(t)$, $\tilde{\alpha}_n(t)$, $\tilde{\alpha}_m(t)$, $\tilde{\alpha}_v(t)$ and $\tilde{d}_v(t)$ to be continuous, positive ω-periodic functions. The explanation of the model parameters is summarized in Table 4.1.

Table 4.1: *Summary of parameters and notations of model* (4.1).

Parameters	Description
μ_h	Humans birth rate
d_h	Humans death rate
θ	Probability of recruitment for humans
δ_n, δ_m	Disease mortality rate for non-immune and semi-immune humans
β	Rate of losing immunity for humans
η_n, η_m, η_r	Relative transmissibility of infectious humans to mosquitoes
γ_n, γ_m	Transfer rate of humans from I_n and I_m to R_m
ν_n, ν_m	Non-immune and semi-immune human incubation rate
ν_v	Mosquitoes incubation rate
α_n, α_m	Baseline value of mosquito-to-human transmission rate
α_v	Baseline value of human-to-mosquio transmission rate
μ_v, d_v	Baseline value of mosquito birth and death rates

We first engage in the study of the existence and uniqueness of solutions of (4.1). Introduce the notation

$$(S_n(0), E_n(0), I_n(0), S_m(0), E_m(0), I_m(0), R_m(0), S_v(0), E_v(0), I_v(0)) = (S_n^0, E_n^0, I_n^0, S_m^0, E_m^0, I_m^0, R_m^0, S_v^0, E_v^0, I_v^0) \in \mathbb{R}_+^{10}.$$

First, we show that (4.1) has a disease-free periodic solution. For the human subsystem of system (4.1) with a positive initial condition

$$(S_n^0, E_n^0, I_n^0, S_m^0, E_m^0, I_m^0, R_m^0, S_v^0, E_v^0, I_v^0) \in \mathbb{R}_+^{10},$$

we have the linear differential equation

$$\frac{\mathrm{d}N_h(t)}{\mathrm{d}t} = \mu_h - d_h N_h(t) - \delta_n I_n(t) - \delta_m I_m(t). \tag{4.2}$$

If the disease is not present in the population, (4.2) has a unique, globally asymptotically stable equilibrium $N_h^* = \frac{\mu_h}{d_h}$, and $N_h(t)$ is bounded.

To obtain the disease-free periodic solution of (4.1), let us consider the equation

$$\frac{\mathrm{d}S_v(t)}{\mathrm{d}t} = \tilde{\mu}_v(t) - \tilde{d}_v(t) S_v(t), \tag{4.3}$$

with initial condition $S_v(0) = S_v^0 \in \mathbb{R}_+$. Equation (4.3) clearly has a single positive ω-periodic solution, given by

$$S_v^*(t) = \left[\int_0^t \tilde{\mu}_v(r) e^{\int_0^r \tilde{d}_v(s)ds} dr + \frac{\int_0^\omega \tilde{\mu}_v(r) e^{\int_0^r \tilde{d}_v(s)ds} dr}{e^{\int_0^\omega \tilde{d}_v(s)ds} - 1} \right] e^{-\int_0^t \tilde{d}_v(s)ds} > 0. \tag{4.4}$$

This solution is globally attractive in $\mathbb{R}_+$ yielding that (4.1) has a single disease-free periodic solution

$$E_0 = \big(S_n^*, 0, 0, S_m^*, 0, 0, 0, S_v^*(t), 0, 0\big),$$

with $S_n^* = \theta \frac{\mu_h}{d_h}$ and $S_m^* = (1-\theta)\frac{\mu_h}{d_h}$.

To introduce the following result, we set $h^L = \sup_{t\in[0,\omega)} h(t)$ and $h^M = \inf_{t\in[0,\omega)} h(t)$ for a positive, continuous ω-periodic function $h(t)$.

Lemma 4.1. *There is $N_v^* = \frac{\mu_v^L}{d_v^M} > 0$ such that each solution in X of (4.1) eventually enters*

$$G_{N^*} := \left\{ (S_n, E_n, I_n, S_m, E_m, I_m, R_m, S_v, E_v, I_v) \in \mathbb{R}_+^{10} : \begin{array}{c} N_h \leqslant N_h^*, \\ N_v \leqslant N_v^* \end{array} \right\},$$

and for each $N_v(t) \geqslant N_v^*$, G_N is positively invariant for system (4.1). Also, we have that

$$\lim_{t\to+\infty} (N_v(t) - S_v^*(t)) = 0.$$

Proof. From (4.1), for the mosquito subsystem we have

$$\frac{\mathrm{d}N_v(t)}{\mathrm{d}t} = \tilde{\mu}_v(t) - \tilde{d}_v(t)N_v(t) \leqslant \mu_v^L - d_v^M N_v(t) \leqslant 0, \quad \text{if } N_v(t) \geqslant N_v^*,$$

which implies that G_N, $N_v(t) \geqslant N_v^*$, is positively invariant and eventually, each forward orbit enters G_{N^*}. To finish the proof, let us assume $y(t) = N_v(t) - S_v^*(t),\ t \geqslant 0$. Hence, we have $\frac{\mathrm{d}y(t)}{\mathrm{d}t} = -\tilde{d}_v(t)y(t)$, from which we have $\lim_{t\to+\infty} y(t) = 0$. Hence, the proof is complete. ■

4.3 Basic reproduction numbers and local stability

In this section, following the technique introduced by Wang and Zhao [103], we will show the local stability of the disease-free periodic solution E_0 of (4.1). First, we identify the basic reproduction number $\mathcal{R}_0$ for system (4.1).

Let $\mathcal{X} = (E_n, I_n, E_m, I_m, R_m, E_v, I_v, S_n, S_m, S_v)^T$ where E_n, I_n, E_m, I_m, R_m, E_v and I_v are infected compartments, and S_n, S_m and S_v are uninfected compartments with

$$\mathcal{F}(t,\mathcal{X}(t)) = \begin{bmatrix} \frac{\tilde{\alpha}_n(t)}{N_h(t)} I_v(t) S_n(t) \\ 0 \\ \frac{\tilde{\alpha}_m(t)}{N_h(t)} I_v(t) S_m(t) \\ 0 \\ 0 \\ \tilde{\alpha}_v(t) \frac{\eta_n I_n(t) + \eta_m I_m(t) + \eta_r R_m(t)}{N_h(t)} S_v(t) \\ 0 \\ 0 \\ 0 \\ 0 \end{bmatrix}, \tag{4.5}$$

$$\mathcal{V}^-(t,\mathcal{X}(t)) = \begin{bmatrix} (\nu_n + d_h)E_n(t) \\ (\gamma_n + d_h + \delta_n)I_n(t) \\ (\nu_m + d_h)E_m(t) \\ (\gamma_m + d_h + \delta_m)I_m(t) \\ (\beta + d_h)R_m(t) \\ (\nu_v + \tilde{d}_v(t))E_v(t) \\ \tilde{d}_v(t)I_v(t) \\ d_h S_n(t) \\ d_h S_m(t) \\ \tilde{d}_v(t)S_v(t) \end{bmatrix}, \quad \mathcal{V}^+(t,\mathcal{X}(t)) = \begin{bmatrix} 0 \\ \nu_n E_n(t) \\ 0 \\ \nu_m E_m(t) \\ \gamma_n I_n(t) + \gamma_m I_m(t) \\ 0 \\ \nu_v E_v(t) \\ \theta\mu_h \\ (1-\theta)\mu_h \\ \tilde{\mu}_v(t) \end{bmatrix}. \tag{4.6}$$

We need to verify that the conditions (A1)–(A7) in Chapter 3 are satisfied. Equation (4.1) is equivalent to

$$\mathcal{X}'(t) = \mathcal{F}(t, \mathcal{X}(t)) - \mathcal{V}(t, \mathcal{X}(t)), \tag{4.7}$$

where we introduce the notation $\mathcal{V}(t, \mathcal{X}(t))$ for $\mathcal{V}^-(t, \mathcal{X}(t)) - \mathcal{V}^+(t, \mathcal{X}(t))$. It is straightforward to check that conditions (A1)–(A5) hold.

It is clear from the above that equation (4.7) has the disease-free periodic solution

$$\mathcal{X}^*(t) = (0, 0, 0, 0, 0, 0, 0, S_n^*, S_m^*, S_v^*(t))\,.$$

Let us introduce $f(t, \mathcal{X}(t))$ for $\mathcal{F}(t, \mathcal{X}(t)) - \mathcal{V}(t, \mathcal{X}(t))$ and the matrix function $M(t) = \left(\frac{\partial f_i(t, \mathcal{X}^*(t))}{\partial \mathcal{X}_j}\right)_{8 \leqslant i,j \leqslant 10}$ where $f_i(t, \mathcal{X}(t))$ is the ith coordinate of $f(t, \mathcal{X}(t))$ and $\mathcal{X}_i$ is the ith component of $\mathcal{X}$. From (4.5) and (4.6), the matrix function $M(t)$ can be calculated as

$$M(t) = \begin{bmatrix} -d_h & 0 & 0 \\ 0 & -d_h & 0 \\ 0 & 0 & -\tilde{d}_v(t) \end{bmatrix}. \tag{4.8}$$

Let us denote by $\Phi_M(t)$ the monodromy matrix of $\frac{\mathrm{d}}{\mathrm{d}t}z = M(t)z$ and we will use the notation $\rho(\Phi_M(t))$ for the spectral radius of $\Phi_M(\omega)$. Hence, $\rho(\Phi_M(t)) < 1$, which implies that $\mathcal{X}^*(t)$ is a linearly asymptotically stable solution in the disease-free subspace $\mathcal{X}_s = \{(0, 0, 0, 0, 0, 0, S_n, S_m, S_v) \in \mathbb{R}_+^{10}\}$. This implies that the condition (A6) holds as well.

We introduce the 7×7 matrix functions $F(t), V(t)$ given as $F(t) = \left(\frac{\partial \mathcal{F}_i(t, \mathcal{X}^*(t))}{\partial \mathcal{X}_j}\right)_{1 \leqslant i,j \leqslant 7}$, $V(t) = \left(\frac{\partial \mathcal{V}_i(t, \mathcal{X}^*(t))}{\partial \mathcal{X}_j}\right)_{1 \leqslant i,j \leqslant 7}$ with $\mathcal{F}_i$ and $\mathcal{V}_i$ denoting the i-th coordinate of the vector functions $\mathcal{F}$ and $\mathcal{V}$, respectively. Then from (4.5) and (4.6), we have

$$\begin{aligned} F(t) &= \begin{bmatrix} 0 & 0 & 0 & 0 & 0 & 0 & \tilde{\alpha}_n(t)\frac{S_n^*}{N_h^*} \\ 0 & 0 & 0 & 0 & 0 & 0 & 0 \\ 0 & 0 & 0 & 0 & 0 & 0 & \tilde{\alpha}_m(t)\frac{S_m^*}{N_h^*} \\ 0 & 0 & 0 & 0 & 0 & 0 & 0 \\ 0 & 0 & 0 & 0 & 0 & 0 & 0 \\ 0 & \eta_n\tilde{\alpha}_v(t)\frac{S_v^*(t)}{N_h^*} & 0 & \eta_m\tilde{\alpha}_v(t)\frac{S_v^*(t)}{N_h^*} & \eta_r\tilde{\alpha}_v(t)\frac{S_v^*(t)}{N_h^*} & 0 & 0 \\ 0 & 0 & 0 & 0 & 0 & 0 & 0 \end{bmatrix}, \\ V(t) &= \begin{bmatrix} \nu_n + d_h & 0 & 0 & 0 & 0 & 0 & 0 \\ -\nu_n & L_n & 0 & 0 & 0 & 0 & 0 \\ 0 & 0 & \nu_m + d_h & 0 & 0 & 0 & 0 \\ 0 & 0 & -\nu_m & L_m & 0 & 0 & 0 \\ 0 & -\gamma_n & 0 & -\gamma_m & \beta + d_h & 0 & 0 \\ 0 & 0 & 0 & 0 & 0 & \nu_v + \tilde{d}_v(t) & 0 \\ 0 & 0 & 0 & 0 & 0 & -\nu_v & \tilde{d}_v(t) \end{bmatrix}, \end{aligned} \tag{4.9}$$

where $L_n = \gamma_n + d_h + \delta_n$ and $L_m = \gamma_m + d_h + \delta_m$. $F(t)$ is a non-negative matrix, and $-V(t)$ is cooperative.

Denote by $Y(t,s),\ t \geqslant s$ the evolution operator of equation

$$\frac{\mathrm{d}y}{\mathrm{d}t} = -V(t)y, \tag{4.10}$$

meaning that, for any $s \in \mathbb{R}$, the 7×7 matrix function $Y(t,s)$ fulfils

$$\frac{\mathrm{d}Y(t,s)}{\mathrm{d}t} = -V(t)Y(t,s), \quad \text{for all } t \geqslant s,\ Y(s,s) = I,$$

with I being the 7×7 unit matrix. From this, $\Phi_{-V}(t)$, the monodromy matrix of (3.2) is equal to $Y(t,0), t \geqslant 0$. We have shown that condition (A7) holds.

Assume that the initial distribution of infected is given by $\phi(s)$, which is ω-periodic in s. $F(s)\phi(s)$ gives the rate of new cases due to those infected who were introduced at time s. For $t \geqslant s$, the formula $Y(t,s)F(s)\phi(s)$ provides the distribution of the infectious individuals who were newly infected at time s and who are still infected at time t. From this we obtain that the distribution of cumulative new infections at t, generated by all infected $\phi(s)$ introduced at any time $s \leqslant t$ is

$$\psi(t) := \int_{-\infty}^{t} Y(t,s)F(s)\phi(s)ds = \int_{0}^{\infty} Y(t,t-a)F(t-a)\phi(t-a)da.$$

Let us introduce the notation C_ω for the ordered Banach space

$$\{h\colon \mathbb{R} \to \mathbb{R}^7 : h \text{ is } \omega\text{-periodic}\},$$

with the maximum norm $\|\cdot\|_\infty$. Consider the positive cone C_ω^+ defined as

$$C_\omega^+ := \{\phi \in C_\omega : \phi(t) \geqslant 0,\ \forall t \in \mathbb{R}\}.$$

Then the linear next infection operator $\mathcal{L}$ from C_ω to C_ω, defined as

$$(\mathcal{L}\phi)(t) = \int_0^\infty Y(t,t-a)F(t-a)\phi(t-a)da, \qquad \forall t \in \mathbb{R},\ \phi \in C_\omega, \tag{4.11}$$

can be used to define the basic reproduction number of (4.1) as the spectral radius of the operator $\mathcal{L}$ [103].

Based on the results so far, we can formulate the following theorem concerning the local stability properties of the disease-free periodic solution E_0 of (4.1).

Theorem 4.1. *The disease-free periodic solution E_0 is locally asymptotically stable if $\mathcal{R}_0 < 1$, while it is unstable in the case $\mathcal{R}_0 > 1$.*

Proof. $J(t)$ is the Jacobian of (4.1) calculated in E_0:

$$J(t) = \begin{bmatrix} F(t) - V(t) & 0 \\ J_1(t) & M(t) \end{bmatrix},$$

with $M(t)$ defined in (4.8) and $J_1(t)$ is given by

$$\begin{bmatrix} 0 & 0 & 0 & 0 & 0 & 0 & -\theta\tilde{\alpha}_n(t) \\ 0 & 0 & 0 & 0 & \beta & 0 & -(1-\theta)\tilde{\alpha}_m(t) \\ 0 & -\eta_n\tilde{\alpha}_v(t)\frac{S_v^*(t)}{N_h^*} & 0 & -\eta_m\tilde{\alpha}_v(t)\frac{S_v^*(t)}{N_h^*} & -\eta_r\tilde{\alpha}_v(t)\frac{S_v^*(t)}{N_h^*} & 0 & 0 \end{bmatrix}.$$

By [100], E_0 is a locally asymptotically stable periodic solution if $\rho(\Phi_M(\omega)) < 1$ as well as $\rho(\Phi_{F-V}(\omega)) < 1$ hold. From condition (A6), we have $\rho(\Phi_M(\omega)) < 1$. It then follows that the stability of E_0 is determined by $\rho(\Phi_{F-V}(\omega))$. Hence, E_0 is locally asymptotically stable if $\rho(\Phi_{F-V}(\omega)) < 1$, and unstable if $\rho(\Phi_{F-V}(\omega)) > 1$. By using Theorem B, we complete the proof. ■

4.3.1 Derivation of the basic reproduction number of the autonomous model

To calculate the basic reproduction number $\mathcal{R}_0^A$ of the autonomous model which we obtain from (4.1) by setting the time-varying parameters mosquito birth ($\tilde{\mu}_v(t) \equiv \mu_v$) and death rates ($\tilde{d}_v(t) \equiv d_v$) and biting rates ($\tilde{\alpha}_n(t) \equiv \alpha_n$, $\tilde{\alpha}_m(t) \equiv \alpha_m$ and $\tilde{\alpha}_v(t) \equiv \alpha_v$) to constant, we follow the general approach established in [37].

Substituting the values in the disease-free equilibrium $S_v^*(t) \equiv S_v^* = \frac{\mu_v}{d_v}$ in equation (4.9), for all $t \geqslant 0$, we obtain the Jacobian F given by

$$F = \begin{bmatrix} 0 & 0 & 0 & 0 & 0 & 0 & \alpha_n\frac{S_n^*}{N_h^*} \\ 0 & 0 & 0 & 0 & 0 & 0 & 0 \\ 0 & 0 & 0 & 0 & 0 & 0 & \alpha_m\frac{S_m^*}{N_h^*} \\ 0 & 0 & 0 & 0 & 0 & 0 & 0 \\ 0 & 0 & 0 & 0 & 0 & 0 & 0 \\ 0 & \eta_n\alpha_v\frac{S_v^*}{N_h^*} & 0 & \eta_m\alpha_v\frac{S_v^*}{N_h^*} & \eta_r\alpha_v\frac{S_v^*}{N_h^*} & 0 & 0 \\ 0 & 0 & 0 & 0 & 0 & 0 & 0 \end{bmatrix},$$

and the Jacobian V given by

$$V = \begin{bmatrix} \nu_n + d_h & 0 & 0 & 0 & 0 & 0 & 0 \\ -\nu_n & L_n & 0 & 0 & 0 & 0 & 0 \\ 0 & 0 & \nu_m + d_h & 0 & 0 & 0 & 0 \\ 0 & 0 & -\nu_m & L_m & 0 & 0 & 0 \\ 0 & -\gamma_n & 0 & -\gamma_m & \beta + d_h & 0 & 0 \\ 0 & 0 & 0 & 0 & 0 & \nu_v + d_v & 0 \\ 0 & 0 & 0 & 0 & 0 & -\nu_v & d_v \end{bmatrix},$$

therefore the characteristic polynomial of the next generation matrix FV^{-1} is

$$\lambda^5\left(\lambda^2-\frac{\alpha_v\nu_vS_v^*}{d_v(d_h+\beta)(\nu_v+d_v)N_h^*}\left(\mathcal{R}_{0n}^2+\mathcal{R}_{0m}^2\right)\right)=0,$$

where

$$\mathcal{R}_{0n}^2=\frac{\theta\alpha_n\nu_n\left(\eta_n(d_h+\beta)+\gamma_n\eta_r\right)}{L_n(d_h+\nu_n)},$$
$$\mathcal{R}_{0m}^2=\frac{(1-\theta)\alpha_m\nu_m\left(\eta_m(d_h+\beta)+\gamma_m\eta_r\right)}{L_m(d_h+\nu_m)}.$$

The characteristic polynomial therefore is the quadratic equation

$$\lambda^2-\frac{\nu_v\alpha_vS_v^*}{d_v(d_h+\beta)(\nu_v+d_v)N_h^*}\left(\mathcal{R}_{0n}^2+\mathcal{R}_{0m}^2\right)=0. \tag{4.12}$$

According to [37], one obtains the basic reproduction number as the largest absolute value eigenvalue of FV^{-1}, i.e. it is given as the root of the quadratic equation (4.12)

$$\mathcal{R}_0^A=\sqrt{\frac{\nu_v\alpha_vS_v^*}{d_v(d_h+\beta)(\nu_v+d_v)N_h^*}\left(\mathcal{R}_{0n}^2+\mathcal{R}_{0m}^2\right)}. \tag{4.13}$$

Remark 4.1. *Given an ω-periodic continuous function $h(t)$, we introduce the integral average (using the notation presented in [72]) as*

$$[h]:=\frac{1}{\omega}\int_0^\omega h(t)\,dt.$$

Then, the time-average reproduction rate, $[\mathcal{R}_0]$, of the associated time-varying model is given by

$$[\mathcal{R}_0]=\sqrt{\frac{\nu_v[\tilde{\alpha}_v][S_v^*]}{[\tilde{d}_v](d_h+\beta)(\nu_v+[\tilde{d}_v])N_h^*}\left([\mathcal{R}_{0n}^2]+[\mathcal{R}_{0m}^2]\right)} \tag{4.14}$$

where

$$[\mathcal{R}_{0n}^2]=\frac{\theta[\tilde{\alpha}_n]\nu_n\left(\eta_n(d_h+\beta)+\gamma_n\eta_r\right)}{L_n(d_h+\nu_n)},$$
$$[\mathcal{R}_{0m}^2]=\frac{(1-\theta)[\tilde{\alpha}_m]\nu_m\left(\eta_m(d_h+\beta)+\gamma_m\eta_r\right)}{L_m(d_h+\nu_m)}.$$

4.4 Threshold dynamics

We will show the global stability of the disease-free periodic solution E_0 and the extinction of the disease if $\mathcal{R}_0$ is less than 1, as well as the persistence of malaria and the existence of a positive periodic solution of (4.1) if $\mathcal{R}_0$ is larger than 1.

4.4.1 Global stability of the disease-free periodic solution

Theorem 4.2. *If $\delta_n = 0$, $\delta_m = 0$ and $\mathcal{R}_0 < 1$, then the disease-free periodic solution E_0 of (4.1) is globally asymptotically stable and if $\mathcal{R}_0 > 1$, then it is unstable.*

Proof. From Theorem B, we know that if $\mathcal{R}_0 > 1$, then E_0 is unstable and if $\mathcal{R}_0 < 1$, then E_0 is locally asymptotically stable. Therefore, it is only left us to show that for $\mathcal{R}_0 < 1$, E_0 is globally attractive. If $\delta_n = 0$ and $\delta_m = 0$, we can rewrite (4.2) as

$$\frac{\mathrm{d}N_h(t)}{\mathrm{d}t} = \mu_h - d_h N_h(t),$$

and from Lemma 4.1, for any ε_1, there exists a $T_1 > 0$ such that $N_v(t) \leqslant S_v^*(t) + \varepsilon_1$ and $N_h(t) \geqslant N_h^* - \varepsilon_1$ for $t > T_1$. We obtain that

$$\frac{S_n(t)}{N_h(t)} \leqslant \frac{S_n^*}{N_h^* - \varepsilon_1}, \qquad \frac{S_m(t)}{N_h(t)} \leqslant \frac{S_m^*}{N_h^* - \varepsilon_1} \quad \text{and} \quad \frac{S_v(t)}{N_h(t)} \leqslant \frac{S_v^*(t) + \varepsilon_1}{N_h^* - \varepsilon_1}.$$

From system (4.1), we get

$$\begin{aligned}
E_n'(t) &\leqslant \tfrac{S_n^*}{N_h^* - \varepsilon_1}\tilde{\alpha}_n(t) I_v(t) - \nu_n E_n(t) - d_h E_n(t),\\
I_n'(t) &= \nu_n E_n(t) - \gamma_n I_n(t) - d_h I_n(t),\\
E_m'(t) &\leqslant \tfrac{S_m^*}{N_h^* - \varepsilon_1}\tilde{\alpha}_m(t) I_v(t) - \nu_m E_m(t) - d_h E_m(t),\\
I_m'(t) &= \nu_m E_m(t) - \gamma_m I_m(t) - d_h I_m(t),\\
R_m'(t) &= \gamma_n I_n(t) + \gamma_m I_m(t) - \beta R_m(t) - d_h R_m(t),\\
E_v'(t) &\leqslant \tilde{\alpha}_v(t)\left(\eta_n I_n(t) + \eta_m I_m(t) + \eta_r R_m(t)\right)\tfrac{S_v^*(t)+\varepsilon_1}{N_h^* - \varepsilon_1} - (\nu_v + \tilde{d}_v(t)) E_v(t),\\
I_v'(t) &= \nu_v E_v(t) - \tilde{d}_v(t) I_v(t),
\end{aligned}$$

for $t > T_1$. Let $M_{\varepsilon_1}(t)$ be the 7×7 matrix function defined by

$$\begin{bmatrix}
-\nu_n - d_h & 0 & 0 & 0 & 0 & 0 & \frac{\tilde{\alpha}_n(t) S_n^*}{N_h^* - \varepsilon_1}\\
\nu_n & -\gamma_n - d_h & 0 & 0 & 0 & 0 & 0\\
0 & 0 & -\nu_m - d_h & 0 & 0 & 0 & \frac{\tilde{\alpha}_m(t) S_m^*}{N_h^* - \varepsilon_1}\\
0 & 0 & \nu_m & -\gamma_m - d_h & 0 & 0 & 0\\
0 & \gamma_n & 0 & \gamma_m & -\beta - d_h & 0 & 0\\
0 & \eta_n \tilde{\alpha}_v(t)\frac{S_v^*(t)+\varepsilon_1}{N_h^* - \varepsilon_1} & 0 & \eta_m \tilde{\alpha}_v(t)\frac{S_v^*(t)+\varepsilon_1}{N_h^* - \varepsilon_1} & \eta_r \tilde{\alpha}_v(t)\frac{S_v^*(t)+\varepsilon_1}{N_h^* - \varepsilon_1} & -\nu_v - \tilde{d}_v(t) & 0\\
0 & 0 & 0 & 0 & 0 & \nu_v & -\tilde{d}_v(t)
\end{bmatrix}.$$

Consider the auxiliary equation

$$\frac{\mathrm{d}\tilde{u}(t)}{\mathrm{d}t} = M_{\varepsilon_1}(t)\tilde{u}(t), \tag{4.15}$$

with $\tilde{u}(t) = \left(\tilde{E}_n(t), \tilde{I}_n(t), \tilde{E}_m(t), \tilde{I}_m(t), \tilde{R}_m(t), \tilde{E}_v(t), \tilde{I}_v(t)\right)$.

Applying Theorem B, it follows that $\mathcal{R}_0 < 1$ is equivalent to $\rho(\Phi_{F-V}(\omega))$ being less

than 1. It is clear that $\lim_{\varepsilon_1\to 0}\Phi_{M_{\varepsilon_1}}(\omega)=\Phi_{F-V}(\omega)$. As $\rho(\Phi_{F-V}(\omega))$ is continuous, we can choose a small enough $\varepsilon_1>0$ for which $\rho(\Phi_{M_{\varepsilon_1}}(\omega))<1$.

By Lemma A, there is an ω-periodic positive function $p_1(t)$ s.t. $p_1(t)\exp(\xi_1 t)$ is a solution of (4.15) and $\xi_1=\frac{1}{\omega}\ln\rho(\Phi_{M_{\varepsilon_1}}(\omega))<0$. For any $h(0)\in\mathbb{R}^7_+$, we can select $K^*\in\mathbb{R}_+$ such that $h(0)\leqslant K^* p_1(0)$ where

$$h(t)=(E_n(t),I_n(t),E_m(t),I_m(t),R_m(t),E_v(t),I_v(t))^T.$$

Applying the comparison principle Theorem E, we obtain $h(t)\leqslant p_1(t)\exp(\xi_1 t)$ for $t>0$. Hence, we get

$$\lim_{t\to\infty}(E_n(t),I_n(t),E_m(t),I_m(t),R_m(t),E_v(t),I_v(t))=(0,0,0,0,0,0,0)\,.$$

Thus, (4.4) and the equations for $S_n'(t)$, $S_m'(t)$ and $S_v'(t)$ in (4.1) yield

$$\lim_{t\to\infty}S_n(t)=S_n^*,\qquad \lim_{t\to\infty}S_m(t)=S_m^*,\quad\text{and}\quad \lim_{t\to\infty}S_v(t)=S_v^*(t),$$

and hence, the proof is complete. ■

4.4.2 Existence of positive periodic solutions

Let us introduce the notations

$$\begin{aligned}X&\coloneqq\left\{(S_n,E_n,I_n,S_m,E_m,I_m,R_m,S_v,E_v,I_v)\in\mathbb{R}^{10}_+\right\},\\ X_0&\coloneqq\left\{(S_n,E_n,I_n,S_m,E_m,I_m,R_m,S_v,E_v,I_v)\in X:\begin{array}{l}E_n>0,I_n>0,\\E_m>0,I_m>0,\\R_m>0,E_v>0,\\I_v>0\end{array}\right\},\end{aligned}\tag{4.16}$$

and

$$\partial X_0\coloneqq X\setminus X_0.$$

Let $P\colon\mathbb{R}^{10}_+\to\mathbb{R}^{10}_+$ defined as the Poincaré map corresponding to (4.1), i.e. the map P is defined as

$$P(x^0)=u(\omega,x^0),\qquad x^0\in\mathbb{R}^{10}_+,$$

with $u(t,x^0)$ being the single solution of (4.1) started from initial condition $x^0\in\mathbb{R}^{10}_+$. Clearly,

$$P^m(x^0)=u(m\omega,x^0),\qquad \forall m\geqslant 0.$$

Lemma 4.2. *If the basic reproduction number $\mathcal{R}_0$ is larger than 1, then there exists a $\sigma>0$ such that for any $(S_n^0,E_n^0,I_n^0,S_m^0,E_m^0,I_m^0,R_m^0,S_v^0,E_v^0,I_v^0)\in X_0$ with*

$$\|(S_n^0,E_n^0,I_n^0,S_m^0,E_m^0,I_m^0,R_m^0,S_v^0,E_v^0,I_v^0)-E_0\|\leqslant\sigma,$$

we have

$$\limsup_{m\to\infty} d\left(P^m\left(S_n^0, E_n^0, I_n^0, S_m^0, E_m^0, I_m^0, R_m^0, S_v^0, E_v^0, I_v^0\right), E_0\right) \geqslant \sigma.$$

Proof. It follows from Theorem B that $\rho(\Phi_{F-V}(\omega)) > 1$ if the basic reproduction number is larger than 1. In this case, there exists an $\eta > 0$ small enough for which $\rho(\Phi_{F-V-M_\eta}(\omega)) > 1$, with $M_\eta(t)$ being the 7×7 matrix function defined by

$$\begin{bmatrix} 0 & 0 & 0 & 0 & 0 & 0 & \tilde{\alpha}_n(t)\eta \\ 0 & 0 & 0 & 0 & 0 & 0 & 0 \\ 0 & 0 & 0 & 0 & 0 & 0 & \tilde{\alpha}_m(t)\eta \\ 0 & 0 & 0 & 0 & 0 & 0 & 0 \\ 0 & 0 & 0 & 0 & 0 & 0 & 0 \\ 0 & \eta_n\tilde{\alpha}_v(t)\eta & 0 & \eta_m\tilde{\alpha}_v(t)\eta & \eta_r\tilde{\alpha}_v(t)\eta & 0 & 0 \\ 0 & 0 & 0 & 0 & 0 & 0 & 0 \end{bmatrix}.$$

Let us choose an arbitrary $\eta > 0$. Applying the continuous dependence of solutions on initial values, there exists a $\sigma = \sigma(\eta) > 0$ such that for any

$$(S_n^0, E_n^0, I_n^0, S_m^0, E_m^0, I_m^0, R_m^0, S_v^0, E_v^0, I_v^0) \in X_0$$

with $\|\left(S_n^0, E_n^0, I_n^0, S_m^0, E_m^0, I_m^0, R_m^0, S_v^0, E_v^0, I_v^0\right) - E_0\| \leqslant \sigma$, it holds that

$$\|u(t, (S_n^0, E_n^0, I_n^0, S_m^0, E_m^0, I_m^0, R_m^0, S_v^0, E_v^0, I_v^0)) - u(t, E_0)\| \leqslant \eta, \text{ for } 0 \leqslant t \leqslant \omega.$$

We further claim that

$$\limsup_{m\to\infty} d\left(P^m\left(S_n^0, E_n^0, I_n^0, S_m^0, E_m^0, I_m^0, R_m^0, S_v^0, E_v^0, I_v^0\right), E_0\right) \geqslant \sigma. \tag{4.17}$$

Suppose that (4.17) is not satisfied. Then

$$\limsup_{m\to\infty} d\left(P^m\left(S_n^0, E_n^0, I_n^0, S_m^0, E_m^0, I_m^0, R_m^0, S_v^0, E_v^0, I_v^0\right), E_0\right) < \sigma$$

holds for some $(S_n^0, E_n^0, I_n^0, S_m^0, E_m^0, I_m^0, R_m^0, S_v^0, E_v^0, I_v^0) \in X_0$. Without loss of generality we may assume that

$$d\left(P^m\left(S_n^0, E_n^0, I_n^0, S_m^0, E_m^0, I_m^0, R_m^0, S_v^0, E_v^0, I_v^0\right), E_0\right) < \sigma, \quad \forall m \geq 0.$$

Then the above discussion implies that

$$\|u(t, P^m\left(S_n^0, E_n^0, I_n^0, S_m^0, E_m^0, I_m^0, R_m^0, S_v^0, E_v^0, I_v^0\right) - u(t, E_0)\| < \sigma, \ \forall m \geq 0, \ t \in [0, \omega].$$

For $t \geqslant 0$, we write t as $t = m\omega + t_1$ with $t_1 \in [0, \omega)$ and $m = [\frac{t}{\omega}]$, which is the greatest integer not larger than $\frac{t}{\omega}$. Then, we obtain

$$\begin{aligned} &\|u\left(t, \left(S_n^0, E_n^0, I_n^0, S_m^0, E_m^0, I_m^0, R_m^0, S_v^0, E_v^0, I_v^0\right)\right) - u\left(t, E_0\right)\| \\ &\qquad = \|u\left(t_1, P^m\left(S_n^0, E_n^0, I_n^0, S_m^0, E_m^0, I_m^0, R_m^0, S_v^0, E_v^0, I_v^0\right)\right) - u(t_1, E_0)\| < \sigma, \end{aligned}$$

for all $t \geqslant 0$, which implies that

$$\frac{S_n(t)}{N_h(t)} \geqslant \frac{S_n^*}{N_h^*} - \eta, \quad \frac{S_m(t)}{N_h(t)} \geqslant \frac{S_m^*}{N_h^*} - \eta \quad \text{and} \quad \frac{S_v(t)}{N_h(t)} \geqslant \frac{S_v^*(t)}{N_h^*} - \eta.$$

Then for $\| (S_n^0, E_n^0, I_n^0, S_m^0, E_m^0, I_m^0, R_m^0, S_v^0, E_v^0, I_v^0) - E_0\| \leqslant \sigma$, we obtain

$$\begin{aligned}
E_n^{'}(t) &\geqslant \tilde{\alpha}_n(t) I_v(t) \left(\tfrac{S_n^*}{N_h^*} - \eta\right) - \nu_n E_n(t) - d_h E_n(t) \\
I_n^{'}(t) &= \nu_n E_n(t) - \gamma_n I_n(t) - (d_h + \delta_n) I_n(t) \\
E_m^{'}(t) &\geqslant \tilde{\alpha}_m(t) I_v(t) \left(\tfrac{S_m^*}{N_h^*} - \eta\right) - \nu_m E_m(t) - d_h E_m(t) \\
I_m^{'}(t) &= \nu_m E_m(t) - \gamma_m I_m(t) - (d_h + \delta_m) I_m(t) \\
R_m^{'}(t) &= \gamma_n I_n(t) + \gamma_m I_m(t) - \beta R_m(t) - d_h R_m(t) \\
E_v^{'}(t) &\geqslant \tilde{\alpha}_v(t) \left(\eta_n I_n(t) + \eta_m I_m(t) + \eta_r R_m(t)\right) \left(\tfrac{S_v^*(t)}{N_h^*} - \eta\right) - (\nu_v + \tilde{d}_v(t)) E_v(t) \\
I_v^{'}(t) &= \nu_v E_v(t) - \tilde{d}_v(t) I_v(t)
\end{aligned}$$

Consider now the auxiliary linear system

$$\frac{\mathrm{d}\hat{u}(t)}{\mathrm{d}t} = (F(t) - V(t) - M_\eta(t))\hat{u}(t), \tag{4.18}$$

where $\hat{u}(t) = \left(\hat{E}_n(t), \hat{I}_n(t), \hat{E}_m(t), \hat{I}_m(t), \hat{R}_m(t), \hat{E}_v(t), \hat{I}_v(t)\right)$.

Now we have that $\rho(\Phi_{F-V-M_\eta}(\omega)) > 1$. Once again by Lemma A, there is an ω-periodic positive function $p_2(t)$ s.t. $p_2(t)\exp(\xi_2 t)$ is a solution of (4.18) and $\xi_2 = \frac{1}{\omega}\ln \rho(\Phi_{F-V-M_\eta}(\omega)) > 0$. For any $h(0) \in \mathbb{R}_+^7$, we can find $K_2^* \in \mathbb{R}_+$ such that $h(0) \geqslant K_2^* p_2(0)$ where

$$h(t) = (E_n(t), I_n(t), E_m(t), I_m(t), R_m(t), E_v(t), I_v(t))^T.$$

Applying the comparison principle Theorem E, we obtain $h(t) \geqslant p_2(t)\exp(\xi_2 t)$ for all $t > 0$, from which it follows that $\lim_{t\to\infty} E_n(t) = \infty$, $\lim_{t\to\infty} I_n(t) = \infty$, $\lim_{t\to\infty} E_m(t) = \infty$, $\lim_{t\to\infty} I_m(t) = \infty$, $\lim_{t\to\infty} R_m(t) = \infty$, $\lim_{t\to\infty} E_v(t) = \infty$ and $\lim_{t\to\infty} I_v(t) = \infty$. This leads to a contradiction, hence the proof is complete. ■

Proposition 4.1. *X_0 and ∂X_0 defined in (4.16) are positively invariant with respect to the flow defined by (4.1).*

Proof. Let $(S_n^0, E_n^0, I_n^0, S_m^0, E_m^0, I_m^0, R_m^0, S_v^0, E_v^0, I_v^0) \in X_0$ be an arbitrary initial condition. By solving (4.1), we obtain

$$\begin{aligned}
S_n(t) &= e^{\int_0^t -a_1(s)\,ds}\left[S_n^0 + \theta\mu_h \int_0^t e^{\int_0^s a_1(r)\,dr}\,ds\right] \\
&\geqslant \theta\mu_h e^{\int_0^t -a_1(s)\,ds}\left[\int_0^t e^{\int_0^s a_1(r)\,dr}\,ds\right] > 0, \quad \forall t > 0,
\end{aligned} \tag{4.19}$$

$$\begin{aligned} E_n(t) &= e^{-(\nu_n+d_h)t}\left[E_n^0+\int_0^t \tfrac{\tilde{\alpha}_n(s)}{N_h(s)} I_v(s)S_n(s)e^{(\nu_n+d_h)s}\,ds\right] \\ &\geqslant e^{-(\nu_n+d_h)t}\left[\int_0^t \tfrac{\tilde{\alpha}_n(s)}{N_h(s)} I_v(s)S_n(s)e^{(\nu_n+d_h)s}\,ds\right] > 0, \quad \forall t>0, \end{aligned} \tag{4.20}$$

$$\begin{aligned} I_n(t) &= e^{-L_n t}\left[I_n^0+\nu_n\int_0^t E_n(s)e^{L_n s}\,ds\right] \\ &\geqslant e^{-L_n t}\left[\nu_n\int_0^t E_n(s)e^{L_n s}\,ds\right] > 0, \quad \forall t>0, \end{aligned} \tag{4.21}$$

$$\begin{aligned} S_m(t) &= e^{\int_0^t -a_2(s)\,ds}\left[S_m^0+\int_0^t \left((1-\theta)\mu_h+\beta R_m(s)\right)e^{\int_0^s a_2(r)\,dr}\,ds\right] \\ &\geqslant e^{\int_0^t -a_2(s)\,ds}\left[\int_0^t \left((1-\theta)\mu_h+\beta R_m(s)\right)e^{\int_0^s a_2(r)\,dr}\,ds\right] \\ &> 0, \quad \forall t>0, \end{aligned} \tag{4.22}$$

$$\begin{aligned} E_m(t) &= e^{-(\nu_m+d_h)t}\left[E_m^0+\int_0^t \tfrac{\tilde{\alpha}_m(s)}{N_h(s)} I_v(s)S_m(s)e^{(\nu_m+d_h)s}\,ds\right] \\ &\geqslant e^{-(\nu_m+d_h)t}\left[\int_0^t \tfrac{\tilde{\alpha}_m(s)}{N_h(s)} I_v(s)S_m(s)e^{(\nu_m+d_h)s}\,ds\right] > 0, \quad \forall t>0, \end{aligned} \tag{4.23}$$

$$\begin{aligned} I_m(t) &= e^{-L_m t}\left[I_m^0+\nu_m\int_0^t E_m(s)e^{L_m s}\,ds\right] \\ &\geqslant e^{-L_m t}\left[\nu_m\int_0^t E_m(s)e^{L_m s}\,ds\right] > 0, \quad \forall t>0, \end{aligned} \tag{4.24}$$

$$\begin{aligned} R_m(t) &= e^{-(\beta+d_h)t}\left[R_m^0+\int_0^t \left(\gamma_n I_n(s)+\gamma_m I_m(s)\right)e^{(\beta+d_h)s}\,ds\right] \\ &\geqslant e^{-(\beta+d_h)t}\left[\int_0^t \left(\gamma_n I_n(s)+\gamma_m I_m(s)\right)e^{(\beta+d_h)s}\,ds\right] > 0, \quad \forall t>0, \end{aligned} \tag{4.25}$$

$$\begin{aligned} S_v(t) &= e^{\int_0^t -(a_3(s)+\tilde{d}_v(s))\,ds}\left[S_v^0+\int_0^t \tilde{\mu}_v(s)e^{\int_0^s (a_3(r)+\tilde{d}_v(r))\,dr}\,ds\right] \\ &\geqslant e^{\int_0^t -(a_3(s)+\tilde{d}_v(s))\,ds}\left[\int_0^t \tilde{\mu}_v(s)e^{\int_0^s (a_3(r)+\tilde{d}_v(r))\,dr}\,ds\right] > 0, \quad \forall t>0, \end{aligned} \tag{4.26}$$

$$\begin{aligned} E_v(t) &= e^{-\int_0^t (\nu_v+\tilde{d}_v(s))\,ds}\left[E_v^0+\int_0^t a_3(s)S_v(s)e^{\int_0^s (\nu_v+\tilde{d}_v(r))\,dr}\,ds\right] \\ &\geqslant e^{-\int_0^t (\nu_v+\tilde{d}_v(s))\,ds}\left[\int_0^t a_3(s)S_v(s)e^{\int_0^s (\nu_v+\tilde{d}_v(r))\,dr}\,ds\right] > 0, \quad \forall t>0, \end{aligned} \tag{4.27}$$

$$\begin{aligned} I_v(t) &= e^{-\int_0^t \tilde{d}_v(s)\,ds}\left[I_v^0+\nu_v\int_0^t E_v(s)e^{\int_0^s \tilde{d}_v(r)\,dr}\,ds\right] \\ &\geqslant \nu_v e^{-\int_0^t \tilde{d}_v(s)\,ds}\left[\int_0^t E_v(s)e^{\int_0^s \tilde{d}_v(r)\,dr}\,ds\right] > 0, \quad \forall t>0, \end{aligned} \tag{4.28}$$

where

$$\begin{aligned} a_1(t) &= \frac{\tilde{\alpha}_n(t)}{N_h(t)}I_v(t)+d_h, \qquad a_2(t) = \frac{\tilde{\alpha}_m(t)}{N_h(t)}I_v(t)+d_h, \\ a_3(t) &= \tilde{\alpha}_v(t)\frac{\eta_n I_n(t)+\eta_m I_m(t)+\eta_r R_m(t)}{N_h(t)}. \end{aligned}$$

Hence we obtain the positive invariance of X_0. The positive invariance of X and the

fact that ∂X_0 is relatively closed in X implies the positive invariance of ∂X_0. ■

Theorem 4.3. *Assume $\mathcal{R}_0 > 1$. Then (4.1) admits at least one positive periodic solution and there is an $\varepsilon > 0$ such that*

$$\liminf_{t\to\infty} E_n(t) \geqslant \varepsilon, \quad \liminf_{t\to\infty} I_n(t) \geqslant \varepsilon, \quad \liminf_{t\to\infty} E_m(t) \geqslant \varepsilon, \quad \liminf_{t\to\infty} I_m(t) \geqslant \varepsilon,$$
$$\liminf_{t\to\infty} R_m(t) \geqslant \varepsilon, \quad \liminf_{t\to\infty} E_v(t) \geqslant \varepsilon, \quad \liminf_{t\to\infty} I_v(t) \geqslant \varepsilon,$$

for all $(S_n^0, E_n^0, I_n^0, S_m^0, E_m^0, I_m^0, R_m^0, S_v^0, E_v^0, I_v^0) \in X_0$.

Proof. First, we prove the uniform persistence of P with respect to $(X_0, \partial X_0)$, as from this, applying Theorem H, we obtain the uniform persistence of the solution of (4.1) with respect to $(X_0, \partial X_0)$. From Proposition 4.1, we have the positive invariance of both X and X_0 and that ∂X_0 is relatively closed in X. Then, from Lemma 4.1 the point dissipativity of system (4.1) follows. Let us introduce

$$M_\partial = \{x^0 \in \partial X_0 : P^m(x^0) \in \partial X_0,\ \forall m \geqslant 0\}.$$

where $x^0 = (S_n^0, E_n^0, I_n^0, S_m^0, E_m^0, I_m^0, R_m^0, S_v^0, E_v^0, I_v^0)$. We will apply the theory of uniform persistence [115] (see also [113, Theorem 2.3]). In order to do this, we first show that

$$M_\partial = \{(S_n, 0, 0, S_m, 0, 0, 0, S_v, 0, 0) : S_n \geqslant 0,\ S_m \geqslant 0,\ S_v \geqslant 0\}. \tag{4.29}$$

Let us note that $M_\partial \supseteq \{(S_n, 0, 0, S_m, 0, 0, 0, S_v, 0, 0) : S_n \geqslant 0,\ S_m \geqslant 0,\ S_v \geqslant 0\}$. It is enough to prove that $M_\partial \subset \{(S_n, 0, 0, S_m, 0, 0, 0, S_v, 0, 0) : S_n \geqslant 0,\ S_m \geqslant 0,\ S_v \geqslant 0\}$, namely, for an arbitrary initial value $\phi \in \partial X_0$, $E_n(n\omega)$ or $I_n(n\omega)$ or $E_m(n\omega)$ or $I_m(n\omega)$ or $I_m(n\omega)$ or $E_v(n\omega)$ or $I_v(n\omega)$ is equal to 0, for any $n \geqslant 0$.

By contradiction assume there is a non-negative integer n_1 for which $E_n(n_1\omega)$, $I_n(n_1\omega)$, $E_m(n_1\omega)$, $I_m(n_1\omega)$, $I_m(n_1\omega)$, $E_v(n_1\omega)$ and $I_v(n_1\omega)$ are all positive. Then, by changing $t = 0$ to $t = n_1\omega$ in (4.19)–(4.28), one gets that $S_n(t)$, $E_n(t)$, $I_n(t)$, $S_m(t)$, $E_m(t)$, $I_m(t)$, $R_m(t)$, $S_v(t)$, $E_v(t)$, $I_v(t)$ are all positive. However, this contradicts the positive invariance of ∂X_0.

We know the weak uniform persistence of P with respect to $(X_0, \partial X_0)$ using Lemma 4.2. Then, Lemma 4.1 yields P has a global attractor. Then we can see E_0 is an isolated invariant subset of X and $W^s(E_0) \cap X_0 = \emptyset$. Each solution in M_∂ tends to E_0 and E_0 is acyclic in M_∂. Applying Theorem I and [115, Remark 1.3.1], we obtain the uniform persistence of P with respect to $(X_0, \partial X_0)$. From this, there is an $\varepsilon > 0$ for which

$$\liminf_{t\to\infty} E_n(t) \geqslant \varepsilon, \quad \liminf_{t\to\infty} I_n(t) \geqslant \varepsilon, \quad \liminf_{t\to\infty} E_m(t) \geqslant \varepsilon, \quad \liminf_{t\to\infty} I_m(t) \geqslant \varepsilon,$$
$$\liminf_{t\to\infty} R_m(t) \geqslant \varepsilon, \quad \liminf_{t\to\infty} E_v(t) \geqslant \varepsilon, \quad \liminf_{t\to\infty} I_v(t) \geqslant \varepsilon.$$

By Theorem J, P has an equilibrium $\bar{\phi} \in X_0$, and thus at least one periodic solution $u(t, \bar{\phi})$ of system (4.1) exists, where

$$\bar{\phi} = \big(\bar{S}_n(0), \bar{E}_n(0), \bar{I}_n(0), \bar{S}_m(0), \bar{E}_m(0), \bar{I}_m(0), \bar{R}_m(0), \bar{S}_v(0), \bar{E}_v(0), \bar{I}_v(0)\big) \in X_0.$$

We show that $\bar{S}_n(0)$, $\bar{S}_m(0)$ and $\bar{S}_v(0)$ are positive. Suppose $\bar{S}_n(0) = \bar{S}_m(0) = \bar{S}_v(0) = 0$, then $\bar{S}_n(0) > 0$, $\bar{S}_m(0) > 0$ and $\bar{S}_v(0) > 0$ for all $t > 0$. However, applying that the solution is periodic, we have $\bar{S}_n(0) = \bar{S}_n(n\omega) = 0$, $\bar{S}_m(0) = \bar{S}_m(n\omega) = 0$ and $\bar{S}_v(0) = \bar{S}_v(n\omega) = 0$, hence, we have arrived at a contradiction. ■

4.5 Numerical simulations

Here we show numerical simulations regarding our model to illustrate and support the theoretical results of the previous sections. From Section 4.4, we see that $\mathcal{R}_0$ serves as a threshold parameter concerning the persistence of the disease in the population (see Theorems 4.2 and 4.3). We show some simulations to demonstrate that our time-periodic model is in accordance with seasonally fluctuation. The functions $\tilde{\mu}_v(t)$, $\tilde{\alpha}_n(t)$, $\tilde{\alpha}_m(t)$, $\tilde{\alpha}_v(t)$ and $\tilde{d}_v(t)$ are time-periodic with one year as a period and, following e.g. [13], they are assumed to be of the form

$$\begin{aligned}
\tilde{\alpha}_i(t) &= \alpha_i \cdot \big(\sin\big(\tfrac{2\pi}{p}t + b\big) + a\big), \qquad i = n, m, v,\\
\tilde{\mu}_v(t) &= \mu_v \cdot \big(\sin\big(\tfrac{2\pi}{p}t + b\big) + a\big),\\
\tilde{d}_v(t) &= d_v \cdot \big(\cos\big(\tfrac{2\pi}{p}t + b\big) + a\big),
\end{aligned}$$

where p is period length (given in months), a, b are free adjustment parameters and μ_v, α_n, α_m, α_v and d_v are the (constant) baseline values of the corresponding time-dependent parameters.

In order to show that the single disease-free periodic solution E_0 is globally asymptotically stable if the basic reproduction number is less than unity, we provide a couple of examples. Our first example (see Figure 4.3), was created with the set of parameters given in Table 4.2 (see Example 1). We can calculate numerically the basic reproduction number $\mathcal{R}_0 = 0.625 < 1$.

In our second example (see Figure 4.4), was created with another set of parameters given in Table 4.2 (see Example 2). Again, we can calculate numerically the basic reproduction number $\mathcal{R}_0 = 0.913 < 1$. Figure 4.3 and Figure 4.4, show that solution of our model in accordance with the analytic results stating that the unique disease-free periodic solution E_0 is globally asymptotically stable when $\mathcal{R}_0 < 1$.

By Theorem 4.3, system (4.1) has a positive ω-periodic solution if $\mathcal{R}_0 > 1$. Figure 4.5 illustrates the uniform persistence of malaria when $\mathcal{R}_0 = 1.721 > 1$. Accordingly, one can see that, the disease compartments are persistent and the epidemic becomes endemic in the population recurring periodically every year.

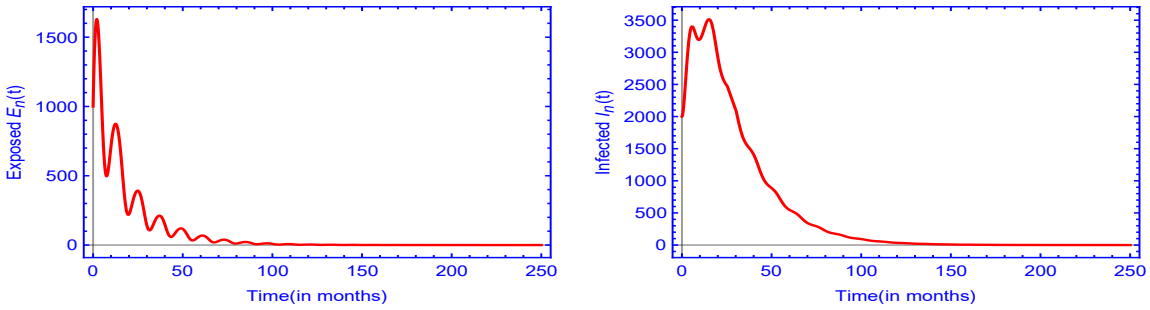

(a) *Non-immune.*

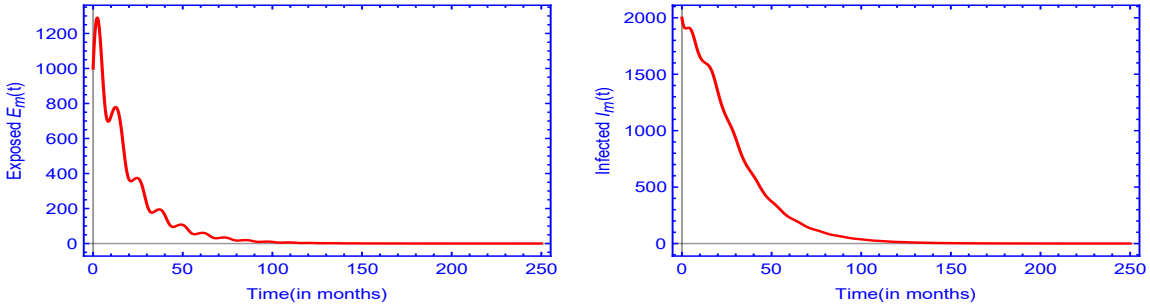

(b) *Semi-immune.*

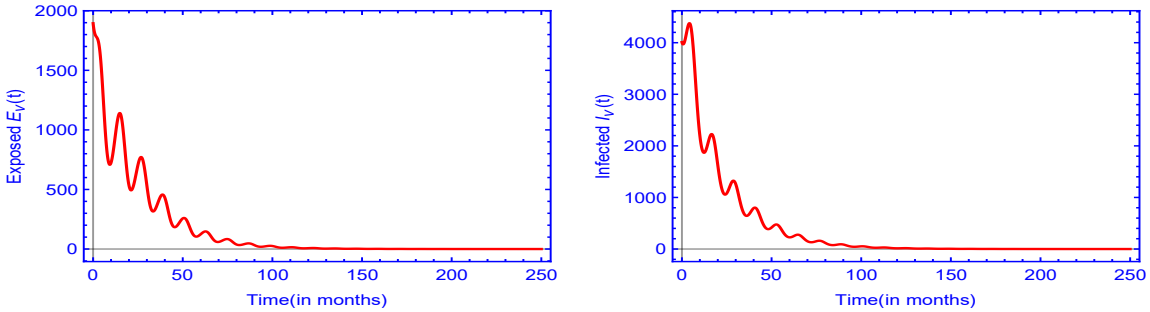

(c) *Mosquitoes.*

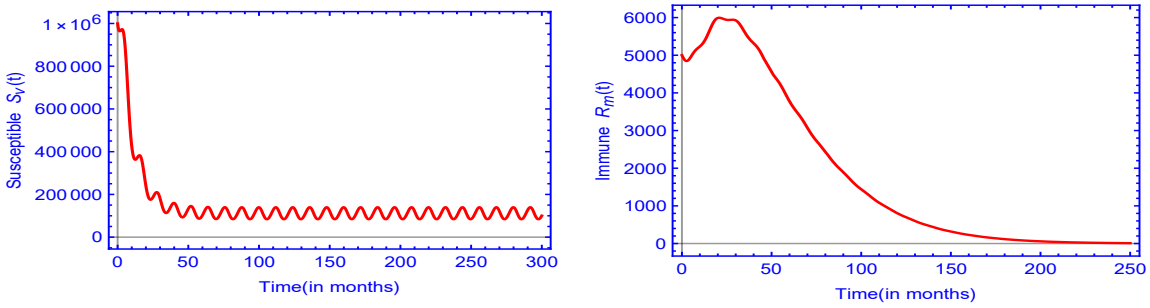

(d) *Mosquitoes and semi-immune.*

Figure 4.3: *Extinction of malaria when* $\mathcal{R}_0 = 0.625 < 1$ *with parameters given in Table 4.2 (see Example 1).*

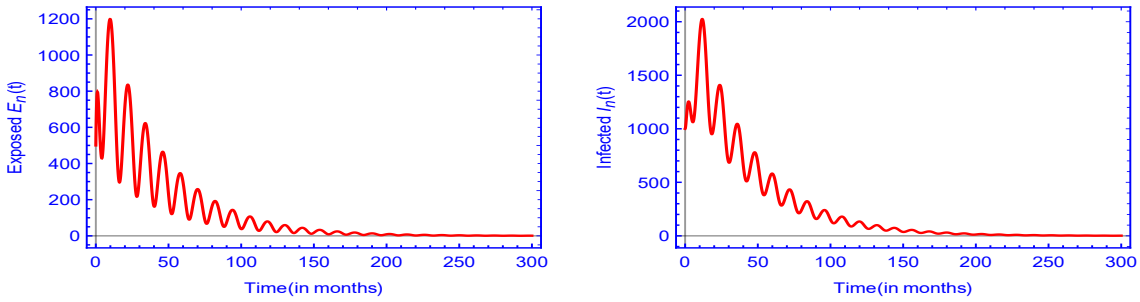

(a) *Non-immune.*

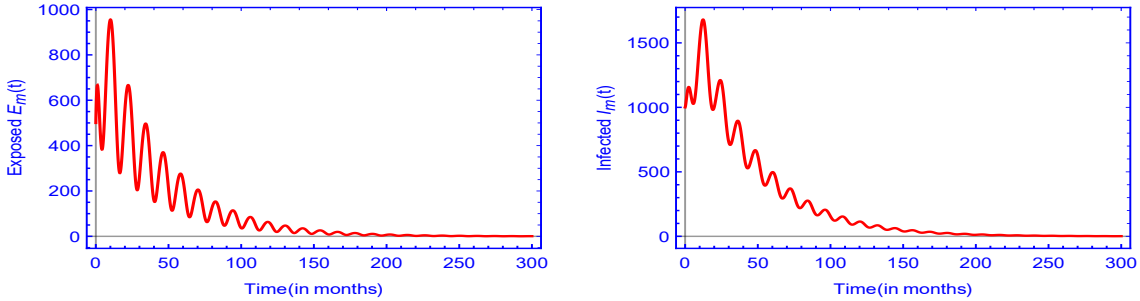

(b) *Semi-immune.*

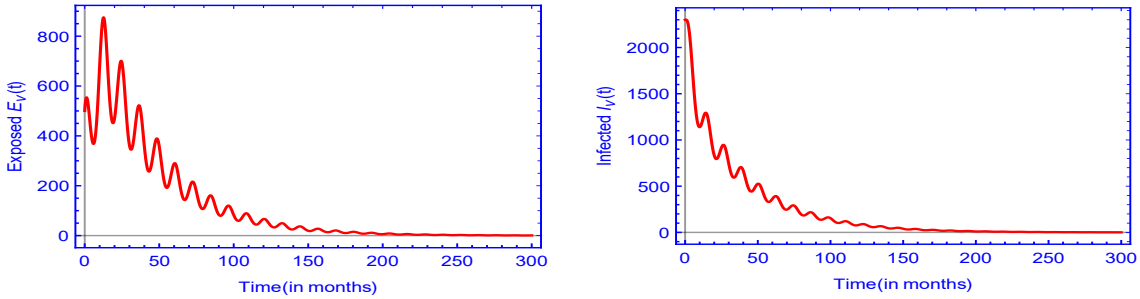

(c) *Mosquitoes.*

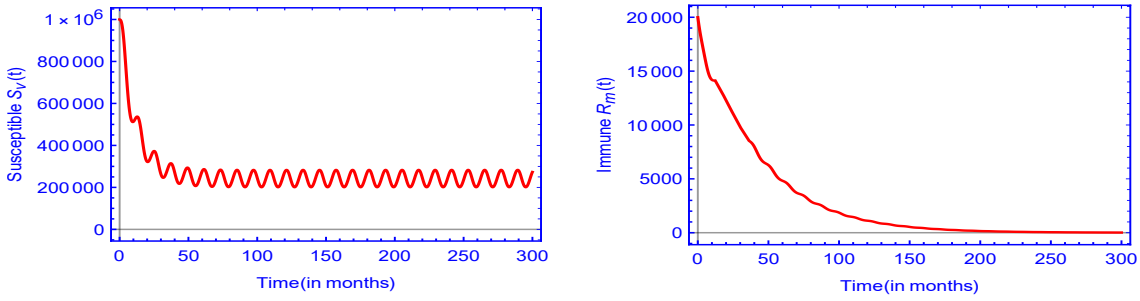

(d) *Mosquitoes and semi-immune.*

Figure 4.4: *Extinction of malaria when* $\mathcal{R}_0 = 0.913 < 1$ *with parameters given in Table 4.2 (see Example 2).*

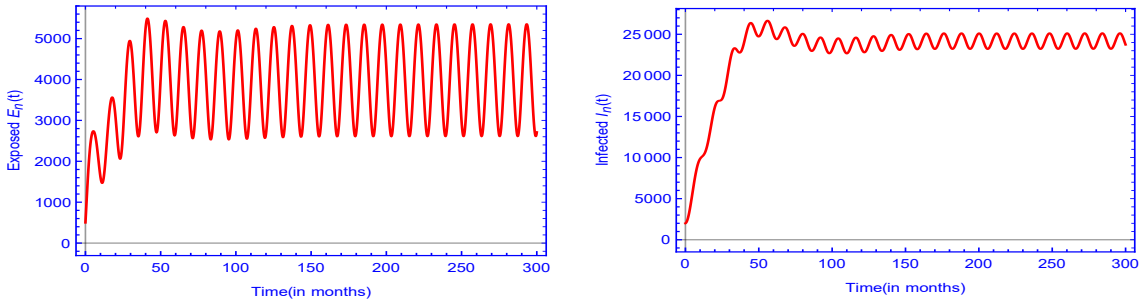

(a) *Non-immune.*

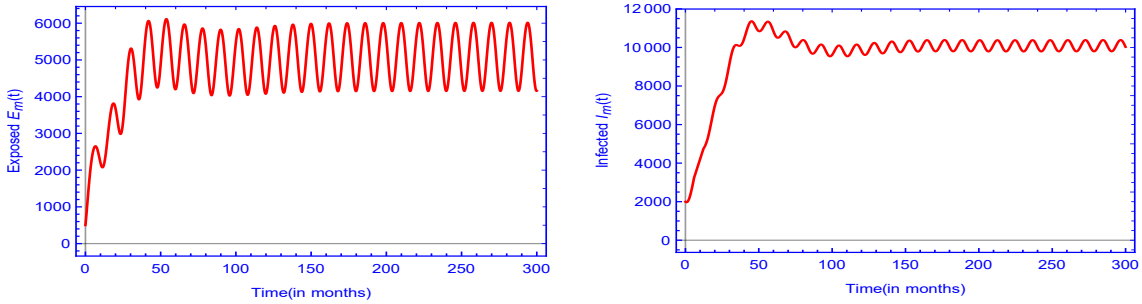

(b) *Semi-immune.*

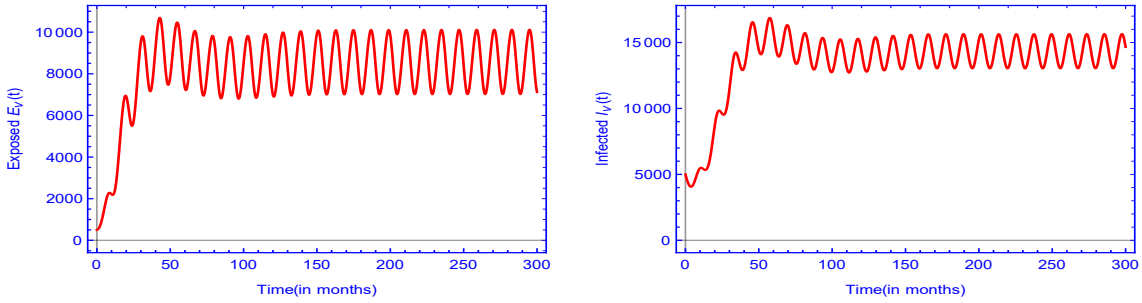

(c) *Mosquitoes.*

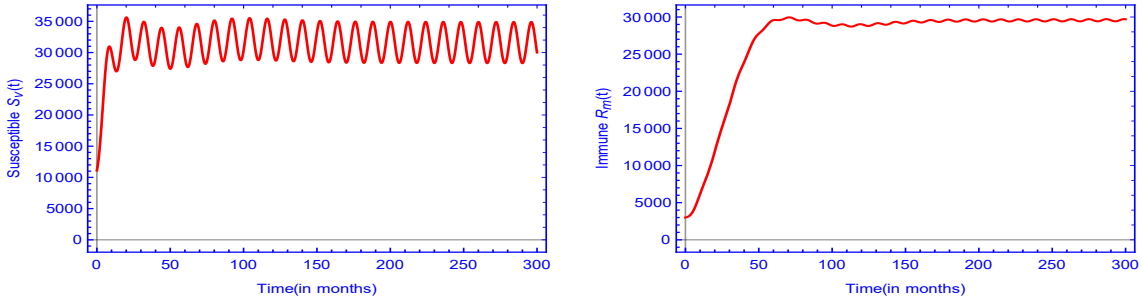

(d) *Mosquitoes and semi-immune.*

Figure 4.5: *Persistence of malaria when* $\mathcal{R}_0 = 1.721 > 1$ *with parameters given in Table 4.2.*

Table 4.2: *Parameters, values for extinction and persistence of model* (4.1).

Parameter	Value for extinction		Value for persistence	Source
	Example 1	Example 2		
μ_h	1600	1000	2000	Assumed
d_h	0.00167	0.00167	0.00167	Assumed
α_n	0.293	0.657	0.595	[39, 57]
α_m	0.17	0.42	0.348	[39, 57]
α_v	0.544	0.281	0.796	[35]
β	0.0901	0.0778	0.0731	[39, 57]
θ	0.19	0.4	0.756	[39, 57]
η_n	0.275	0.2	0.275	[39, 57]
η_m	0.219	0.2	0.219	[39, 57]
η_r	0.002	0.0021	0.002	[39, 57]
γ_n	0.088	0.35	0.0568	[39, 57]
γ_m	0.096	0.25	0.083	[39, 57]
δ_n	0	0	0.0026	[39, 57]
δ_m	0	0	0.0005	[39, 57]
ν_n	0.366	0.706	0.366	[39, 57]
ν_m	0.168	0.549	0.168	[39, 57]
ν_v	0.094	0.1	0.094	[35]
μ_v	10000	15000	2000	[35]
$1/d_v$	10	15	27	[35]
a	1.1	1.3	1.5	Assumed
b	1.83	9.43	5.9	Assumed

4.5.1 Reproduction numbers

Substituting the (time-changing) parameter values into formulas (4.13) and (6.9) provide the reproduction numbers ($\mathcal{R}_0^A, [\mathcal{R}_0]$), respectively, for any time instant.

In Figure 4.6 and Figure 4.7, we show the reproduction rate, $\mathcal{R}_0^A$, of the corresponding time-constant system (see Figure 4.6a and Figure 4.7a) and the time-average basic reproduction rate, $[\mathcal{R}_0]$, of the time-dependent system (see Figure 4.6b and Figure 4.7b), depending on mosquito birth and death rates, respectively, as well as transmission rates from humans to mosquitoes and mosquitoes to humans. The figures suggest that mosquito control, especially the control of mosquito births, highly influences the transmission of malaria and that control of the mosquito population may be sufficient to control the disease. At the same time, decreasing the mosquito-to-human transmission rates can also efficiently contribute to reduce the basic reproduction number. Figure 4.7 (in accordance with Ross' fundamental work [93]) suggests that above a certain level, killing mosquitoes has only a reduced effect.

Numerically, we can plot the reproduction ratio $\mathcal{R}_0$, the time-average reproduc-

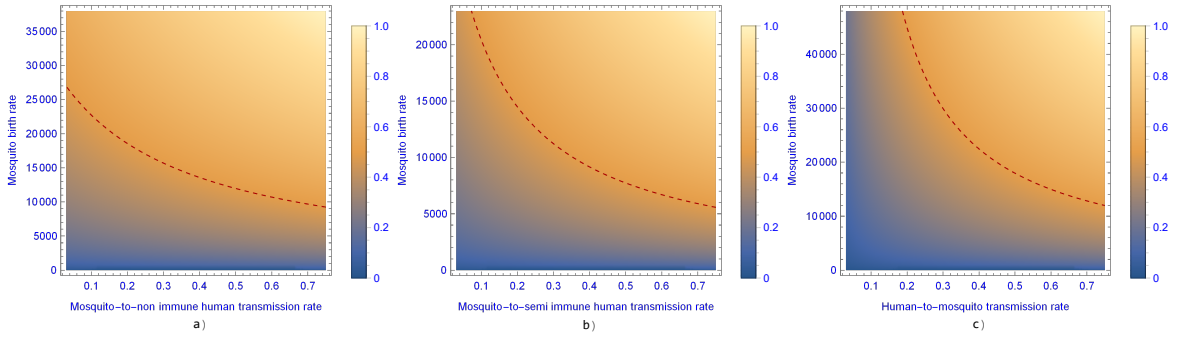

(a) *Contour plot of the basic reproduction number,* $\mathcal{R}_0^A$.

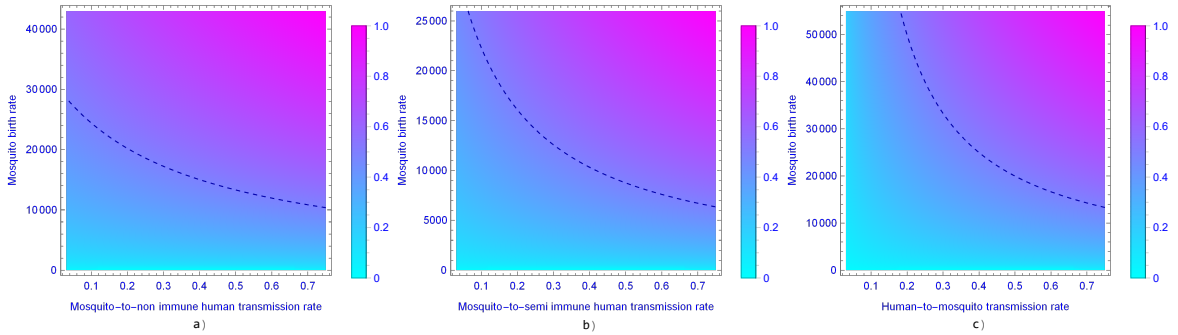

(b) *Contour plot of the time-average reproduction number,* $[\mathcal{R}_0]$.

Figure 4.6: *Contour plot of the basic reproduction number,* $\mathcal{R}_0^A$ *in (a) and the time-average basic reproduction number,* $[\mathcal{R}_0]$ *in (b), depending on mosquito birth rate* (μ_v) *and a) mosquito-to-non-immune human transmission rate* (α_n)*, b) mosquito-to-semi-immune human transmission rate* (α_m) *and c) human-to-mosquito transmission rate* (α_v)*. The dashed curve is the contour of* $\mathcal{R}_0^A = 0.5$ *in (a), and* $[\mathcal{R}_0] = 0.5$ *in (b). Parameter values are given in Table 4.2 (see Example 1).*

tion number $[\mathcal{R}_0]$, and the reproduction number $\mathcal{R}_0^A$ of the constant model with respect to mosquito birth rate (μ_v), mosquito-to-human transmission rates (α_n, α_m) and human-to-mosquito transmission rate (α_v), respectively, in Figure 4.8.

The calculations show that the time-averaged reproduction number $[\mathcal{R}_0]$ is less than the reproduction ratio $\mathcal{R}_0$, suggesting that the time-averaged reproduction number provides an underestimation of the risk of disease transmission. From this aspect, our results are similar to the those in [103] and [54]. We note that various papers present different results on under- and overestimation of the average basic reproduction number. In [9] the authors gave an approximate formula of the reproduction number for a class of epidemic models with vectorial transmission in a seasonal environment with a small perturbation parameter.

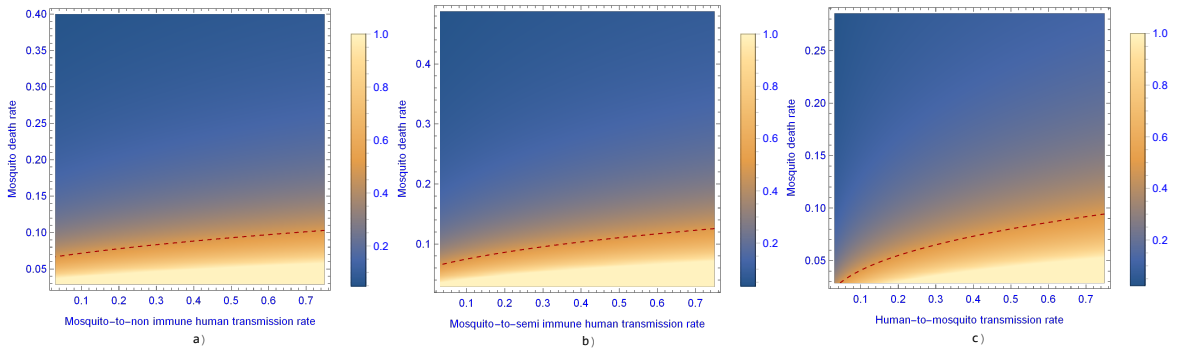

(a) *Contour plot of the basic reproduction number,* $\mathcal{R}_0^A$.

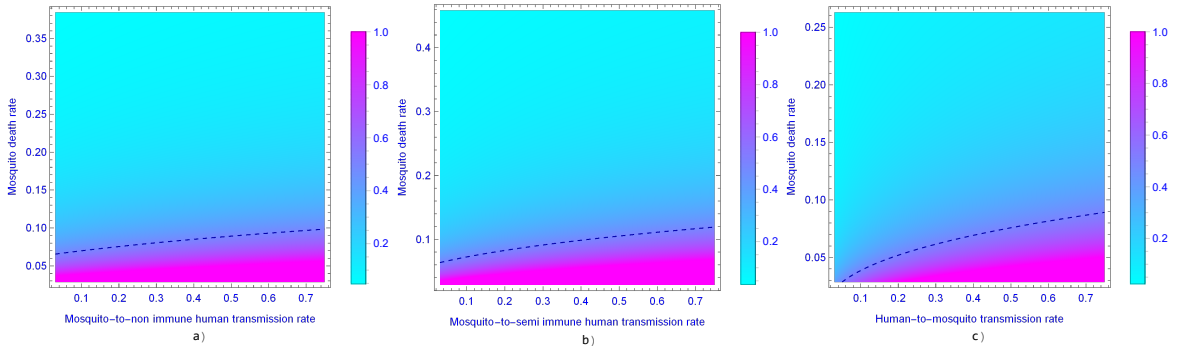

(b) *Contour plot of the time-average reproduction number,* $[\mathcal{R}_0]$.

Figure 4.7: *Contour plot of the basic reproduction number,* $\mathcal{R}_0^A$ *in (a) and the time-average basic reproduction number,* $[\mathcal{R}_0]$ *in (b), depending on mosquito death rate (*d_v*) and a) mosquito-to-non-immune human transmission rate (*α_n*), b) mosquito-to-semi-immune human transmission rate (*α_m*) and c) human-to-mosquito transmission rate (*α_v*). The dashed curve is the contour of* $\mathcal{R}_0^A = 0.5$ *in (a), and* $[\mathcal{R}_0] = 0.5$ *in (b). Parameter values are given in Table 4.2 (see Example 1).*

4.6 Discussion

We have established a compartmental model to describe malaria transmission in a seasonal environment with periodic mosquito birth, death and biting rates, where human hosts are divided into two classes: those who do not have any immunity and those who have a partial immunity due an earlier malaria infection or due to their genetics. Although mathematical modelling of malaria transmission has a quite extensive literature, up to our knowledge, the present one is the first paper to include both partial immunity of humans and periodicity in mosquito vital dynamics. For a disease like malaria, the spread of which is strongly correlated with the size of mosquito populations, it is of special importance to include weather seasonality which highly affects the abundance of vectors. Determining the variance between groups with dif-

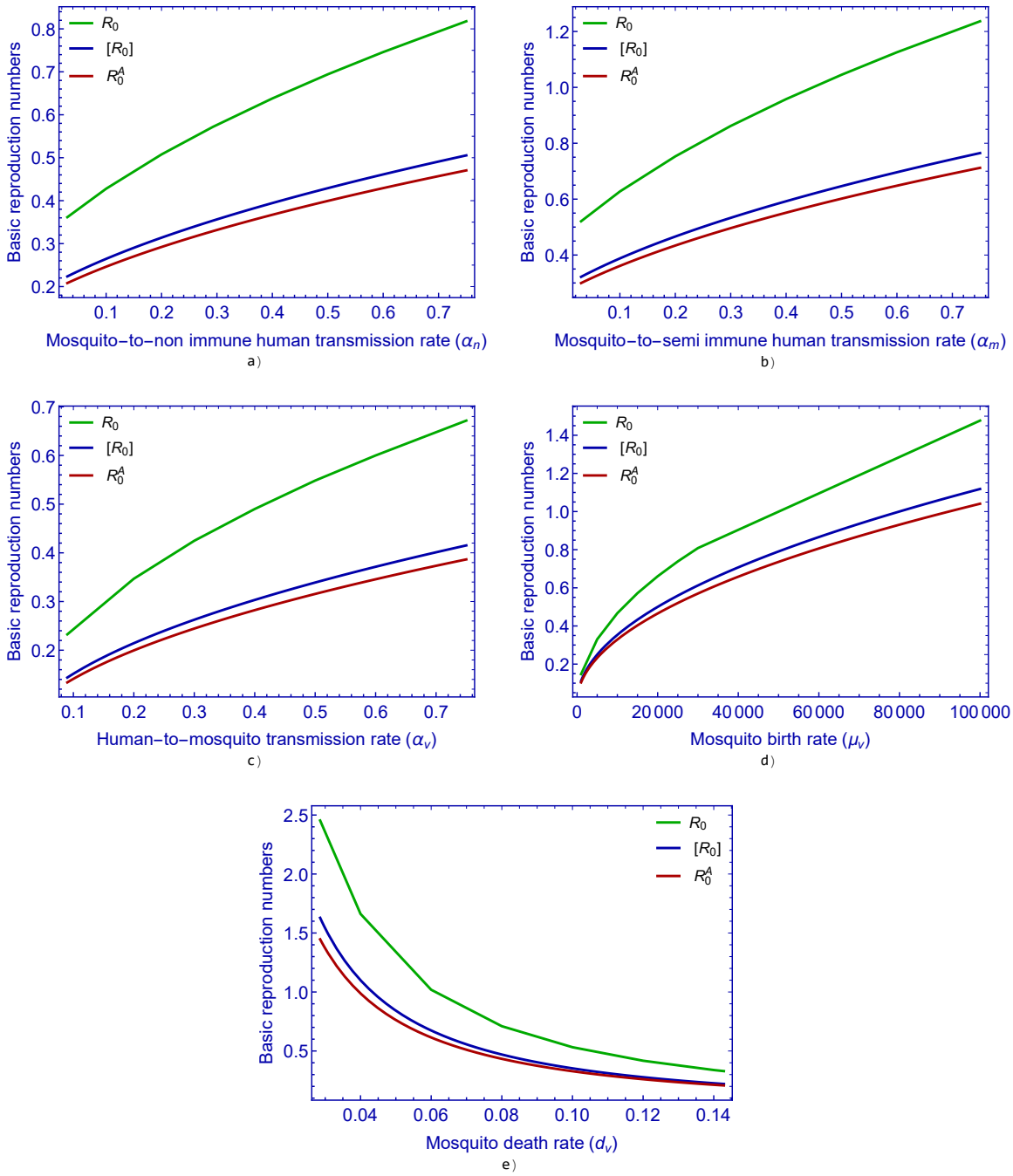

Figure 4.8: *The curves of the reproduction ratio $\mathcal{R}_0$, the time-averaged reproduction number $[\mathcal{R}_0]$ and the reproduction number of the constant model $\mathcal{R}_0^A$ versus in a) mosquito-to-non-immune human transmission rate (α_n), b) mosquito-to-semi-immune human transmission rate (α_m), c) human-to-mosquito transmission rate (α_v), d) mosquito birth rate (μ_v) and e) mosquito death rate (d_v). Parameter values are given in Table 4.2 (see Example 1).*

ferent level of immunity and applying the more realistic periodic setting might help to understand the different levels of risk the different groups to establish intervention strategies applied to these groups.

We have shown that the global dynamics of the system is characterized by the reproduction number: if $\mathcal{R}_0 < 1$, we have shown the global asymptotic stability of the disease-free periodic solution E_0, in this case the disease goes extinct. If $\mathcal{R}_0 > 1$, malaria becomes endemic in the population and the existence of at least one positive periodic solution is proved. We have also shown numerical simulations in accordance with these theoretical results (see Figure 4.3, Figure 4.4 and Figure 4.5).

The reproduction numbers were calculated as a function of the parameters α_n, α_m, α_v, μ_v and d_v. Our simulations suggest that vector control is an important factor in malaria transmission and that mosquito control, above all the control of mosquito births, may prove to be sufficient in controlling the disease (see Figure 4.6 and Figure 4.7). At the same time, personal protection resulting in a decrease of transmission rates is also an important tool to reduce the basic reproduction number. As is observed, the time-averaged reproduction number $[\mathcal{R}_0]$ is smaller than the reproduction number $\mathcal{R}_0$ (see Figure 4.8). This implies that the time-average basic reproduction number provides an underestimation of the risk of disease transmission, while the risk is overestimated in case the basic reproduction number is applied.

Our model has several possibilities for further development. As mentioned above, in regions with high transmission, the most vulnerable are young children, hence an age-structured model could be applied. To incorporate extrinsic incubation period, i.e. the length of the development of the malaria parasite within the mosquito, a time-delayed model could be formulated. Although currently there is no available vaccine against malaria, there are several vaccine constructs under evaluated in clinical trials or in advanced development. Furthermore, there are several medications used to prevent malaria. The (possibly temporary) effect of these currently used medicines or future vaccines can also be incorporated in our model, either by a direct movement from the non-immune to the semi-immune compartment, or by introducing new compartments for the temporary protection obtained by using medication or for the vaccinated population. To make the model more realistic, one could also consider different phases of the mosquitoes' life cycle. These questions might be topics of future research.

Chapter 5

Threshold dynamics in a model for Zika virus disease with seasonality

In this chapter, we present a compartmental population model for the spread of Zika virus disease including sexual and vectorial transmission as well as asymptomatic carriers. We apply a non-autonomous model with time-dependent mosquito birth, death and biting rates to integrate the impact of the periodicity of weather on the spread of Zika. We define the basic reproduction number $\mathcal{R}_0$ as the spectral radius of a linear integral operator and show that the global dynamics is determined by this threshold parameter: if $\mathcal{R}_0 < 1$, then the disease-free periodic solution is globally asymptotically stable, while if $\mathcal{R}_0 > 1$, then the disease persists. We show numerical examples to study what kind of parameter changes might lead to a periodic recurrence of Zika.

The content of this chapter has been published in

[54] M. A. Ibrahim and A. Dénes. Threshold dynamics in a model for Zika virus disease with seasonality. *Bulletin of Mathematical Biology*, 83:27, 2021. https://doi.org/10.1007/s11538-020-00844-6

5.1 Introduction

Zika virus disease or Zika fever is a mosquito-borne disease caused by the Zika virus (ZIKV). This *Flavivirus* was first identified in monkeys in Uganda in 1947 [36], then identified in humans in 1952 in Uganda and Tanzania [98]. The first cases of Zika infection in South America were detected in Brazil in spring 2015 and several further countries from the region reported Zika cases in the same year. Zika virus is chiefly spread in tropical and subtropical regions by the bite of infected female mosquitoes from the *Aedes* genus (by *Aedes aegypti* above all) [see, e.g., 87], the same species that is responsible for dengue, chikungunya and yellow fever transmission. Zika

virus is also spread via sexual contacts, principally from men to women [67]. Studies suggest that ZIKV might remain in male genital secretions for a longer period (up to six months) than in other bodily fluids, hence, in this way, a transmission of the disease is possible even several months after recovery [71]. Mothers can transmit the disease to their fetus during pregnancy or during delivery. This transmission might result in microcephaly (a medical condition with improper brain development and head size smaller than normal) and further congenital malformations. These are collectively denominated as congenital Zika syndrome. The incubation period of Zika virus disease is around 3–14 days. Most of the infected people do not show any symptoms or only mild ones including fever, rash, muscle and joint pain, conjunctivitis and headache, in general lasting for 2–7 days [108]. Figure 5.1 shows the possible methods of Zika transmission.

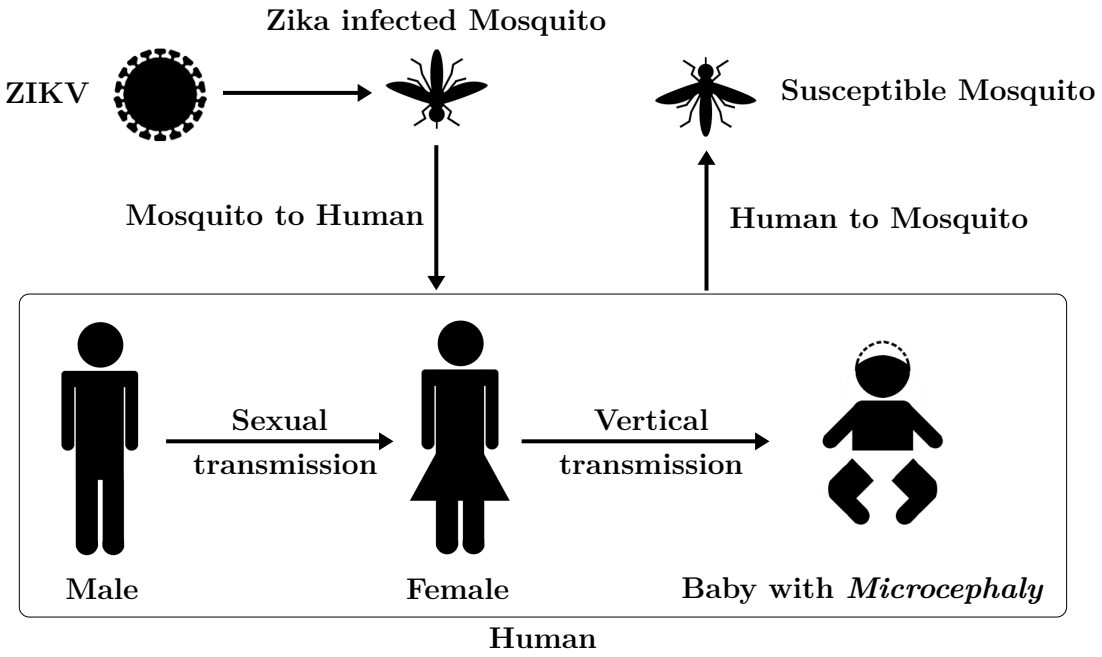

Figure 5.1: *Biology of Zika Virus (ZIKV). The figure shows modes of transmission and illustrates the critical pathological manifestation (microcephaly) associated with Zika infection.*

A number of sophisticated mathematical models for the spread of Zika virus disease have been previously developed, see e.g. [8, 20, 83]. [46] presented an autonomous compartmental model of Zika spread considering mosquito-borne and sexual transmission proposing an $SEIR$-type model for the human population with S, E and I compartments for vectors. They separated asymptomatically infected humans from those who had symptoms. [95] established a stage-structured model to study the effect of sexual transmission. [22] and [74] formulated compartmental models of

Zika transmission which considers the importance of weather and climate changes. In [35] a non-autonomous model was established considering most of the important features regarding Zika transmission: sexual and vector-borne transmission, the role of asymptomatically infected humans, the prolonged period of infectiousness after recovery and assessed the importance of the seasonality of weather. In [51], this model was extended to improve the estimation of microcephaly risk due to Zika. However, most models so far have not considered seasonality, although the number of mosquitoes – and thus the number of infections – is highly dependent on the periodically changing weather circumstances. Hence, in the present work, we establish and study a model with nine compartments describing the spread of Zika virus disease in a periodically changing environment: we set the mosquito birth and death rates as well as the biting rates to be periodic with one year as period, following the annual change of weather. The study of such models was initiated and further extended in [10, 11, 90, 103], where a general definition was introduced for the basic reproduction number of periodic compartmental models, more details can be found in Chapter 3. Since then, several papers have used the methods introduced in the above works, see e.g. [13, 62, 77, 102, 113].

Our aim is to determine the basic reproduction number for our newly established periodic model which serves as a threshold parameter regarding the persistence of the disease. In the analysis we follow the methods established in the above-cited papers, however, the techniques need to be adapted to the present model including both human–human and mosquito–human transmission. Further, it is an utmost important question to know what might lead to a regular recurrence of the epidemic. Several vector-borne diseases–malaria, dengue, chikungunya–tend to reappear from year to year, following the annual periodicity of weather. Up to now, unlike these diseases, after 1–3 major outbreaks in following years in various countries, Zika has not shown a periodic recurrence. Our hope is that our model might help to understand which changes in the parameters may contribute to such a phenomenon. This is especially important in the days of climate change, which might provoke important modifications in the mosquito-related parameters. Furthermore, other factors like mutations of the virus might also change sexual transmission rates as well.

The chapter is organized as follows. In Section 5.2, we introduce our periodic compartmental model for Zika fever transmission. In Section 5.3, we determine the basic reproduction number and study the local asymptotic stability of the disease-free periodic solution. In Section 5.4, we study the global stability of the disease-free equilibrium in the case of $\mathcal{R}_0 < 1$ the persistence of the disease in case of $\mathcal{R}_0 > 1$. We also calculate the basic reproduction number of the time-constant variant of the model. In Section 5.5, we present a case study for two South American countries. We estimate the parameter values for both countries and perform sensitivity analysis to determine the parameters which have the largest effect on the outcome of

the epidemic. We provide numerical simulations to study the possible effects of an alteration of various parameters to see what kind of changes might lead to an annual recurrence of the disease. The chapter is closed by a discussion.

5.2 Mathematical model

We divide the total human population into six compartments: susceptible $S_h(t)$, exposed $E_h(t)$, symptomatically infected $I_s(t)$, asymptomatically infected $I_a(t)$, convalescent $I_r(t)$, and recovered $R(t)$ at time $t > 0$, while the vector population is divided into three classes: susceptible $S_v(t)$, exposed $E_v(t)$ and infectious $I_v(t)$ individuals.

The total human population $N_h(t)$ and the total mosquito population $N_v(t)$ are given by:

$$N_h(t) = S_h(t) + E_h(t) + I_a(t) + I_s(t) + I_r(t) + R(t),$$

and

$$N_v(t) = S_v(t) + E_v(t) + I_v(t).$$

Our model takes the form

$$\begin{aligned}
S_h'(t) &= \mu_h - \beta \frac{\tau_e E_h(t) + \tau_a I_a(t) + I_s(t) + \tau_r I_r(t)}{N_h(t)} S_h(t) - \frac{\tilde{\alpha}_h(t)}{N_h(t)} I_v(t) S_h(t) \\
&\quad - d_h S_h(t), \\
E_h'(t) &= \beta \frac{\tau_e E_h(t) + \tau_a I_a(t) + I_s(t) + \tau_r I_r(t)}{N_h(t)} S_h(t) + \frac{\tilde{\alpha}_h(t)}{N_h(t)} I_v(t) S_h(t) \\
&\quad - \nu_h E_h(t) - d_h E_h(t), \\
I_a'(t) &= q\nu_h E_h(t) - \gamma_a I_a(t) - d_h I_a(t), \\
I_s'(t) &= (1-q)\nu_h E_h(t) - \gamma_s I_s(t) - d_h I_s(t), \\
I_r'(t) &= \gamma_a I_a(t) + \gamma_s I_s(t) - \gamma_r I_r(t) - d_h I_r(t), \\
R'(t) &= \gamma_r I_r(t) - d_h R(t), \\
S_v'(t) &= \tilde{\mu}_v(t) - \tilde{\alpha}_v(t) \frac{\eta_e E_h(t) + \eta_a I_a(t) + I_s(t)}{N_h(t)} S_v(t) - \tilde{d}_v(t) S_v(t), \\
E_v'(t) &= \tilde{\alpha}_v(t) \frac{\eta_e E_h(t) + \eta_a I_a(t) + I_s(t)}{N_h(t)} S_v(t) - \nu_v E_v(t) - \tilde{d}_v(t) E_v(t), \\
I_v'(t) &= \nu_v E_v(t) - \tilde{d}_v(t) I_v(t),
\end{aligned} \tag{5.1}$$

where $\tilde{\mu}_v(t)$, $\tilde{\alpha}_h(t)$, $\tilde{\alpha}_v(t)$ and $\tilde{d}_v(t)$ denote mosquito birth rate, transmission rate from an infectious mosquito to a susceptible human, the transmission rate from infected humans to susceptible mosquitoes and mosquito death rate, respectively. In our model we assumed $\tilde{\mu}_v(t)$, $\tilde{\alpha}_h(t)$, $\tilde{\alpha}_v(t)$ and $\tilde{d}_v(t)$ to be continuous, positive ω-

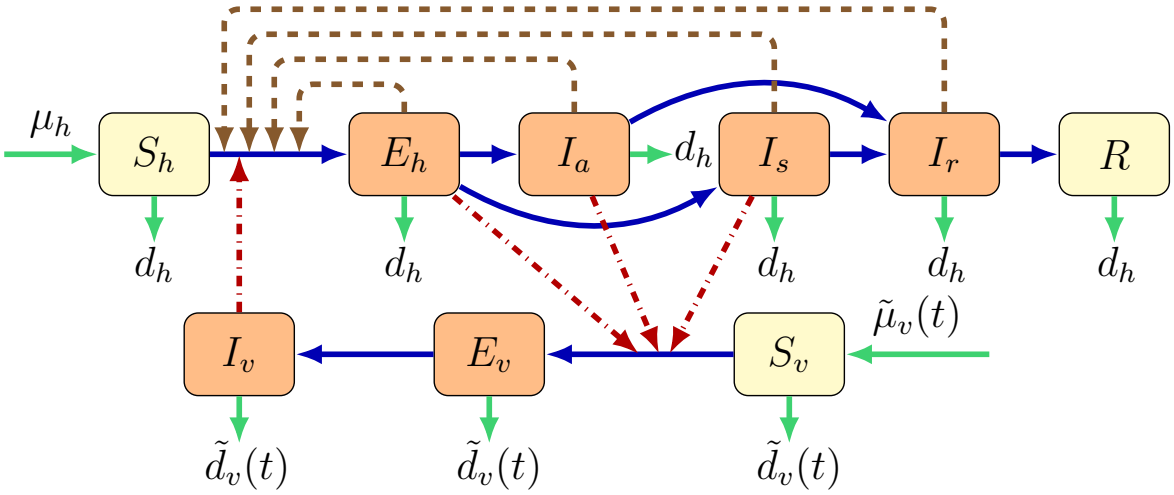

Figure 5.2: *Zika virus dynamics spread including vectorial and sexual transmission. Brown nodes are infectious and yellow nodes are non-infectious. Blue solid arrows show the progression of infection, while brown dashed arrows show direction of human-to-human transmission and red dash-dotted arrows show direction of transmission between humans and mosquitoes. Green arrows show birth and death.*

Table 5.1: *Description of parameters of model* (5.1).

Parameter	Description
μ_h	Human birth rate
d_h	Human death rate
β	Transmission rate from infected humans to susceptible humans
α_h	Baseline value of transmission rate from mosquitoes to humans
α_v	Baseline value of transmission rate from humans to mosquitoes
q	Proportion of asymptomatic infections
τ_e, τ_a, τ_r	Relative human-to-human transmissibility of (exposed, asymptomatic and convalescent) humans to symptomatic humans
η_a, η_e	Relative human-to-mosquito transmissibility of (asymptomatically infected and exposed) humans to symptomatically infected humans
γ_a	Progression rate from I_a to I_r
γ_s	Progression rate from I_s to I_r
γ_r	Recovery rate of convalescent humans
ν_h	Human incubation rate
ν_v	Mosquitoes incubation rate
μ_v	Baseline value of mosquito birth rate
d_v	Baseline value of mosquito death rate

periodic functions. An individual may progress from susceptible (S_h) to exposed (E_h) upon contracting the disease. An exposed individual moves either to the symp-

tomatically infected class I_s or to the asymptomatically infected class I_a, depending on whether that person shows symptoms or not. Infected people with or without symptoms move to the convalescent compartment I_r including those who have already recovered, but who can still transmit the disease via sexual contact. After the convalescent period, one moves to the recovered compartment R. Mosquitoes may progress from susceptible (S_v) to exposed (E_v) and then to infectious (I_v) class. The description of the model parameters is summarized in Table 5.1, while the transmission diagram of the model can be seen in Figure 5.2. We note that although the population is non-constant, the recruitment term in our model is given as μ_h instead of $\mu_h N_h$, as the countries studied in this work can be expected to be close to constant within a reasonable time interval. Doing so, we also followed among others the works [11, 62, 89, 102]. We emphasize that a similar model was established and studied in [35], which also included differentiation of the two sexes. However, no stability analysis was performed in that paper, only numerical results were presented.

We define $X_h = (S_h, E_h, I_a, I_s, I_r, R)$ and the functions $g_1, g_2, g_3 \in C(\mathbb{R}^6_+, \mathbb{R}_+)$ by

$$
\begin{aligned}
g_1(X_h) &= \begin{cases} 0, & \text{if } X_h = (0,0,0,0,0,0), \\ \frac{\tau_e E_h + \tau_a I_a + I_s + \tau_r I_r}{S_h + E_h + I_a + I_s + I_r + R} S_h, & \text{if } X_h \in \mathbb{R}^6_+ \setminus \{(0,0,0,0,0,0)\} \end{cases} \\
g_2(X_h) &= \begin{cases} 0, & \text{if } X_h = (0,0,0,0,0,0), \\ \frac{1}{S_h + E_h + I_a + I_s + I_r + R} S_h, & \text{if } X_h \in \mathbb{R}^6_+ \setminus \{(0,0,0,0,0,0)\} \end{cases} \\
g_3(X_h) &= \begin{cases} 0, & \text{if } X_h = (0,0,0,0,0,0), \\ \frac{\eta_e E_h(t) + \eta_a I_a(t) + I_s(t)}{S_h + E_h + I_a + I_s + I_r + R}, & \text{if } X_h \in \mathbb{R}^6_+ \setminus \{(0,0,0,0,0,0)\} \end{cases}
\end{aligned}
\tag{5.2}
$$

Clearly, $g_1(X_h)$, $g_2(X_h)$ and $g_3(X_h)$ are continuous on $\mathbb{R}^6_+$. Also, $g_1(X_h)$, $g_2(X_h)$ and $g_3(X_h)$ are globally Lipschitz on $\mathbb{R}^6_+$. By a change of variable $N_h = S_h + E_h + I_a + I_s + I_r + R$ and from (5.2), system (5.1) is equivalent to

$$
\begin{aligned}
S_h'(t) &= \mu_h - \beta g_1(S_h, E_h, I_a, I_s, I_r, N_h) - \tilde{\alpha}_h(t) g_2(S_h, E_h, I_a, I_s, I_r, N_h) I_v(t), \\
&\quad - d_h S_h(t), \\
E_h'(t) &= \beta g_1(S_h, E_h, I_a, I_s, I_r, N_h) + \tilde{\alpha}_h(t) g_2(S_h, E_h, I_a, I_s, I_r, N_h) I_v(t), \\
&\quad - \nu_h E_h(t) - d_h E_h(t), \\
I_a'(t) &= q\nu_h E_h(t) - \gamma_a I_a(t) - d_h I_a(t), \\
I_s'(t) &= (1-q)\nu_h E_h(t) - \gamma_s I_s(t) - d_h I_s(t), \\
I_r'(t) &= \gamma_a I_a(t) + \gamma_s I_s(t) - \gamma_r I_r(t) - d_h I_r(t), \\
N_h'(t) &= \mu_h - d_h N_h(t), \\
S_v'(t) &= \tilde{\mu}_v(t) - \tilde{\alpha}_v(t) g_3(S_h, E_h, I_a, I_s, I_r, N_h) S_v(t) - \tilde{d}_v(t) S_v(t), \\
E_v'(t) &= \tilde{\alpha}_v(t) g_3(S_h, E_h, I_a, I_s, I_r, N_h) S_v(t) - \nu_v E_v(t) - \tilde{d}_v(t) E_v(t),
\end{aligned}
\tag{5.3}
$$

$$I_v'(t) = \nu_v E_v(t) - \tilde{d}_v(t) I_v(t).$$

We now prove the existence of a disease-free periodic solution of (5.3). For the human subsystem of system (5.3) with initial condition

$$X^0 = (S_h(0), E_h(0), I_a(0), I_s(0), I_r(0), N_h(0), S_v(0), E_v(0), I_v(0)) \in \mathbb{R}_+^9,$$

we have the linear differential equation

$$\frac{\mathrm{d}N_h}{\mathrm{d}t} = \mu_h - d_h N_h(t). \tag{5.4}$$

One can easily see that (5.4) has a single equilibrium $N_h^* = \frac{\mu_h}{d_h}$, which is globally asymptotically stable and $N_h(t)$ is bounded.

To determine the disease-free periodic solution of (5.3), we study equation

$$S_v'(t) = \tilde{\mu}_v(t) - \tilde{d}_v(t) S_v(t) \tag{5.5}$$

with initial value $S_v(0) \in \mathbb{R}_+$. Equation (6.4) has a single positive ω-periodic solution $S_v^*(t)$, globally attractive in $\mathbb{R}_+$ and thus, system (5.3) has a single disease-free periodic solution $E_0 = \big(N_h^*, 0, 0, 0, 0, N_h^*, S_v^*(t), 0, 0\big)$.

To formulate our next result, we introduce the notations $h^L = \sup_{t\in[0,\omega)} h(t)$ and $h^M = \inf_{t\in[0,\omega)} h(t)$ for a continuous, positive ω-periodic function $h(t)$.

Lemma 5.1. *There exists an* $N_v^* = \frac{\tilde{\mu}_v^L}{\tilde{d}_v^L} > 0$ *such that every forward solution in*

$$X := \left\{ (S_h, E_h, I_a, I_s, I_r, N_h, S_v, E_v, I_v) \in \mathbb{R}_+^9 : \begin{array}{l} N_h \geqslant S_h + E_h + I_a + I_s + I_r, \\ N_v \geqslant S_v + E_v + I_v \end{array} \right\},$$

of (5.3) *eventually enters*

$$G_{N^*} := \{(S_h, E_h, I_a, I_s, I_r, N_h, S_v, E_v, I_v) \in X : N_h \leqslant N_h^*,\ S_v + E_v + I_v \leqslant N_v^* < \infty\}$$

and for each $N_v(t) \geqslant N_v^*$, G_N *is positively invariant for* (5.3). *Further, it holds that*

$$\lim_{t\to+\infty} (N_v(t) - S_v^*(t)) = 0$$

where $N_v(t) = S_v(t) + E_v(t) + I_v(t)$.

Proof. From (5.3), for the mosquito subsystem we have

$$N_v'(t) = \tilde{\mu}_v(t) - \tilde{d}_v(t) N_v(t) \leqslant \mu_v^L - d_v^M N_v(t) \leqslant 0 \quad \text{if } N_v(t) \geqslant N_v^*,$$

which implies that G_N, $N_v(t) \geqslant N_v^*$, is forward invariant and eventually, every posi-

tive orbit will enter G_{N^*}. For the second part of the proof, let us assume that

$$y(t) = N_v(t) - S_v^*(t),\ t \geqslant 0.$$

We then have that $y'(t) = -\tilde{d}_v(t)y(t)$, which implies that $\lim_{t\to+\infty} y(t) = 0$. Hence, the proof is complete. ■

5.3 Basic reproduction number and local stability

Following the technique introduced by [103], we show the local stability of the disease-free periodic equilibrium $E_0 = \left(N_h^*, 0, 0, 0, 0, N_h^*, S_v^*(t), 0, 0\right)$ of (5.3) for appropriate parameter values. We introduce the basic reproduction number $\mathcal{R}_0$ for system (5.3) with

$$\mathcal{F}(t,\mathcal{X}(t)) = \begin{bmatrix} \beta\frac{\tau_e E_h(t)+\tau_a I_a(t)+I_s(t)+\tau_r I_r(t)}{N_h(t)} S_h(t) + \frac{\tilde{\alpha}_h(t)}{N_h(t)} I_v(t) S_h(t) \\ 0 \\ 0 \\ 0 \\ \tilde{\alpha}_v(t)\frac{\eta_e E_h(t)+\eta_a I_a(t)+I_s(t)}{N_h(t)} S_v(t) \\ 0 \\ 0 \\ 0 \\ 0 \end{bmatrix},$$

$$\mathcal{V}^-(t,\mathcal{X}(t)) = \begin{bmatrix} (\nu_h + d_h)E_h(t) \\ (\gamma_a + d_h)I_a(t) \\ (\gamma_s + d_h)I_s(t) \\ (\gamma_r + d_h)I_r(t) \\ (\nu_v + \tilde{d}_v(t))E_v(t) \\ \tilde{d}_v(t)I_v(t) \\ L_1(t)S_h(t) + d_h S_h(t) \\ d_h N_h(t) \\ L_2(t)S_v(t) + \tilde{d}_v(t)S_v(t) \end{bmatrix},\ \mathcal{V}^+(t,\mathcal{X}(t)) = \begin{bmatrix} 0 \\ q\nu_h E_h(t) \\ (1-q)\nu_h E_h(t) \\ \gamma_a I_a(t) + \gamma_s I_s(t) \\ 0 \\ \nu_v E_v(t) \\ \mu_h \\ \mu_h \\ \tilde{\mu}_v(t) \end{bmatrix}, \tag{5.6}$$

where $L_1(t) = \frac{\tilde{\alpha}_h(t)}{N_h(t)} I_v(t) + \beta\frac{\tau_e E_h(t)+\tau_a I_a(t)+I_s(t)+\tau_r I_r(t)}{N_h(t)}$, $L_2(t) = \tilde{\alpha}_v(t)\frac{\eta_e E_h(t)+\eta_a I_a(t)+I_s(t)}{N_h(t)}$ and $\mathcal{X} = (E_h, I_a, I_s, I_r, E_v, I_v, S_h, N_h, S_v)^T$.

Now, let us check the conditions (A1)–(A7) in Chapter 3. From the above, equation (5.1) is equivalent to

$$\mathcal{X}'(t) = \mathcal{F}(t,\mathcal{X}(t)) - \mathcal{V}(t,\mathcal{X}(t)) \tag{5.7}$$

where $\mathcal{V}(t,\mathcal{X}(t)=\mathcal{V}^{-}(t,\mathcal{X}(t)-\mathcal{V}^{+}(t,\mathcal{X}(t)$. It is straightforward to see that the conditions (A1)–(A5) are satisfied.

We know that (5.7) has the disease-free periodic solution

$$\mathcal{X}^{*}(t)=(0,0,0,0,0,0,N_h^{*},N_h^{*},S_v^{*}(t))\,.$$

Now, we define $f(t,\mathcal{X}(t))=\mathcal{F}(t,\mathcal{X}(t))-\mathcal{V}(t,\mathcal{X}(t))$ and $M(t)=\left(\frac{\partial f_i(t,\mathcal{X}^{*}(t))}{\partial\mathcal{X}_j}\right)_{7\leqslant i,j\leqslant 9}$ where $f_i(t,\mathcal{X}(t))$ and $\mathcal{X}_i$ is the ith component of $f(t,\mathcal{X}(t))$ and $\mathcal{X}$, respectively. Clearly, from (5.6), we obtain

$$M(t)=\begin{bmatrix}-d_h & 0 & 0\\ 0 & -d_h & 0\\ 0 & 0 & -\tilde{d}_v(t)\end{bmatrix}.$$

Let $\Phi_M(t)$ and $\rho(\Phi_M(t))$ be the monodromy matrix of the linear ω-periodic system $\frac{d}{dt}z=M(t)z$ and the spectral radius of $\Phi_M(\omega)$, respectively. Hence, $\rho(\Phi_M(t))<1$, which implies that $\mathcal{X}^{*}(t)$ is linearly asymptotically stable in the disease-free subspace $\mathcal{X}_s=(0,0,0,0,0,0,S_h,N_h,S_v)\in\mathbb{R}_{+}^{9}$. Thus, the condition (A6) also holds.

Let us introduce $F(t)$ and $V(t)$ defined by

$$F(t)=\left(\frac{\partial\mathcal{F}_i(t,\mathcal{X}^{*}(t))}{\partial\mathcal{X}_j}\right)_{1\leqslant i,j\leqslant 6},\qquad V(t)=\left(\frac{\partial\mathcal{V}_i(t,\mathcal{X}^{*}(t))}{\partial\mathcal{X}_j}\right)_{1\leqslant i,j\leqslant 6}$$

where $\mathcal{F}_i(t,\mathcal{X}(t))$ and $\mathcal{V}_i(t,\mathcal{X}(t)$ is the i-th component of $\mathcal{F}(t,\mathcal{X}(t))$ and $\mathcal{V}(t,\mathcal{X}(t)$, respectively. Then from (5.6), we have

$$F(t)=\begin{bmatrix}\beta\tau_e & \beta\tau_a & \beta & \beta\tau_r & 0 & \tilde{\alpha}_h(t)\\ 0 & 0 & 0 & 0 & 0 & 0\\ 0 & 0 & 0 & 0 & 0 & 0\\ 0 & 0 & 0 & 0 & 0 & 0\\ \frac{\eta_e\tilde{\alpha}_v(t)}{N_h^{*}}S_v^{*}(t) & \frac{\eta_a\tilde{\alpha}_v(t)}{N_h^{*}}S_v^{*}(t) & \frac{\tilde{\alpha}_v(t)}{N_h^{*}}S_v^{*}(t) & 0 & 0 & 0\\ 0 & 0 & 0 & 0 & 0 & 0\end{bmatrix},\tag{5.8}$$

$$V(t)=\begin{bmatrix}\nu_h+d_h & 0 & 0 & 0 & 0 & 0\\ -q\nu_h & \gamma_a+d_h & 0 & 0 & 0 & 0\\ -(1-q)\nu_h & 0 & \gamma_s+d_h & 0 & 0 & 0\\ 0 & -\gamma_a & -\gamma_s & \gamma_r+d_h & 0 & 0\\ 0 & 0 & 0 & 0 & \nu_v+\tilde{d}_v(t) & 0\\ 0 & 0 & 0 & 0 & -\nu_v & \tilde{d}_v(t)\end{bmatrix},\tag{5.9}$$

Furthermore, $F(t)$ is non-negative, and $-V(t)$ is cooperative. Also $F(t)-V(t)$ is

irreducible for all t. It is straightforward to see that the conditions (A1)–(A6) are satisfied, and $\mathcal{X}^*(t)$ is linearly asymptotically stable in the disease-free subspace

$$\mathcal{X}_s = (0, 0, 0, 0, 0, 0, S_h, N_h, S_v) \in \mathbb{R}^9_+.$$

Assume $Y(t, s), t \geqslant s$ is the evolution operator of the linear ω-periodic system

$$\frac{dy}{dt} = -V(t)y. \tag{5.10}$$

That is, for each $s \in \mathbb{R}$, the 6×6 matrix $Y(t, s)$ satisfies

$$\frac{d}{dt}Y(t, s) = -V(t)Y(t, s), \qquad \forall t \geqslant s,\ Y(s, s) = I,$$

where I is the 6×6 identity matrix. Thus, the monodromy matrix $\Phi_{-V}(t)$ of (5.10) is equal to $Y(t, 0),\ t \geqslant 0$. Therefore, the condition (A7) holds.

Following the setting in Section 3.2, the basic reproduction number of (5.1) is defined as $\mathcal{R}_0 := \rho(L)$, i.e. the spectral radius of the next infection operator L.

From the above discussion and using Theorem B, the disease-free periodic solution E_0 is locally asymptotically stable if $\mathcal{R}_0 < 1$, and unstable if $\mathcal{R}_0 > 1$.

5.3.1 Derivation of the basic reproduction number of the autonomous model

To calculate the basic reproduction ratio $\mathcal{R}_0^A$ of the autonomous model obtained from (5.3) by setting the time-dependent parameters (mosquito birth ($\tilde{\mu}_v(t) \equiv \mu_v$) and death rates ($\tilde{d}_v(t) \equiv d_v$) and biting rates ($\tilde{\alpha}_h(t) \equiv \alpha_h$ and $\tilde{\alpha}_v(t) \equiv \alpha_v$) to constant, we follow the general approach established by [37].

Substituting the values in the disease-free equilibrium $S_v^* = \frac{\mu_v}{d_v}$ in equations (5.8) and (5.9), for all $t \geqslant 0$, we obtain the Jacobian F given by

$$F = \begin{bmatrix} \beta\tau_e & \beta\tau_a & \beta & \beta\tau_r & 0 & \alpha_h \\ 0 & 0 & 0 & 0 & 0 & 0 \\ 0 & 0 & 0 & 0 & 0 & 0 \\ 0 & 0 & 0 & 0 & 0 & 0 \\ \eta_e\alpha_v\dfrac{\mu_v d_h}{\mu_h d_v} & \eta_a\alpha_v\dfrac{\mu_v d_h}{\mu_h d_v} & \alpha_v\dfrac{\mu_v d_h}{\mu_h d_v} & 0 & 0 & 0 \\ 0 & 0 & 0 & 0 & 0 & 0 \end{bmatrix}$$

and the Jacobian V given by

$$V = \begin{bmatrix} \nu_h + d_h & 0 & 0 & 0 & 0 & 0 \\ -q\nu_h & \gamma_a + d_h & 0 & 0 & 0 & 0 \\ -(1-q)\nu_h & 0 & \gamma_s + d_h & 0 & 0 & 0 \\ 0 & -\gamma_a & -\gamma_s & \gamma_r + d_h & 0 & 0 \\ 0 & 0 & 0 & 0 & \nu_v + d_v & 0 \\ 0 & 0 & 0 & 0 & -\nu_v & d_v \end{bmatrix},$$

therefore the characteristic polynomial of the next generation matrix FV^{-1} is

$$\lambda^4 \left(\lambda^2 - \mathcal{R}_{hh}\lambda - \mathcal{R}_{hv}\mathcal{R}_{vh}\right) = 0, \tag{5.11}$$

where

$$\mathcal{R}_{hh} = \frac{\beta}{d_h + \nu_h}\left(\tau_e + \frac{q\tau_a\nu_h}{\gamma_a + d_h} + \frac{(1-q)\nu_h}{\gamma_s + d_h} + \frac{\tau_r\nu_h(\gamma_s(\gamma_a + d_h) + q(\gamma_a - \gamma_s)d_h)}{(\gamma_a + d_h)(\gamma_r + d_h)(\gamma_s + d_h)}\right),$$
$$\mathcal{R}_{hv} = \frac{\alpha_v d_h \mu_v}{d_v \mu_h (d_h + \nu_h)}\left(\eta_e + \frac{q\eta_a\nu_h}{\gamma_a + d_h} + \frac{(1-q)\nu_h}{\gamma_s + d_h}\right), \qquad \mathcal{R}_{vh} = \frac{\alpha_h\nu_v}{d_v(d_v + \nu_v)}.$$

The characteristic polynomial therefore is the quadratic equation

$$\lambda^2 - \mathcal{R}_{hh}\lambda - \mathcal{R}_{hv}\mathcal{R}_{vh} = 0. \tag{5.12}$$

According to [37], the basic reproduction number is the spectral radius of FV^{-1}. Thus, the basic reproduction number corresponds to the dominant eigenvalue given by the root of the quadratic equation (5.12)

$$\mathcal{R}_0^A = \frac{\mathcal{R}_{hh} + \sqrt{\mathcal{R}_{hh}^2 + 4\mathcal{R}_{hv}R_{vh}}}{2}, \tag{5.13}$$

where $\mathcal{R}_{hh}$ and $\mathcal{R}_v = \mathcal{R}_{hv}\mathcal{R}_{vh}$ are the basic reproduction numbers corresponding to sexual transmission and vector-borne transmission, respectively. From (5.13) we found that $\mathcal{R}_{hh} + \mathcal{R}_v < 1$ is the necessary and sufficient condition for $\mathcal{R}_0^A < 1$.

5.4 Threshold dynamics

Here we study the global stability of the disease-free equilibrium of model (5.3) and the persistence of the infectious compartments. We use the general theory for the extinction or persistence of infectious given by [90] to show that if the basic reproduction ratio $\mathcal{R}_0$ is less than 1, then the unique disease-free equilibrium $\mathcal{X}^*(t) = \left(0, 0, 0, 0, 0, 0, N_h^*, N_h^*, S_v^*(t)\right)$ is globally asymptotically stable (G.A.S.) and the disease dies out, while if the basic reproduction ratio $\mathcal{R}_0$ is larger than 1, the disease persists. Moreover, we follow [62, 77, 89, 113] to prove the existence of a

positive periodic solution of (5.3) if $\mathcal{R}_0 > 1$.

5.4.1 Global stability of the disease-free equilibrium

In this subsection, we use the general method given by [90] to show that the disease-free equilibrium is G.A.S. if $\mathcal{R}_0 < 1$.

Theorem 5.1. *If $\mathcal{R}_0 < 1$, then the disease-free periodic solution $\mathcal{X}^*(t)$ of system (4.7) is globally asymptotically stable and if $\mathcal{R}_0 > 1$, then it is unstable.*

Proof. By Theorem B, we know that $\mathcal{X}^*(t)$ is unstable if $\mathcal{R}_0 > 1$ and if $\mathcal{R}_0 < 1$, then $\mathcal{X}^*(t)$ is locally asymptotically stable. According to the above discussion in Section 5.3, the conditions (A1) to (A7) in Chapter 3 are satisfied. Moreover $\mathcal{X}^*(t)$ is the unique periodic solution in the set of the disease-free states $\mathcal{X}_s$.

Clearly, $S(t) \leqslant N_h(t)$, for all $t \geqslant 0$. From Lemma 5.1, for any $\epsilon > 0$, there exists $t(\epsilon) > 0$ such that $S_v(t) \leqslant N_v(t) \leqslant S_v^*(t) + \epsilon$ for all $t \geqslant t(\epsilon)$. Substituting into system (5.3), we obtain

$$
\begin{aligned}
E_h'(t) &\leqslant \beta\left(\tau_e E_h(t) + \tau_a I_a(t) + I_s(t) + \tau_r I_r(t)\right) + \tilde{\alpha}_h(t) I_v(t) - (\nu_h + d_h) E_h(t),\\
I_a'(t) &\leqslant q\nu_h E_h(t) - \gamma_a I_a(t) - d_h I_a(t),\\
I_s'(t) &\leqslant (1-q)\nu_h E_h(t) - \gamma_s I_s(t) - d_h I_s(t),\\
I_r'(t) &\leqslant \gamma_a I_a(t) + \gamma_s I_s(t) - \gamma_r I_r(t) - d_h I_r(t),\\
E_v'(t) &\leqslant \tilde{\alpha}_v(t)\frac{\eta_e E_h(t) + \eta_a I_a(t) + I_s(t)}{N_h^*}\left(S_v^*(t) + \epsilon\right) - (\nu_v + \tilde{d}_v(t)) E_v(t),\\
I_v'(t) &\leqslant \nu_v E_v(t) - \tilde{d}_v(t) I_v(t),
\end{aligned}
$$

for all $t \geqslant t(\epsilon)$.

Set $\mu(\epsilon) := \min\{S_v^*(\cdot)/\left(S_v^*(\cdot) + \epsilon\right)\}$. Then we have the following system:

$$
\frac{\mathrm{d}\tilde{U}(t)}{\mathrm{d}t} \leqslant \left(\frac{F(t)}{\mu(\epsilon)} - V(t)\right)\tilde{U}(t), \quad \forall t \geqslant t(\epsilon), \tag{5.14}
$$

where $\tilde{U}(t) = \left(\tilde{E}_h(t), \tilde{I}_a(t), \tilde{I}_s(t), \tilde{I}_r(t), \tilde{E}_v(t), \tilde{I}_v(t)\right)$. Then $\tilde{U}(t) \to 0$ as $t \to \infty$ and the disease dies out.

By applying the first part of Theorem D, we conclude that the disease-free periodic solution $\mathcal{X}^*(t)$ is G.A.S. since it is G.A.S. in $\mathcal{X}_s$. ■

5.4.2 Persistence of the infective compartments

In this subsection, we will show that the infectives are persistent if $\mathcal{R}_0 > 1$, by using the general method given by [90].

Theorem 5.2. *If $\mathcal{R}_0 > 1$ then system (5.3) is persistent with respect to E_h, I_a, I_s, I_r, E_v and I_v.*

Proof. Persistence of $E_h + I_a + I_s$ implies persistence of E_h, I_a and I_s, and hence, persistence of I_r, E_v and I_v. If there exists $\epsilon > 0$ such that

$$\lim_{t\to+\infty} \inf \left(E_h + I_a + I_s\right) \geqslant \epsilon,$$

then $E_h \geqslant \frac{\epsilon}{3} - I_a - I_s$ for large t. Thus, from system (5.3), we obtain

$$\begin{aligned} I_a' &\geqslant q\nu_h \frac{\epsilon}{3} - (q\nu_h + \gamma_a + d_h)I_a - q\nu_h I_s, \\ I_s' &\geqslant (1-q)\nu_h \frac{\epsilon}{3} - ((1-q)\nu_h + \gamma_s + d_h)I_s - (1-q)\nu_h I_a. \end{aligned} \tag{5.15}$$

Thus, we have

$$\begin{aligned} I_a(t) &\geqslant \frac{\epsilon}{3} \frac{q\nu_h}{q\nu_h + \gamma_a + d_h} =: \kappa_a(\epsilon), \\ I_s(t) &\geqslant \frac{\epsilon}{3} \frac{(1-q)\nu_h}{(1-q)\nu_h + \gamma_s + d_h} =: \kappa_s(\epsilon). \end{aligned} \tag{5.16}$$

By introducing the inequality (5.16) into the fifth equation of system (5.3), we get

$$I_r' \geqslant \gamma_a \kappa_a(\epsilon) + \gamma_s \kappa_s(\epsilon) - (\gamma_r + d_h)I_r, \tag{5.17}$$

and hence,

$$I_r(t) \geqslant \frac{\gamma_a \kappa_a(\epsilon) + \gamma_s \kappa_s(\epsilon)}{\gamma_r + d_h} =: \kappa_r(\epsilon). \tag{5.18}$$

Consider $E_h \leqslant \epsilon$, $I_a \leqslant \epsilon$, $I_s \leqslant \epsilon$, $I_r \leqslant \epsilon$, $R \leqslant \epsilon$, $E_v \leqslant \epsilon$ and $I_v \leqslant \epsilon$ for all $t \geqslant t_0$. There exists $t_1 \geqslant t_0$ such that $|N_h(t) - S_h^*| \leqslant \epsilon$ and $|N_v(t) - S_v^*(t)| \leqslant \epsilon$ for all $t \geqslant t_1$. Therefore, $S_h(t) = N_h(t) - E_h(t) - I_a(t) - I_s(t) - I_r(t) - R(t) \geqslant S_h^* - 5\epsilon$ and $S_v(t) = N_v(t) - E_v(t) - I_v(t) \geqslant S_v^*(t) - 3\epsilon$ for all $t \geqslant t_1$. From the equation for E_v' of system (5.3), we have

$$E_v' \geqslant \tilde{\alpha}_v(t) \frac{\eta_e \frac{\epsilon}{3} + (\eta_a - \eta_e)I_a + (1-\eta_e)I_s}{N_h^*} (S_v^*(t) - 3\epsilon) - (\nu_v + \tilde{d}_v(t))E_v, \tag{5.19}$$

By [90, Lemma 1], we obtain that

$$E_v(t) \geqslant \frac{\tilde{\alpha}_v^M \left(\eta_e \frac{\epsilon}{3} + (\eta_a - \eta_e)\kappa_a(\epsilon) + (1-\eta_e)\kappa_s(\epsilon)\right)(S^{*M}_v(t) - 3\epsilon)}{2N_h^*(\nu_v + \tilde{d}_v^L)} =: \kappa_e(\epsilon). \tag{5.20}$$

Substituting the inequality (5.20) into the equation for I_v' of system (5.3), we obtain

$$I_v' \geqslant \nu_v \kappa_e(\epsilon) - \tilde{d}_v(t) I_v,$$

and again by [90, Lemma 1], we have

$$I_v(t) \geqslant \frac{\nu_v \kappa_e(\epsilon)}{2\tilde{d}_v^L} =: K_v(\epsilon).$$

Set $\lambda(\epsilon) := \max\{1/\big(1 - \frac{5\epsilon}{N_h^*}\big), \max\big(S_v^*(\cdot)/(S_v^*(\cdot) - 3\epsilon\big)\}$. From the equations of system (5.3), for sufficiently large $t \geqslant t_1$, we obtain

$$\begin{aligned}
E_h'(t) &\geqslant \beta\big(\tau_e E_h(t) + \tau_a I_a(t) + I_s(t) + \tau_r I_r(t) + \tilde{\alpha}_h(t) I_v(t)\big)\left(1 - \frac{5\epsilon}{N_h^*}\right) - (\nu_h + d_h)E_h(t)\\
&\geqslant \beta\big(\tau_e E_h(t) + \tau_a I_a(t) + I_s(t) + \tau_r I_r(t) + \tilde{\alpha}_h(t) I_v(t)\big)\frac{1}{\lambda(\epsilon)} - (\nu_h + d_h)E_h(t),\\
I_a'(t) &\geqslant q\nu_h E_h(t) - \gamma_a I_a(t) - d_h I_a(t),\\
I_s'(t) &\geqslant (1-q)\nu_h E_h(t) - \gamma_s I_s(t) - d_h I_s(t),\\
I_r'(t) &\geqslant \gamma_a I_a(t) + \gamma_s I_s(t) - \gamma_r I_r(t) - d_h I_r(t),\\
E_v'(t) &\geqslant \tilde{\alpha}_v(t)\big(\eta_e E_h(t) + \eta_a I_a(t) + I_s(t)\big)\left(\frac{S_v^*(t)}{N_h^*} - \frac{3\epsilon}{N_h^*}\right) - (\nu_v + \tilde{d}_v(t))E_v(t)\\
&\geqslant \tilde{\alpha}_v(t)\big(\eta_e E_h(t) + \eta_a I_a(t) + I_s(t)\big)\frac{S_v^*(t)}{\lambda(\epsilon)} - (\nu_v + \tilde{d}_v(t))E_v(t),\\
I_v'(t) &\geqslant \nu_v E_v(t) - \tilde{d}_v(t) I_v(t).
\end{aligned}$$

From Lemma 5.1, it is clear that condition (A8) is satisfied. Therefore, the assumptions of Theorem G are satisfied and system (5.3) is persistent with respect to E_h, I_a, I_s, I_r, E_v, and I_v. ■

5.4.3 Existence of positive periodic solutions

Define

$$\begin{aligned}
X &:= \left\{(S_h, E_h, I_a, I_s, I_r, N_h, S_v, E_v, I_v) \in \mathbb{R}_+^9\right\},\\
X_0 &:= \left\{(S_h, E_h, I_a, I_s, I_r, N_h, S_v, E_v, I_v) \in \mathbb{R}_+ \times \mathrm{Int}(\mathbb{R}_+^4) \times \mathbb{R}_+^2 \times \mathrm{Int}(\mathbb{R}_+^2)\right\}
\end{aligned}$$

and

$$\partial X_0 := X \setminus X_0 = \left\{(S_h, E_h, I_a, I_s, I_r, N_h, S_v, E_v, I_v) : E_h I_a I_s I_r E_v I_v = 0\right\}.$$

Let $P\colon \mathbb{R}_+^9 \to \mathbb{R}_+^9$ be the Poincaré map associated with (5.3), that is,

$$P(x^0) = u(\omega, x^0), \quad \text{for } x^0 \in \mathbb{R}_+^9,$$

where $u(t, x^0)$ is the unique solution of (5.3) with $u(0, x^0) = x^0$. It is easy to see that

$$P^m(x^0) = u(m\omega, x^0), \qquad \forall m \geqslant 0.$$

Let $d(x,y)$ denote Euclidean distance in $\mathbb{R}^9$. The following lemma is analogous with [62, Lemma 3.1].

Lemma 5.2. *If $\mathcal{R}_0 > 1$, then there exists a $\sigma^* > 0$ such that for any $x^0 \in X_0$, with $\|x^0 - E_0\| \leqslant \sigma^*$ we have*

$$\limsup_{m\to\infty} d\left(P^m(x^0), E_0\right) \geqslant \sigma^*.$$

Proof. By Theorem B, we have that $\rho(\Phi_{F-V}(\omega)) > 1$ if $\mathcal{R}_0 > 1$. Then, we can choose $\eta > 0$ small enough such that $\rho(\Phi_{F-V-M_\eta}(\omega)) > 1$ where

$$M_\eta(t) = \begin{bmatrix} 0 & 0 & 0 & 0 & 0 & 0 \\ 0 & 0 & 0 & 0 & 0 & 0 \\ 0 & 0 & 0 & 0 & 0 & 0 \\ 0 & 0 & 0 & 0 & 0 & 0 \\ \frac{2\eta}{N_h^*+\eta}\eta_e\tilde{\alpha}_v(t) & \frac{2\eta}{N_h^*+\eta}\eta_a\tilde{\alpha}_v(t) & \frac{2\eta}{N_h^*+\eta}\tilde{\alpha}_v(t) & 0 & 0 & 0 \\ 0 & 0 & 0 & 0 & 0 & 0 \end{bmatrix}.$$

The equation $\frac{\mathrm{d}S_h}{\mathrm{d}t} = \mu_h - d_h S_h$ has a unique equilibrium $S_h^* = N_h^*$ which is a global attractor in $\mathbb{R}_+$.

The perturbed system

$$\frac{\mathrm{d}\hat{S}_h(t)}{\mathrm{d}t} = (\mu_h - \beta\sigma_1 - \tilde{\alpha}_h(t)\sigma_2) - d_h\hat{S}_h(t), \tag{5.21}$$

has a unique solution

$$\hat{S}_h(t,\sigma_1,\sigma_2) = e^{-d_h t}\left(\hat{S}_h(0,\sigma_1,\sigma_2) + \int_0^t e^{-d_h s}\left(\mu_h - \beta\sigma_1 - \alpha_h(s)\sigma_2\right)\,ds\right),$$

through any initial value $\hat{S}_h(0,\sigma_1,\sigma_2)$, and it has a unique periodic solution

$$\hat{S}_h^*(t,\sigma_1,\sigma_2) = e^{-d_h t}\left(\hat{S}_h^*(0,\sigma_1,\sigma_2) + \int_0^t e^{-d_h s}\left(\mu_h - \beta\sigma_1 - \alpha_h(s)\sigma_2\right)\,ds\right),$$

where

$$\hat{S}_h^*(0,\sigma_1,\sigma_2) = \frac{\int_0^\omega e^{-d_h s}\left(\mu_h - \beta\sigma_1 - \alpha_h(s)\sigma_2\right)\,ds}{e^{-d_h\omega} - 1}.$$

It is clear that $|\hat{S}_h(t,\sigma_1,\sigma_2) - \hat{S}_h^*(t,\sigma_1,\sigma_2)| \to 0$ as $t \to \infty$, and from this we obtain that $\hat{S}_h^*(t,\sigma_1,\sigma_2)$ is globally attractive on $\mathbb{R}_+$. One can easily see that $\hat{S}_h^*(0,\sigma_1,\sigma_2)$ is continuous in σ_1 and σ_2. As the solution $\hat{S}_h^*(t,\sigma_1,\sigma_2)$ depends continuously on the initial condition and the parameter values, we obtain that $\hat{S}_h^*(t,\sigma_1,\sigma_2) > S_h^* - \eta$ holds for sufficiently small σ_1 and small σ_2, and all $t \in [0,\omega]$. By the periodicity of $\hat{S}_h^*(t,\sigma_1,\sigma_2)$ and constant $S_h^* - \eta$, we see that $\hat{S}_h^*(t,\sigma_1,\sigma_2) > S_h^* - \eta$ holds for sufficiently small σ_1 and small σ_2, and all $t \geqslant 0$.

Now, let us consider the following perturbed equation

$$\frac{\mathrm{d}\hat{S}_v(t)}{\mathrm{d}t} = \tilde{\mu}_v(t) - (\tilde{\alpha}_v(t)\sigma_3 + \tilde{d}_v(t))\hat{S}_v(t). \tag{5.22}$$

The Poincaré map associated with (5.22) has a unique positive fixed point $\hat{S}_v^*(0,\sigma_3)$ which is globally attractive in $\mathbb{R}_+$. Applying the implicit function theorem, we get that $\hat{S}_v^*(0,\sigma_3)$ is continuous in σ_3. Thus, we further fix $\sigma_3 > 0$ small enough such that

$$\hat{S}_v^*(t,\sigma_3) > S_v^* - \eta.$$

By the continuous dependence of the solutions on the parameters and initial values and by choosing $\sigma := \min\{\sigma_1,\sigma_2,\sigma_3\}$, there exists a $\sigma^* > 0$ such that for all $x^0 \in X_0$ with $\|x^0 - E_0\| \leqslant \sigma^*$, it holds that

$$\|u(t,x^0) - u(t,E_0)\| \leqslant \sigma, \text{ for } 0 \leqslant t \leqslant \omega.$$

We further claim that

$$\limsup_{m\to\infty} d\left(P^m(x^0)\right) \geqslant \sigma^*. \tag{5.23}$$

Suppose, by contradiction, that (5.23) does not hold. Then we have

$$\limsup_{m\to\infty} d\left(P^m(x^0), E_0\right) < \sigma^*,$$

for some $x^0 \in X_0$. Without loss of generality, we assume that $d\left(P^m(x^0), E_0\right) < \sigma^*$, for all $m \geq 0$. Then, from the above discussion, we have that

$$\|u(t,P^m(x^0)) - u(t,E_0)\| < \sigma, \ \forall m \geq 0, \ t \in [0,\omega].$$

For any $t \geqslant 0$, let $t = m\omega + t_1$, where $t_1 \in [0,\omega)$ and $m = [\frac{t}{\omega}]$, which is the greatest integer less than or equal to $\frac{t}{\omega}$. Then, we get

$$\|u(t,x^0) - u(t,E_0)\| = \|u(t_1,P^m(x^0)) - u(t_1,E_0)\| < \sigma, \ \forall t \geqslant 0.$$

Set

$$(S_h(t),E_h(t),I_a(t),I_s(t),I_r(t),N_h(t),S_v(t),E_v(t),I_v(t)) = u(t,x^0).$$

It follows that $E_h(t) < \sigma$, $I_a(t) < \sigma$, $I_s(t) < \sigma$, $I_r(t) < \sigma$, $I_v(t) < \sigma$, for all $t \geqslant 0$ and from system (5.3), we have

$$\frac{dS_h(t)}{dt} \geqslant (\mu_h - \beta\sigma - \tilde{\alpha}_h(t)\sigma) - d_h S_h(t),$$

$$\frac{dS_v(t)}{dt} \geqslant \tilde{\mu}_v(t) - (\tilde{\alpha}_v(t)\sigma + \tilde{d}_v(t))S_v(t).$$

As the periodic solution $\hat{S}_h^*(t,\sigma)$ of equation (5.21) is globally attractive on $\mathbb{R}_+$ and $\hat{S}_h^*(t,\sigma) > S_h^* - \eta$, we have

$$S_h(t) \geqslant S_h^* - \eta,$$

for t large enough. Also, the fixed point $\hat{S}_v^*(t,\sigma)$ of the Poincaré map corresponding to (5.22) is globally attractive and $\hat{S}_v^*(t,\sigma) > S_v^*(t) - \eta$, there exists a t large enough such that

$$S_v(t,\sigma) > S_v^*(t) - \eta.$$

From the equations of system (5.3), for sufficiently large t, we obtain

$$\begin{aligned}
E_h'(t) &\geqslant \beta\left(\tau_e E_h(t) + \tau_a I_a(t) + I_s(t) + \tau_r I_r(t) + \tilde{\alpha}_h(t) I_v(t)\right)\left(1 - \frac{2\eta}{N_h^* + \eta}\right) - \nu_h E_h(t) \\
&\quad - d_h E_h(t), \\
I_a'(t) &= q\nu_h E_h(t) - \gamma_a I_a(t) - d_h I_a(t), \\
I_s'(t) &= (1-q)\nu_h E_h(t) - \gamma_s I_s(t) - d_h I_s(t), \\
I_r'(t) &= \gamma_a I_a(t) + \gamma_s I_s(t) - \gamma_r I_r(t) - d_h I_r(t), \\
E_v'(t) &\geqslant \tilde{\alpha}_v(t)\left(\eta_e E_h(t) + \eta_a I_a(t) + I_s(t)\right)\left(\frac{S_v^*(t)}{N_h^*} - \frac{2\eta}{N_h^* + \eta}\right) - (\nu_v + \tilde{d}_v(t)) E_v(t), \\
I_v'(t) &= \nu_v E_v(t) - \tilde{d}_v(t) I_v(t).
\end{aligned}$$

Next we consider the system

$$\begin{aligned}
\frac{\mathrm{d}\hat{E}_h(t)}{\mathrm{d}t} &= \beta\left(\tau_e \hat{E}_h(t) + \tau_a \hat{I}_a(t) + \hat{I}_s(t) + \tau_r \hat{I}_r(t) + \tilde{\alpha}_h(t)\hat{I}_v(t)\right)\left(1 - \frac{2\eta}{N_h^* + \eta}\right) \\
&\quad - \nu_h \hat{E}_h(t) - d_h \hat{E}_h(t), \\
\frac{\mathrm{d}\hat{I}_a(t)}{\mathrm{d}t} &= q\nu_h \hat{E}_h(t) - \gamma_a \hat{I}_a(t) - d_h \hat{I}_a(t), \\
\frac{\mathrm{d}\hat{I}_s(t)}{\mathrm{d}t} &= (1-q)\nu_h \hat{E}_h(t) - \gamma_s \hat{I}_s(t) - d_h \hat{I}_s(t), \\
\frac{\mathrm{d}\hat{I}_r(t)}{\mathrm{d}t} &= \gamma_a \hat{I}_a(t) + \gamma_s \hat{I}_s(t) - \gamma_r \hat{I}_r(t) - d_h \hat{I}_r(t), \\
\frac{\mathrm{d}\hat{E}_v(t)}{\mathrm{d}t} &= \tilde{\alpha}_v(t)(\eta_e \hat{E}_h(t) + \eta_a \hat{I}_a(t) + \hat{I}_s(t))\left(\frac{S_v^*(t)}{N_h^*} - \frac{2\eta}{N_h^* + \eta}\right) - \nu_v \hat{E}_v(t) \\
&\quad - \tilde{d}_v(t)\hat{E}_v(t), \\
\frac{\mathrm{d}\hat{I}_v(t)}{\mathrm{d}t} &= \nu_v \hat{E}_v(t) - \tilde{d}_v(t)\hat{I}_v(t).
\end{aligned} \tag{5.24}$$

Now we have that $\rho(\Phi_{F-V-M_\eta}(\omega)) > 1$. Once again by Lemma A, there exists a positive, ω-periodic function $p_2(t)$ such that $p_2(t)\exp(\xi_2 t)$ is a solution of (5.24) and $\xi_2 = \frac{1}{\omega}\ln\rho(\Phi_{F-V+M_\eta}(\omega)) > 0$. For any $J(0) \in \mathbb{R}_+^6$, we can choose a real number

$K_2^* > 0$ such that $J(0) \geqslant K_2^* p_2(0)$ where

$$J(t) = (E_h(t), I_a(t), I_s(t), I_r(t), E_v(t), I_v(t))^T.$$

Applying the comparison principle Theorem E, we obtain $J(t) \geqslant p_2(t)\exp(\xi_2 t)$ for all $t > 0$, which implies that $\lim_{t\to\infty} E_h(t) = \infty$, $\lim_{t\to\infty} I_a(t) = \infty$, $\lim_{t\to\infty} I_s(t) = \infty$, $\lim_{t\to\infty} I_r(t) = \infty$, $\lim_{t\to\infty} E_v(t) = \infty$ and $\lim_{t\to\infty} I_v(t) = \infty$. This leads to a contradiction, which completes the proof. ■

Theorem 5.3. *Assume that $\mathcal{R}_0 > 1$. Then system (5.3) has at least one positive periodic solution and there exists an $\varepsilon > 0$ such that*

$$\liminf_{t\to\infty} E_h(t) \geqslant \varepsilon, \quad \liminf_{t\to\infty} I_a(t) \geqslant \varepsilon, \quad \liminf_{t\to\infty} I_s(t) \geqslant \varepsilon, \quad \liminf_{t\to\infty} I_r(t) \geqslant \varepsilon,$$
$$\liminf_{t\to\infty} E_v(t) \geqslant \varepsilon, \quad \liminf_{t\to\infty} I_v(t) \geqslant \varepsilon,$$

for all $(S_h(0), E_h(0), I_a(0), I_s(0), I_r(0), N_h(0), S_v(0), E_v(0), I_v(0)) \in X_0$.

Proof. First, we prove that P is uniformly persistent with respect to $(X_0, \partial X_0)$, as from this, applying Theorem H it follows that the solution of (5.3) is uniformly persistent with respect to $(X_0, \partial X_0)$.

Let $\phi = (S_h(0), E_h(0), I_a(0), I_s(0), I_r(0), N_h(0), S_v(0), E_v(0), I_v(0)) \in X_0$ be any initial condition. By solving (5.1) for all $t > 0$, we get that

$$S_h(t) = e^{-\int_0^t (a_h(s)+d_h)\,ds}\left[S_h(0) + \int_0^t \mu_h e^{\int_0^s (a_h(r)+d_h)\,dr}\,ds\right] > 0, \tag{5.25}$$

$$E_h(t) = e^{-(\nu_h+d_h)t}\left[E_h(0) + \int_0^t a_h(s)S_h(s)e^{(\nu_h+d_h)s}\,ds\right] > 0, \tag{5.26}$$

$$I_a(t) = e^{-(\gamma_a+d_h)t}\left[I_a(0) + q\nu_h\int_0^t E_h(s)e^{(\gamma_a+d_h)s}\,ds\right] > 0, \tag{5.27}$$

$$I_s(t) = e^{-(\gamma_s+d_h)t}\left[I_s(0) + (1-q)\nu_h\int_0^t E_h(s)e^{(\gamma_s+d_h)s}\,ds\right] > 0, \tag{5.28}$$

$$I_r(t) = e^{-(\gamma_r+d_h)t}\left[I_r(0) + \int_0^t \big(\gamma_a I_a(z) + \gamma_s I_s(z)\big)e^{(\gamma_r+d_h)z}\,dz\right] > 0, \tag{5.29}$$

$$S_v(t) = e^{-\int_0^t (a_v(s)+\tilde{d}_v(s))\,ds}\left[S_v(0) + \int_0^t \tilde{\mu}_v(s)e^{\int_0^s (a_v(r)+\tilde{d}_v(r))\,dr}\,ds\right] > 0, \tag{5.30}$$

$$E_v(t) = e^{-\int_0^t (\nu_v+\tilde{d}_v(s))\,ds}\left[E_v(0) + \int_0^t a_v(s)S_h(s)e^{\int_0^s (\nu_v+\tilde{d}_v(r))\,dr}\,ds\right] > 0, \tag{5.31}$$

$$I_v(t) = e^{-\int_0^t \tilde{d}_v(s)\,ds}\left[I_v(0) + \nu_v\int_0^t E_v(s)e^{\int_0^s \tilde{d}_v(r)\,dr}\,ds\right] > 0, \tag{5.32}$$

where

$$a_h(t) = \beta\frac{\tau_e E_h(t) + \tau_a I_a(t) + I_s(t) + \tau_r I_r(t)}{N_h(t)} + \tilde{\alpha}_h(t)\frac{I_v(t)}{N_h(t)},$$

$$a_v(t) = \tilde{\alpha}_v(t)\frac{\eta_e E_h(t) + \eta_a I_a(t) + I_s(t)}{N_h(t)}.$$

Hence, we get the positively invariant of X_0. Since X is also positively invariant and ∂X_0 is relatively closed in X, it gives ∂X_0 is positively invariant. Furthermore, from Lemma 5.1 it follows that system (5.3) is point dissipative.

Let us introduce

$$M_\partial = \{x^0 \in \partial X_0 : P^m(x^0) \in \partial X_0,\ \forall m \geqslant 0\}.$$

We will apply the theory of uniform persistence developed in [115] (see also [113, Theorem 2.3]). In order to do this, we first show that

$$M_\partial = \{(S_h, 0, 0, 0, 0, N_h, S_v, 0, 0) : S_h \geqslant 0,\ N_h \geqslant 0,\ S_v \geqslant 0\}.$$

Let us note that $M_\partial \supseteq \{(S_h, 0, 0, 0, 0, N_h, S_v, 0, 0) : S_h \geqslant 0,\ N_h \geqslant 0,\ S_v \geqslant 0\}$. It suffices to prove that for arbitrary initial condition $x^0 \in \partial X_0$, $E_h(n\omega) = 0$ or $I_a(n\omega) = 0$ or $I_s(n\omega) = 0$ or $I_r(n\omega) = 0$ or $E_v(n\omega) = 0$ or $I_v(n\omega) = 0$, for all $n \geqslant 0$.

By contradiction assume there exists an $n_1 \geqslant 0$ for which

$$\big(E_h(n_1\omega), I_a(n_1\omega), I_s(n_1\omega), I_r(n_1\omega), E_v(n_1\omega), I_v(n_1\omega)\big)^T > 0.$$

Thus, (5.25) implies $N_h(t) \geqslant S_h(t) > 0,\ \forall t > n_1\omega$. Then, by replacing $t = 0$ to $t = n_1\omega$ in (5.25)–(5.32), we obtain that $S_h(t) > 0$, $E_h(t) > 0$, $I_a(t) > 0$, $I_s(t) > 0$, $I_r(t) > 0$, $N_h(t) > 0$, $S_v(t) > 0$, $E_v(t) > 0$, $I_v(t) > 0$. This is in contradiction with the positive invariance of ∂X_0.

By Lemma 5.2, P is weakly uniformly persistent with respect to $(X_0, \partial X_0)$. From Lemma 5.1, P has a global attractor. It follows that E_0 is an isolated invariant set in X and $W^s(E_0) \cap X_0 = \emptyset$. It is clear that every solution in M_∂ converges to E_0 and E_0 is acyclic in M_∂. By Theorem I and [115, Remark 1.3.1], we obtain that P is uniformly persistent with respect to $(X_0, \partial X_0)$. Hence, there exists an $\varepsilon > 0$ such that

$$\liminf_{t\to\infty} E_h(t) \geqslant \varepsilon, \quad \liminf_{t\to\infty} I_a(t) \geqslant \varepsilon, \quad \liminf_{t\to\infty} I_s(t) \geqslant \varepsilon, \quad \liminf_{t\to\infty} I_r(t) \geqslant \varepsilon,$$
$$\liminf_{t\to\infty} E_v(t) \geqslant \varepsilon, \quad \liminf_{t\to\infty} I_v(t) \geqslant \varepsilon.$$

By Theorem J, P has a fixed point

$$\bar{\phi} = \big(\bar{S}_h(0), \bar{E}_h(0), \bar{I}_a(0), \bar{I}_s(0), \bar{I}_r(0), \bar{N}_h(0), \bar{S}_v(0), \bar{E}_v(0), \bar{I}_v(0)\big) \in X_0,$$

and hence at least one periodic solution $u(t, \bar{\phi})$ of system (5.3) exists. Now, we show that $\bar{S}_h(0)$ and $\bar{S}_v(0)$ are positive. If $\bar{S}_h(0) = 0 = \bar{S}_v(0)$, then from (5.25) and (5.30) we get that $\bar{S}_h(0) > 0$ and $\bar{S}_v(0) > 0$ for all $t > 0$. However, using the periodicity of solution, we have $\bar{S}_h(0) = \bar{S}_h(n\omega) = 0$ and $\bar{S}_v(0) = \bar{S}_v(n\omega) = 0$ for all $n \geqslant 1$, that leads to a contradiction. ■

5.5 Case study for Ecuador and Colombia: what changes in the parameters might lead to a regular recurrence of Zika fever?

In this section, we apply our model to study the spread of Zika in Ecuador during the 2015–17 and in Colombia during the 2015–17 Zika virus epidemic. From Section 5.4, we see that $\mathcal{R}_0$ is a threshold parameter for the persistence of the disease in the population (see Theorems 5.1 and 5.3). The functions $\tilde{\mu}_v(t)$, $\tilde{\alpha}_h(t)$, $\tilde{\alpha}_v(t)$ and $\tilde{d}_v(t)$ are assumed to be time-periodic with one year as a period and, following e.g. [13], they are assumed to be of the form $\mu_v \cdot \left(\sin\left(\frac{2\pi}{p}t + b\right) + a\right)$, $\alpha_h \cdot \left(\sin\left(\frac{2\pi}{p}t + b\right) + a\right)$, $\alpha_v \cdot \left(\sin\left(\frac{2\pi}{p}t + b\right) + a\right)$ and $d_v \cdot \left(\cos\left(\frac{2\pi}{p}t + b\right) + a\right)$ where p is period length, a, b are free adjustment parameters and $\mu_v, \alpha_h, \alpha_v, d_v$ are the (constant) baseline values of the corresponding time-dependent parameters.

5.5.1 Parameter estimation for Ecuador and Colombia

To give an estimate for the values of the parameters providing the best fit, we applied Latin Hypercube Sampling, a method used in statistics to assess simultaneous variation of multiple parameters (see, e.g., [70]).

Figure 5.3 shows model (5.1) fitted to data from Ecuador and Colombia [84, 85]. Our model gives a reasonably good fit for both countries, reproducing the single peak of Zika fever in Colombia and the two peaks of Zika fever experienced in Ecuador in two subsequent years. This shows that model (5.1) is able to reproduce the two types of outcomes of the Zika epidemic observed in South America. We note that in our simulation for Ecuador, before dying out, the epidemic shows a very minor third peak for the following year 2018. This is in accordance with real world data, as sources report a small number of Zika infections in this year. Our model slightly overestimates the number of cases in 2018, however, as in most cases, Zika fever does not cause severe symptoms and that public awareness was reduced by the decreasing number of Zika cases, probably less people visited their doctors during this third year.

Figure 5.3 is in accordance with the analytic results stating that the unique disease-free equilibrium E_0 is globally asymptotically stable when $\mathcal{R}_0 < 1$. By Theorem 5.2, system (5.1) is persistent with respect to the infective compartments if $\mathcal{R}_0 > 1$. Figure 5.4 shows the persistence of the disease when $\mathcal{R}_0 > 1$.

5.5.2 Parameter changes

One of our main interests was to see what changes in the parameters might lead to a regular reappearance of the epidemic. Up to now, after 1–3 consecutive years

with outbreaks, Zika did not appear in high numbers again. However, in the days of climate change, one can expect that some of the parameters will change in the future as mosquitoes adapt to new circumstances and mutations of the virus appear. This might lead to a periodic annual recurrence of the epidemic, just like in the case of other mosquito-borne diseases like dengue fever or malaria. Because of the high number of parameters, it is not easy to assess rigorously which of the parameters have the most important role in the variation of the dynamics, so we only try to demonstrate the possible alterations through a couple of examples.

Our first example (see Figure 5.4a) was created with the above determined parameters for the Zika epidemic in Ecuador except the mosquito-related parameters $\alpha_h, \alpha_v, \beta, \mu_v$, i.e. we increased human-to-human and human-to-mosquito transmission rates and mosquito birth rate, while mosquito-to-human transmission rate was decreased. We can calculate numerically the value of the basic reproduction number $\mathcal{R}_0 = 1.2465 > 1$. In the second example (see Figure 5.4b), similar changes were performed for the parameters determined for Colombia. Again, we can calculate numerically the value of the basic reproduction number $\mathcal{R}_0 = 1.707 > 1$. Accordingly, one can see that with these parameters, the disease compartments are persistent and the epidemic becomes endemic in the population recurring periodically every year.

In Figure 5.5 we present how changes in some of the key parameters (human-to-human, human-to-mosquito and mosquito-to human transmission rates as well as mosquito birth rates) might affect the course of Zika epidemics. The simulations suggest that an increase of any of these four parameters – either due to climate change or to genetic mutation of the virus – can lead to a periodic annual reappearance of the epidemic.

Knowing the seasonal fluctuation, one may rightly suppose that mosquito control is limited to the peak months of mosquito abundance. Hence, we also show an example where mosquito control only occurs during five months when the highest number of vectors are present to see whether control measures implemented only during a limited period of the year might have a sufficient effect to eradicate the disease. Mosquito killing is incorporated into the model by considering a step function multiplier of the mosquitoes' death rate. Namely, we increase the death rate during a five-month-long period of each year.

For a better assessment of the effect of additional mosquito killing, we assume a periodic recurrence of the disease, just like given in Figure 5.4 and Table 5.2. In Figure 5.6 we show some seasonal measures to control Zika virus disease both in Ecuador and Colombia. The figure suggests that even a mosquito control limited to the peak period of mosquito abundance might have a significant impact to control the disease.

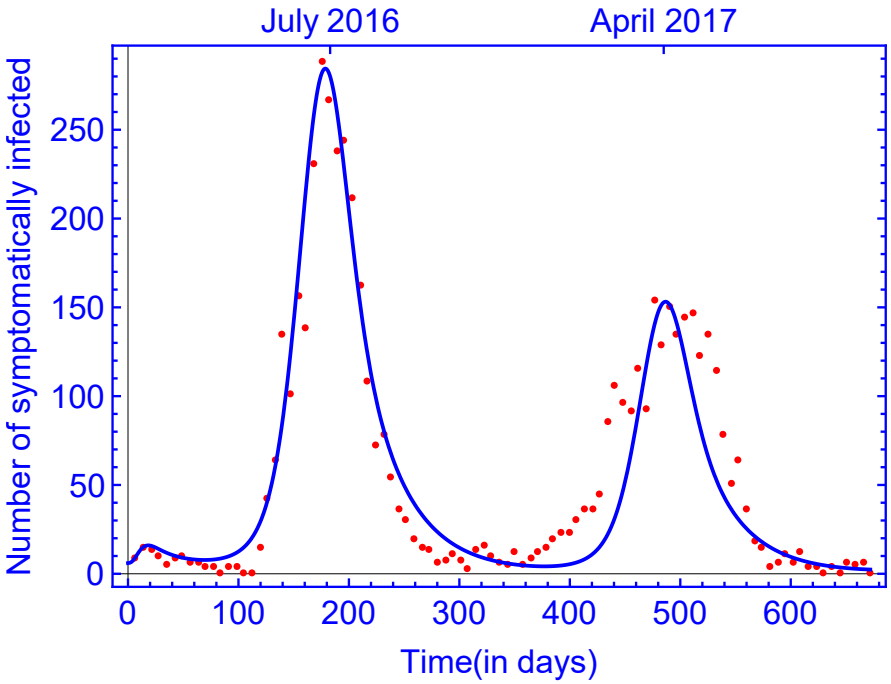

(a) *The model fitted to 2016–17 data from Ecuador when* $\mathcal{R}_0 = 0.945 < 1$.

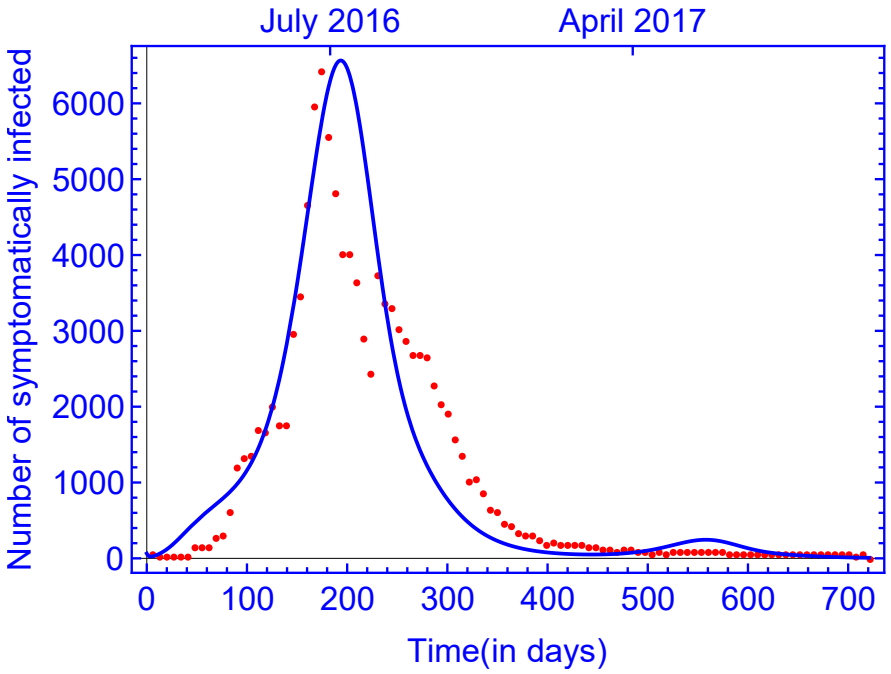

(b) *The model fitted to 2015–17 data from colombia when* $\mathcal{R}_0 = 0.989 < 1$.

Figure 5.3: *The model fitted to in (a) 2016–17 data from Ecuador and in (b) 2015–17 data from Colombia when* $\mathcal{R}_0 < 1$ *with parameter values in Table 5.2.*

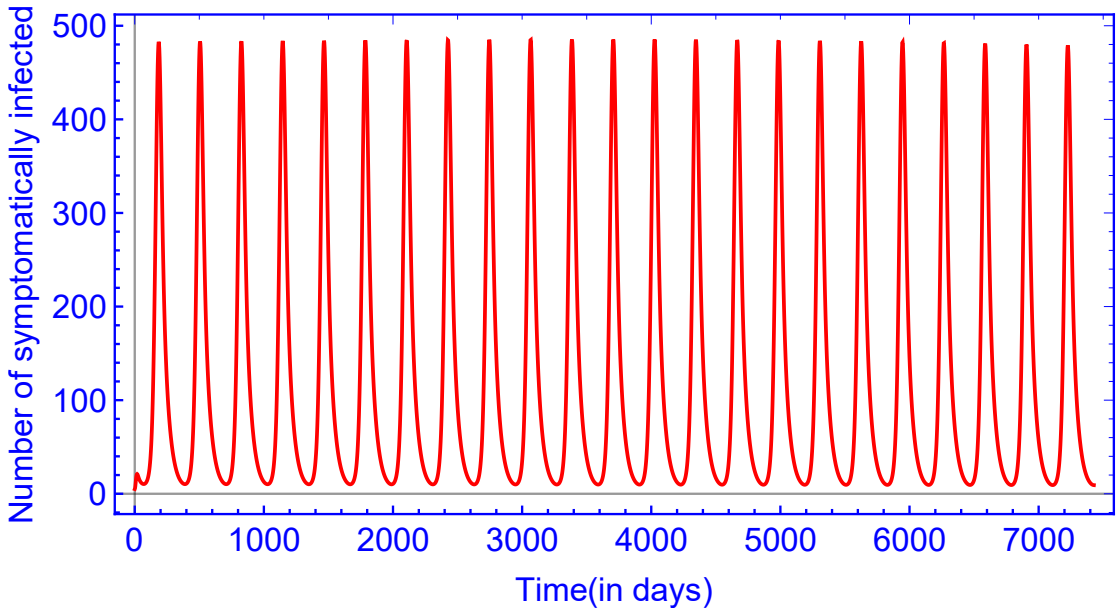

(a) *The uniform persistence of the disease in Ecuador when* $\alpha_h = 0.545$, $\alpha_v = 0.56$, $\beta = 0.0256$, $\mu_v = 26,800$ *and* $\mathcal{R}_0 = 1.2465 > 1$.

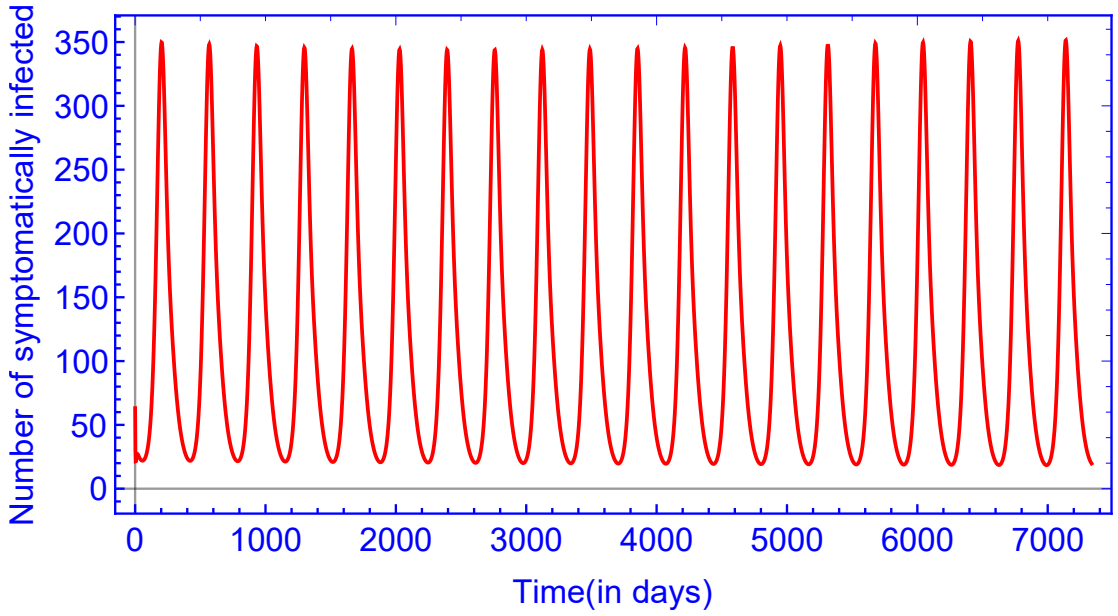

(b) *The uniform persistence of the disease in Colombia when* $\alpha_h = 0.641$, $\alpha_v = 0.083$, $\beta = 0.0552$, $\mu_v = 54,200$ *and* $\mathcal{R}_0 = 1.707 > 1$.

Figure 5.4: *The uniform persistence of the disease in (a) Ecuador and in (b) Colombia when* $\mathcal{R}_0 > 1$. *The rest of the parameter values are the same as those in Table 5.2.*

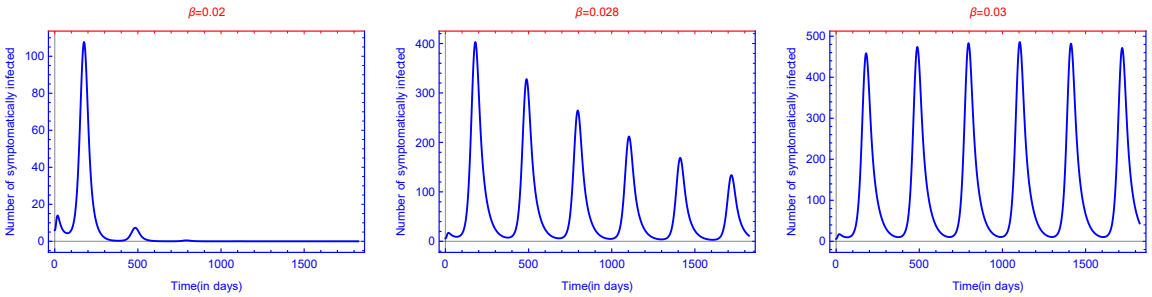

(a) *The model solution with different values of* β.

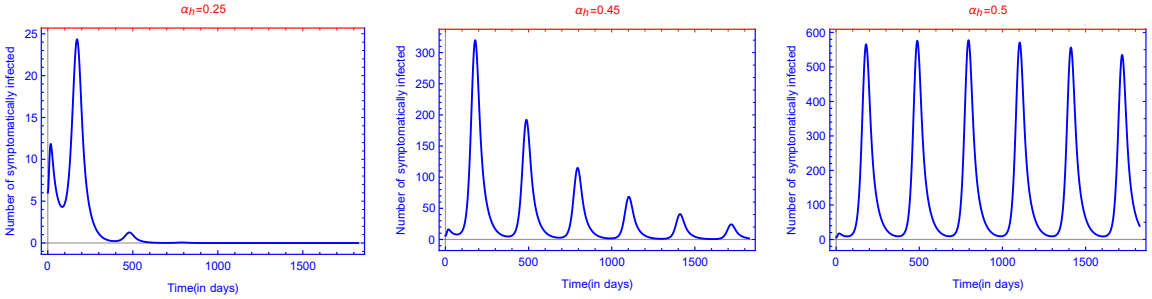

(b) *The solution of model* (5.1) *with three different values of* α_h.

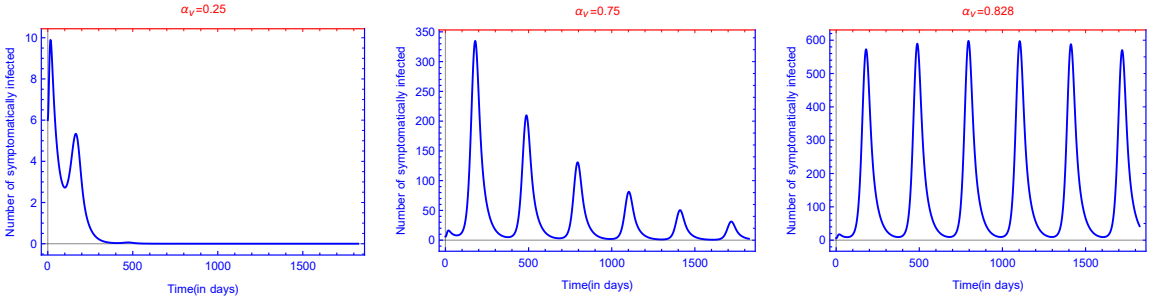

(c) *The solution of model* (5.1) *with three different values of* α_v.

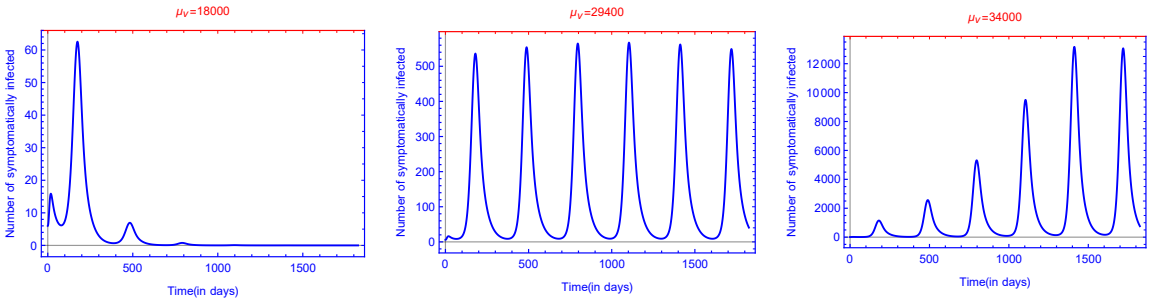

(d) *The solution of model* (5.1) *with three values of* μ_v.

Figure 5.5: *The solution of model* (5.1) *with three different values of in (a) human-to-human transmission rate* (β)*, in (b) baseline value of mosquito-to-human transmission rate* (α_h)*, in (c) baseline value of human-to-mosquito transmission rate* (α_v) *and in (d) baseline value of mosquito birth rate* (μ_v)*. The rest of the parameter values are the same as those for Ecuador in Table 5.2.*

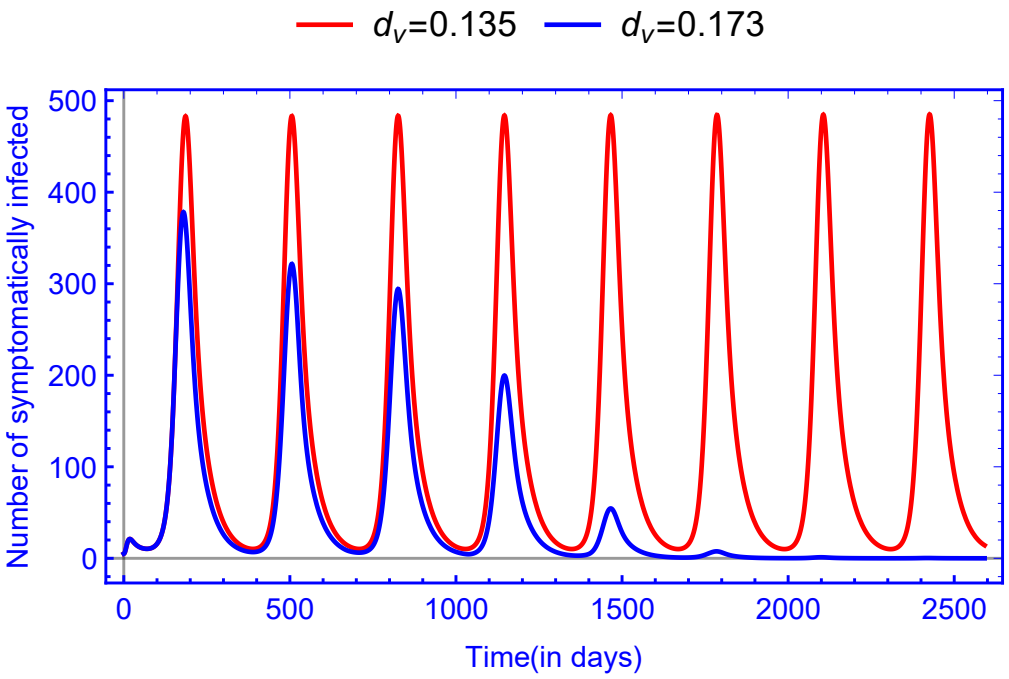

(a) *Ecuador.*

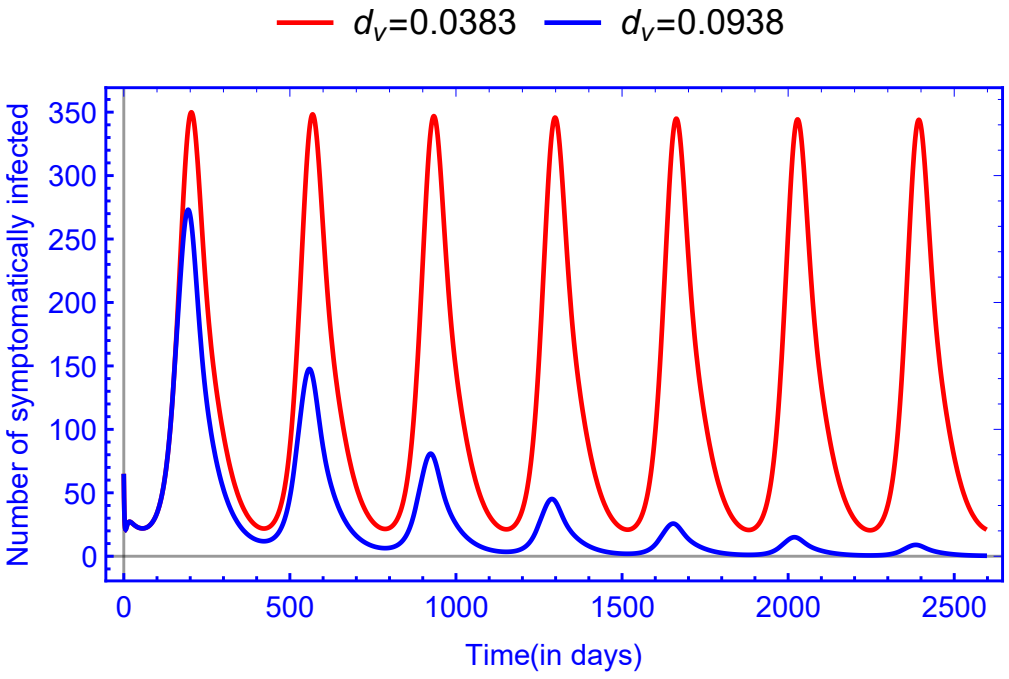

(b) *Colombia.*

Figure 5.6: *Seasonal measures to control ZIKV in (a) Ecuador and in (b) Colombia. The rest of the parameter values are the same as those in Figure 5.4 and Table 5.2.*

Table 5.2: *Parameters of model (5.1) and fitted values in the case of Ecuador and Colombia.*

Parameter	Range	Value (Ecuador)	Value (Colombia)	Source
μ_h	–	608.142	1826.81	[106]
d_h	–	0.0000359	0.0000368	[106]
β	0.01–0.1	0.0249	0.0435	[46]
α_h	0.03–0.75	0.44	0.218	[6, 29]
α_v	0.09–0.75	0.727	0.347	[6, 29]
q	0.75–0.9	0.765	0.824	[40, 46]
τ_e	0.2–1	0.796	0.382	[46]
τ_a	0.2–1	0.7902	0.263	[46]
τ_r	0.2–0.8	0.576	0.585	[46]
η_e	0.2–0.7	0.636	0.653	[46]
η_a	0.2–0.7	0.591	0.471	[46]
γ_a	0.05–0.4	0.1169	0.165	[46]
γ_s	0.2–0.5	0.1059	0.477	[15]
γ_r	0.01–0.07	0.0545	0.06	[47, 76]
ν_h	0.1–0.5	0.292	0.421	[15]
ν_v	0.08–0.125	0.106	0.0965	[6, 18]
μ_v	500–40, 000	25, 800	32, 200	Fitted
$1/d_v$	4–35	8	26.05	[6]
a	–	1.35	1.1	–
b	–	6.48	138.51	–

5.5.3 Sensitivity analysis

Sensitivity analysis, using Partial Rank Correlation Coefficients (PRCC, see, e.g. [17]), is carried out to determine the parameters that have the greatest influence on the dynamics of the diseases. The PRCC-based sensitivity analysis measures the effect of the parameters on the response function (in our cases, the number of infected cases), while we vary the parameters (relevant to the dynamics of the diseases in Ecuador and Colombia) in the given ranges (see Table 5.2).

Figure 5.7 shows the comparison of the PRCC values obtained for the parameters $\beta, \alpha_h, \alpha_v, \mu_v$ and d_v, i.e. those parameters which can typically be affected by control measures. The results suggest that the most relevant factors in Zika transmission, and hence in the elevation of the number of infected cases are birth and death rates of mosquitoes. Spread via sexual contacts is shown to have a smaller effect, however, it is still an important factor. Based on the sensitivity analysis, we can assess that the most effective measures to reduce transmission are control of mosquito populations and protection against their bites.

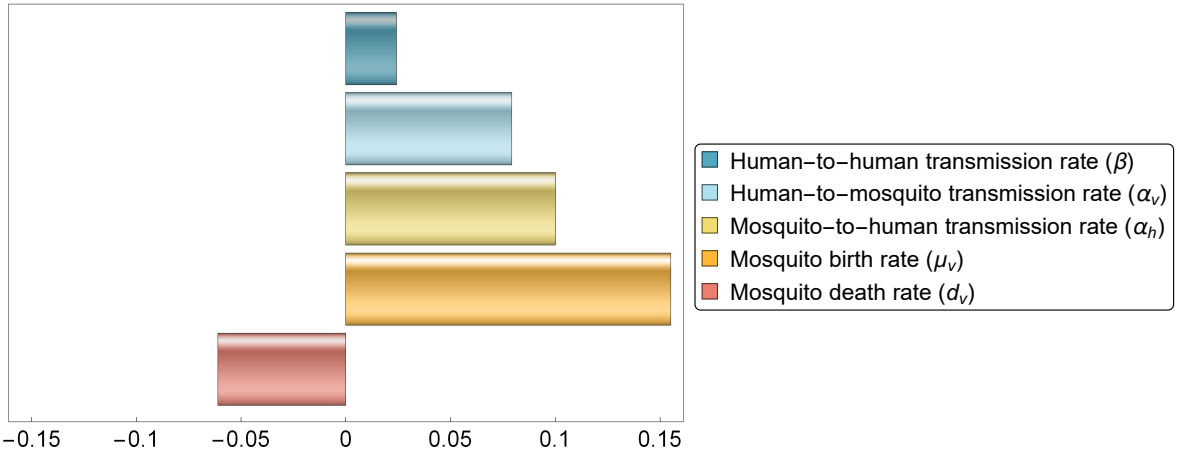

Figure 5.7: *Partial rank correlation coefficients of the five parameters subject to intervention measures. Parameters with positive PRCC values are positively correlated with the cumulative number of cases. Parameters with negative PRCC values are negatively correlated with the cumulative number of infections.*

5.5.4 Reproduction numbers

To calculate the reproduction numbers, we use the parameters as obtained in the fitting to Ecuador data in Table 5.2. Formula (5.13) provides us the basic reproduction number in any time point by substituting the parameter values. Figure 5.8 shows the basic reproduction number of the time-constant model with respect to baseline value of mosquito birth rate, baseline value of human-to-mosquito transmission rates and human-to-human transmission rate, suggesting that control of mosquito population and sexual protection both have a significant effect in Zika fever transmission. The results also imply that vector control might not be enough to contain the disease spread in case of a high sexual transmission rate.

Further, by numerical calculations we get the curves of the basic reproduction ratio $\mathcal{R}_0$, the time-average basic reproduction number $[\mathcal{R}_0]$ (using the notation presented by [72]) and the basic reproduction number $\mathcal{R}_0^A$ of the autonomous model with respect to baseline value of mosquito birth rate (μ_v), human-to-human transmission rate (β), baseline value of mosquito-to-human transmission rate (α_h) and baseline value of human-to-mosquito transmission rate (α_v), respectively, in Figure 5.9.

The calculations show that the time-average basic reproduction number $[\mathcal{R}_0]$ is always less than the basic reproduction ratio $\mathcal{R}_0$, suggesting that the time-average basic reproduction number underestimates the disease transmission risk. From this aspect, our results are similar to those of [103]. We note that there are some other cases of underestimation and overestimation for the average basic reproduction number can be found in [9], where an approximate formula of the basic reproduction number was obtained for a class of periodic vector-borne disease models with a small

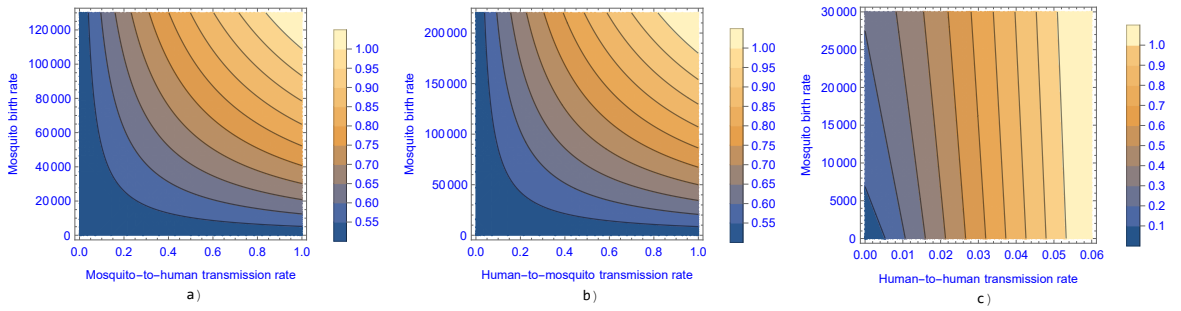

(a) *Ecuador.*

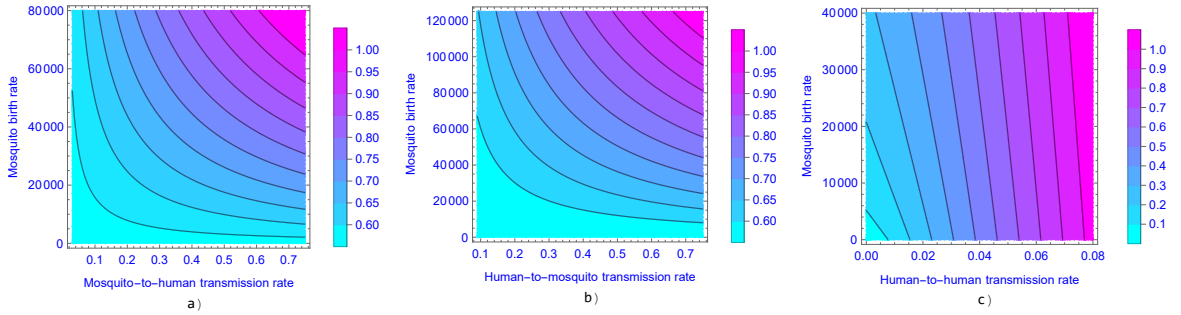

(b) *Colombia.*

Figure 5.8: *Contour plot of the basic reproduction number as a function of baseline value of mosquito birth rate (μ_v) and a) baseline value of mosquito-to-human transmission rate (α_h), b) baseline value of human-to-mosquito transmission rate (α_v) and c) human-to-human transmission rate (β).*

perturbation parameter.

5.6 Discussion

We have developed a compartmental population model to describe the transmission of Zika virus disease in a periodic environment (by including periodic coefficients). We have shown that the global dynamics of the model is determined by the basic reproduction number $\mathcal{R}_0$. For $\mathcal{R}_0$ less than 1, we have shown the global asymptotic stability of the disease-free periodic solution E_0, while the disease persists if $\mathcal{R}_0 > 1$. Using our model and taking Ecuador and Colombia as two examples, the fitted curves match the data very well (see Figure 5.3). Our numerical simulations suggest that there exists a single positive periodic solution which is globally asymptotically stable for $\mathcal{R}_0 > 1$ (see Figure 5.4).

The reproduction numbers were calculated as a function of the parameters μ_v, α_h, α_v and β. As is observed, the time-average basic reproduction number $[\mathcal{R}_0]$ is always

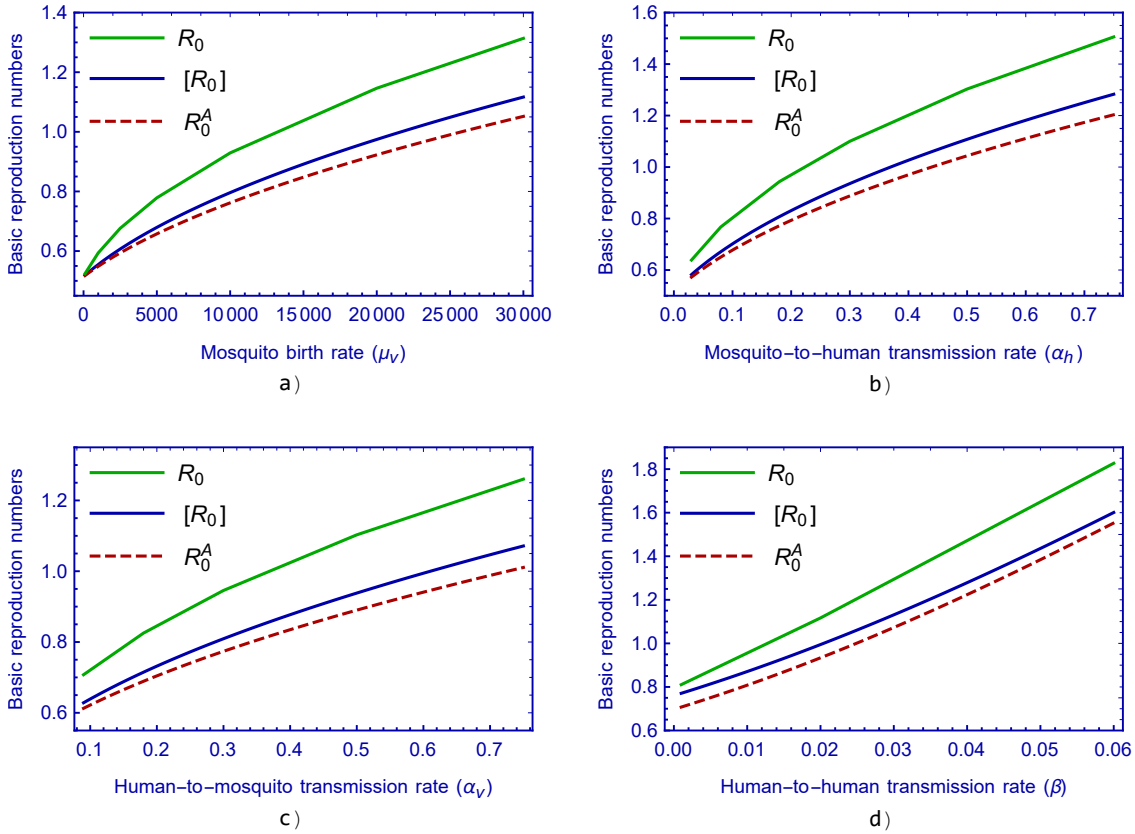

Figure 5.9: *The curves of the basic reproduction number $\mathcal{R}_0$, the time-average basic reproduction number $[\mathcal{R}_0]$ and the basic reproduction number of the autonomous model $\mathcal{R}_0^A$ versus a) baseline value of mosquito birth rate (μ_v), b) baseline value of mosquito-to-human transmission rate (α_h), c) baseline value of human-to-mosquito transmission rate (α_v) and d) human-to-human transmission rate (β).*

less than the basic reproduction number $\mathcal{R}_0$ (see Figure 5.9). This implies that the time-average basic reproduction number underrates the risk of disease transmission, while the risk of infection is overestimated by the basic reproduction number.

Although a regular periodic recurrence of Zika has not been observed so far, it is expected that this might be altered by climate change. Our model allows us to estimate what kind of parameter changes might lead to a periodic recurrence of Zika. Using numerical simulations, we found that mosquito birth and death rates are the most significant factors in a possible periodic recurrence of Zika, however, sexual transmission also has a significant effect on the prevalence of the disease.

Chapter 6

A mathematical model for Lassa fever transmission dynamics in a seasonal environment with a view to the 2017–20 epidemic in Nigeria

In this chapter, we formulate and study a compartmental model for Lassa fever transmission dynamics considering human-to-human, rodent-to-human transmission and the vertical transmission of the virus in rodents. To incorporate the impact of periodicity of weather on the spread of Lassa, we introduce a non-autonomous model with time-dependent parameters for rodent birth rate and carrying capacity of the environment with respect to rodents. We introduce the basic reproduction number and show that it can be used as a threshold parameter concerning the global dynamics. It also shown that the disease-free periodic solution is globally asymptotically stable in the case of $\mathcal{R}_0 < 1$ and if $\mathcal{R}_0 > 1$, then the disease persists. We show numerical studies for the Lassa fever in Nigeria and give examples to describe what kind of parameter changes might trigger the periodic recurrence of Lassa fever.

The content of this chapter has been published in

[52] M. A. Ibrahim and A. Dénes. A mathematical model for Lassa fever transmission dynamics in a seasonal environment with a view to the 2017–20 epidemic in Nigeria. *Nonlinear Analysis: Real World Applications*, 60:103310, 2021. https://doi.org/10.1016/j.nonrwa.2021.103310.

6.1 Introduction

Lassa haemorrhagic fever (LHF), or Lassa fever for short is a zoonotic, acute viral hemorrhagic fever caused by the Lassa virus from the *Arenaviridae* family [110]. The

disease was first described in the 1950s, though the virus causing it was only identified in 1969 [21]. The disease was named after the Nigerian town Lassa, where the first cases were observed. LHF is usually transmitted to humans via direct or indirect exposure to food or other items contaminated with urine or feces of infected multimammate rats (*Mastomys natalensis*), through the respiratory or gastrointestinal tracts. Person-to-person transmission has also been observed [92]. The virus remains in body fluids even after recovery: in urine for 3–9 weeks from infection and for three months in male genital secretions [92]. Lassa fever is endemic among rats in parts of West Africa, while it is endemic in humans in several countries of the region. In these regions, the number of infections per year is estimated between 100,000 and 300,000, with around 5,000 deaths. Lassa menaces mostly those who live in rural areas where multimammate rats are present, especially where poor sanitation and crowded living conditions are typical. Figure 6.1 shows the possible methods of LHF transmission.

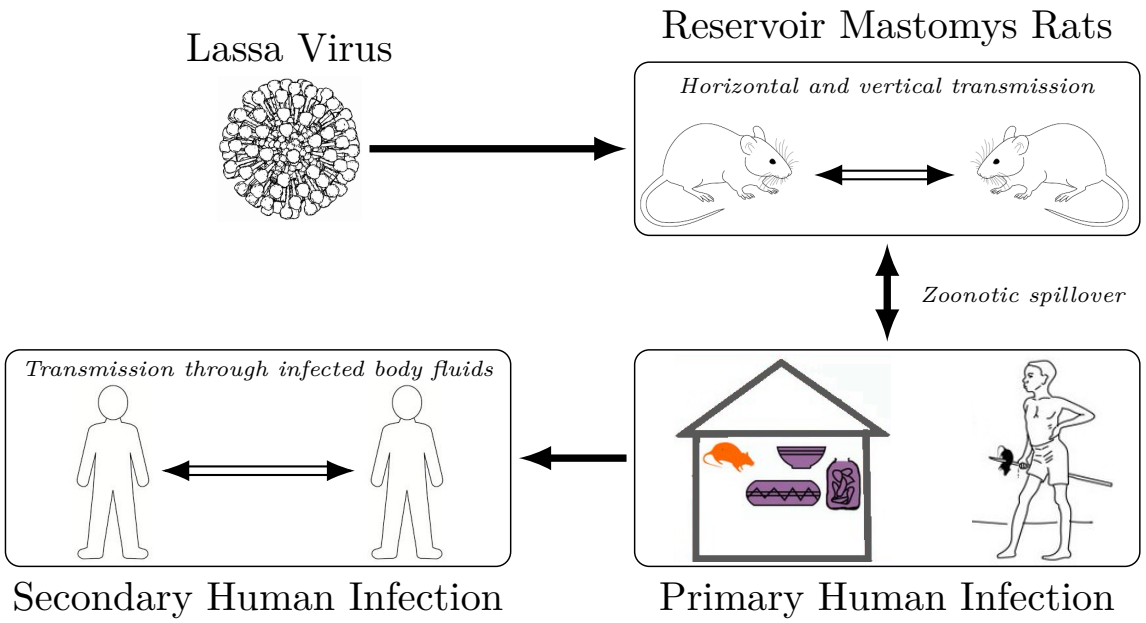

Figure 6.1: *Lassa fever transmission. The figure shows modes of transmission (human-to-human, human-to-rodent, rodent-to-human and rodent-to-rodent).*

About 80% of people infected with Lassa fever have only mild or no symptoms. Symptom onset occurs usually 1–3 weeks after exposure, these include fever, tiredness, weakness, and headache. 20% of infected develop a severe multisystem disease with symptoms including bleeding gums, respiratory distress, vomiting, chest, back and abdomen pain, facial swelling, low blood pressure. Neurological problems can also be observed, such as hear loss, tremors, encephalitis. Approximately 1% of infections result in death due to multi-organ failure. However, the disease is particularly

severe in women in the third trimester of their pregnancy, with high rates of maternal death (29%) observed, while an estimated 80–95% fetal and neonatal mortality is reported [23, 88, 110].

Treatment of Lassa fever includes antiviral medication, fluid replacement and blood transfusions. For women in late pregnancy, inducing delivery is necessary.

Although Lassa fever appears in WHO's Blueprint list of diseases to be prioritized for research and development [107], compared with other infectious diseases, a relatively small number of mathematical modelling studies have been published up to now. Onah et al. [81] extended an SIR–SI-type compartmental model by introducing different control intervention measures, e.g. external protection, treatment, isolation and rodent control. They used optimal control theory to determine how to reduce disease transmission with minimal cost. Musa et al. [75] established a model describing the interaction between humans and rodents including quarantine, isolation and hospitalization. The authors showed the presence of a forward bifurcation with a stability switch between the disease-free and the endemic equilibrium. Also, they fitted the model to data from 2016–19 to find that initial susceptibility increased across the three outbreaks in these years. Zhao et al. [114] studied the epidemiological features of Lassa epidemics in various regions of Nigeria. They assessed the connection between the reproduction number and rainfall. They determined the infectivity of Lassa by the reproduction number estimated from four types of growth models. They fitted the models to Lassa surveillance data and estimated the reproduction number in various regions. Akhmetzanov et al. [5] applied a model to study the datasets of human infection, population changes of rodents as well as weather changes to quantify the seasonal drivers of Lassa fever transmission. They obtained that seasonal migration of rats plays a key role in regulating the periodicity of Lassa epidemics. The peak exposure of humans to rats is shortly after the beginning of the dry season and correlates with the mating period of rodents.

Although some of the above works put an emphasis on the time-changing nature of Lassa transmission dynamics, so far, no compartmental model with time-dependent parameters has been established. In this work, we set up and study a compartmental epidemic model for Lassa fever transmission dynamics considering infected humans with mild or severe symptoms, treatment, human-to-human and rodent-to human transmission as well as time-dependent parameters. Namely, modelling the annual periodic change of weather, we introduce time-periodic parameters for rodent birth rate and carrying capacity of the environment with respect to rodents. To study the dynamics of our time-periodic model, we will apply the theory initiated in [10, 11, 90, 103, 113] and detailed in Chapter 3, later applied in several periodic epidemic models (see, e.g. [53, 54, 61, 62, 63, 78, 89, 102]). Here we adapt these methods to our system with human-to-human and rodent-to-human transmission with a logistic growth of rodents.

The rest of the paper is structured as follows. In the next section we introduce the time-dependent mathematical model for Lassa fever transmission dynamics. In Section 6.3 we study the existence of the disease-free periodic solution. In Section 6.4 we calculate the basic reproduction number of our model using various methods. In Section 6.5, we show that depending on the basic reproduction number, either the disease-free periodic solution is globally asymptotically stable or the disease persists in the population. In Section 6.6 we provide numerical simulations for both scenarios supporting the theoretical results.

6.2 Seasonal model for Lassa fever transmission

We divide the human population into six compartments: susceptible $S_h(t)$, exposed $E_h(t)$, symptomatically infected $I_s(t)$, mildly infected $I_m(t)$, treated $I_T(t)$, and recovered individuals with temporary immunity $R(t)$. The total size of the human population at any time t is denoted by

$$N_h(t) = S_h(t) + E_h(t) + I_m(t) + I_s(t) + I_T(t) + R(t).$$

An individual may proceed from susceptible (S_h) to exposed (E_h) upon contracting

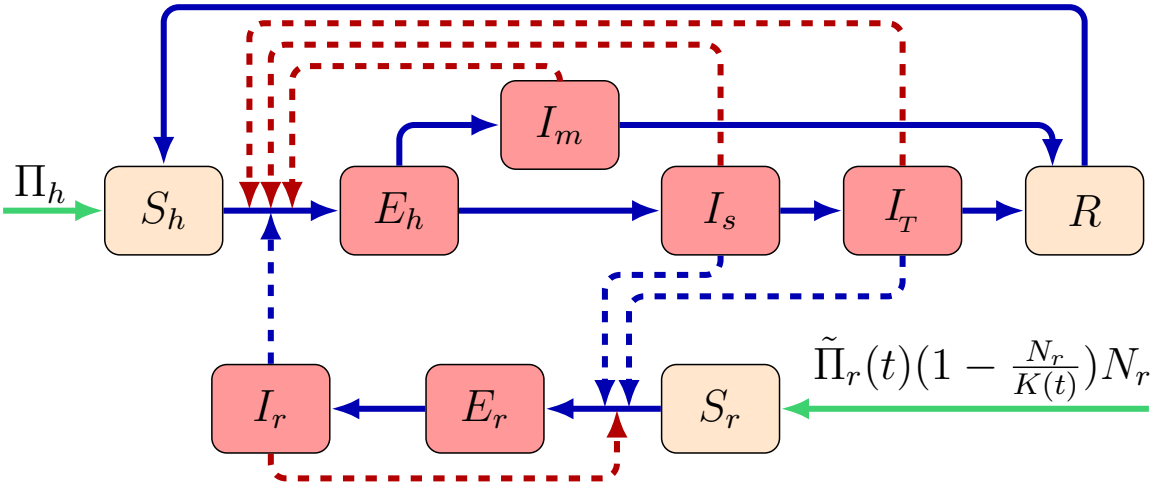

Figure 6.2: *Schematic diagram of the LHF transmission among rodents and humans. Red nodes denote infectious, brown nodes denote non-infectious states. Blue solid arrows demonstrate infection progress, while red dashed arrows represent direction of human-to-human transmission and rodent-to-rodent transmission. Blue dashed arrows show direction of transmission between humans and rodents. Green arrows show recruitment rate for humans and maximum growth rate of the rodents.*

the disease. Individuals in the exposed compartment have no symptoms yet. After the incubation time, an exposed individual moves either to the symptomatically

infected class (I_s) or to the mildly infected class (I_m), depending on whether that person shows symptoms or not. Infected people from I_s may move to the treated compartment ($I_{_T}$), including those who need hospital treatment. After the infection period, recovered persons move to the class R.

The vector population (*Mastomys natalensis* rat) at time t, denoted by $N_r(t)$, is divided into three compartments: susceptible $S_r(t)$, exposed $E_r(t)$ and infectious $I_r(t)$, respectively. Thus

$$N_r(t) = S_r(t) + E_r(t) + I_r(t).$$

The transmission dynamics is shown in the flow diagram (see Figure 6.2) and our model takes the form

$$\begin{aligned}
\frac{\mathrm{d}S_h(t)}{\mathrm{d}t} &= \Pi_h - \frac{\beta_m I_m(t) + \beta_s I_s(t) + \beta_{_T} I_{_T}(t)}{N_h(t)} S_h(t) - \beta_{rh}\frac{I_r(t)}{N_h(t)} S_h(t) - dS_h(t) \\
&\quad + \xi R(t), \\
\frac{\mathrm{d}E_h(t)}{\mathrm{d}t} &= \frac{\beta_m I_m(t) + \beta_s I_s(t) + \beta_{_T} I_{_T}(t)}{N_h(t)} S_h(t) + \beta_{rh}\frac{I_r(t)}{N_h(t)} S_h(t) - \nu_h E_h(t) \\
&\quad - dE_h(t), \\
\frac{\mathrm{d}I_m(t)}{\mathrm{d}t} &= \theta\nu_h E_h(t) - \gamma_m I_m(t) - dI_m(t), \\
\frac{\mathrm{d}I_s(t)}{\mathrm{d}t} &= (1-\theta)\nu_h E_h(t) - \gamma_s I_s(t) - (d+\delta_s) I_s(t), \\
\frac{\mathrm{d}I_{_T}(t)}{\mathrm{d}t} &= \gamma_s I_s(t) - \gamma_{_T} I_{_T}(t) - (d+\delta_{_T}) I_{_T}(t), \\
\frac{\mathrm{d}R(t)}{\mathrm{d}t} &= \gamma_m I_m(t) + \gamma_{_T} I_{_T}(t) - \xi R(t) - dR(t), \\
\frac{\mathrm{d}S_r(t)}{\mathrm{d}t} &= \tilde{\Pi}_r(t)\left(1 - \frac{N_r(t)}{K(t)}\right) N_r(t) - \beta_{hr}\frac{\eta_s I_s(t) + \eta_{_T} I_{_T}(t)}{N_h(t)} S_r(t) - \mu S_r(t) \\
&\quad - \beta_r \frac{I_r(t)}{N_r(t)} S_r(t), \\
\frac{\mathrm{d}E_r(t)}{\mathrm{d}t} &= \beta_{hr}\frac{\eta_s I_s(t) + \eta_{_T} I_{_T}(t)}{N_h(t)} S_r(t) + \beta_r \frac{I_r(t)}{N_r(t)} S_r(t) - \nu_r E_r(t) - \mu E_r(t), \\
\frac{\mathrm{d}I_r(t)}{\mathrm{d}t} &= \nu_r E_r(t) - \mu I_r(t),
\end{aligned} \tag{6.1}$$

where $\tilde{\Pi}_r(t)$ and $K(t)$ denote the time-dependent per capita birth rate and maximal carrying capacity of the *Mastomys natalensis* rats. In our model we assumed $\tilde{\Pi}_r(t)$ and $K(t)$ are continuous, positive ω-periodic functions. We denote by Π_h and d the human birth and death rate, respectively. There is also an additional disease-induced death rate, denoted by δ_s and $\delta_{_T}$ for those in the compartments I_s and $I_{_T}$, respectively.

The description of the model parameters are summarized in Table 6.1.

Table 6.1: *Description of parameters of model* (6.1).

Parameters	Description
Π_h	Recruitment rate for humans
d	Natural death rates of humans
$\delta_s, \delta_{_T}$	Disease-induced death rates for humans
$\beta_m, \beta_s, \beta_{_T}$	Transmission rates from human-to-human
β_{hr}	Transmission rate from human-to-rodent
β_{rh}	Transmission rate from rodent-to-human
β_r	Transmission rate from rodent-to-rodent
$\eta_s, \eta_{_T}$	Relative transmissibility of infectious human-to-rodent
θ	Proportion of mild infections
γ_s	Progression rate from I_s to $I_{_T}$
$\gamma_m, \gamma_{_T}$	Recovery rates
ν_h, ν_r	Humans and rodent incubation rate
ξ	Rate of relapse from R to S_h
K_r	Average carrying capacity of the environment for the rodents
Π_r	Baseline value of rodents birth rate
μ	Natural death rates of rodents
b	Phase angle (month of peak in seasonal forcing)
Λ	Amplitude of seasonality

6.3 The disease-free periodic solution

6.3.1 Existence of the disease-free ω-periodic solution

In this section, we study the existence and uniqueness of the disease-free periodic solution of system (6.1). Define

$$\phi = \big(S_h(0), E_h(0), I_m(0), I_s(0), I_{_T}(0), R(0), S_r(0), E_r(0), I_r(0)\big) \in \mathbb{R}^9_+.$$

In case of no disease, for the total human population N_h with a positive initial condition $\phi \in \mathbb{R}^9_+$, we have the equation

$$\frac{\mathrm{d}N_h(t)}{\mathrm{d}t} = \Pi_h - dN_h(t), \tag{6.2}$$

from which we obtain

$$N_h(t) = N_h(0)e^{-dt} + \frac{\Pi_h}{d}(1 - e^{-dt}). \tag{6.3}$$

with an arbitrary initial value $N_h(0)$. Equation (6.3) has a unique equilibrium $N_h^* = \frac{\Pi_h}{d}$ in $\mathbb{R}_+$. Consequently, $|N_h(t) - N_h^*| \to 0$ as $t \to \infty$ and N_h^* is globally attractive on $\mathbb{R}_+$.

To identify the disease-free periodic solution of (6.1), consider

$$\frac{\mathrm{d}S_r(t)}{\mathrm{d}t} = \tilde{\Pi}_r(t)\left(1 - \frac{S_r(t)}{K(t)}\right)S_r(t) - \mu S_r(t), \tag{6.4}$$

with initial condition $S_r(0) \in \mathbb{R}_+$. Equation (6.4) has a unique positive ω-periodic solution

$$S_r^*(t) = \frac{e^{\int_0^t (\tilde{\Pi}_r(s)-\mu)\,ds}}{\int_0^t \frac{\tilde{\Pi}_r(\tau)}{K(\tau)} e^{\int_0^\tau (\tilde{\Pi}_r(s)-\mu)\,ds}\,d\tau + \frac{\int_0^\omega \frac{\tilde{\Pi}_r(\tau)}{K(\tau)} e^{\int_0^\tau (\tilde{\Pi}_r(s)-\mu)\,ds}\,d\tau}{e^{\int_0^\omega (\tilde{\Pi}_r(s)-\mu)\,ds}-1}} > 0, \tag{6.5}$$

which is globally attractive in $\mathbb{R}_+$. Thus, system (6.1) has a unique disease-free periodic solution $E_0 = \left(S_h^*, 0, 0, 0, 0, 0, S_r^*(t), 0, 0\right)$, where $S_h^* = \frac{\Pi_h}{d}$.

Lemma 6.1. *There is* $N_r^* = \limsup_{t\to\infty} \frac{K(t)(\tilde{\Pi}_r(t)-\mu)}{\tilde{\Pi}_r(t)} > 0$ *such that any forward solution in* $\mathbb{R}_+^9$ *of* (6.1) *enters eventually*

$$\Omega_{N_r^*} := \left\{(S_h, E_h, I_m, I_s, I_T, R, S_r, E_r, I_r) \in \mathbb{R}_+^9 : N_h \leqslant N_h^*,\ N_r \leqslant N_r^*\right\},$$

and for each $N_r(t) \geqslant N_r^*$, Ω_N *is a positively invariant set with respect to* (6.1). *Further, it holds that*

$$\lim_{t\to+\infty} (N_r(t) - S_r^*(t)) = 0.$$

Proof. From (6.1), we have

$$\begin{aligned}\frac{\mathrm{d}N_r(t)}{\mathrm{d}t} &= \tilde{\Pi}_r(t)\left(1 - \frac{N_r(t)}{K(t)}\right)N_r(t) - \mu N_r(t)\\ &\leqslant \left(\tilde{\Pi}_r(t) - \mu - \frac{\tilde{\Pi}_r(t)}{K(t)}N_r(t)\right)N_r(t) \leqslant 0 \quad \text{if } N_r(t) \geqslant N_r^*,\end{aligned}$$

which implies that Ω_N, $N_r(t) \geqslant N_r^*$, is positively invariant and each forward orbit enters Ω_{N^*} eventually. For the second part of the proof, let us assume that

$$z(t) = N_r(t) - S_r^*(t),\ t \geqslant 0.$$

Then, it follows that

$$\frac{\mathrm{d}z(t)}{\mathrm{d}t} = -\mu z(t),$$

which implies that $\lim_{t\to+\infty} z(t) = 0$. ■

6.4 Basic reproduction numbers and local stability

Based on the method established by Wang and Zhao [103], we demonstrate the local stability of the disease-free periodic equilibrium E_0 of (6.1) in terms of the basic reproduction number $\mathcal{R}_0$.

Linearizing the system (6.1) at E_0, we obtain the equations for exposed and infectious human and rodent populations, respectively:

$$\begin{aligned}
\frac{\mathrm{d}E_h(t)}{\mathrm{d}t} &= \frac{\beta_m I_m(t) + \beta_s I_s(t) + \beta_T I_T(t)}{N_h^*} S_h^* - \beta_{rh} \frac{I_r(t)}{N_h^*} S_h^* - (\nu_h + d) E_h(t),\\
\frac{\mathrm{d}I_m(t)}{\mathrm{d}t} &= \theta \nu_h E_h(t) - \gamma_m I_m(t) - d I_m(t),\\
\frac{\mathrm{d}I_s(t)}{\mathrm{d}t} &= (1-\theta)\nu_h E_h(t) - \gamma_s I_s(t) - (d+\delta_s) I_s(t),\\
\frac{\mathrm{d}I_T(t)}{\mathrm{d}t} &= \gamma_s I_s(t) - \gamma_T I_T(t) - (d+\delta_T) I_T(t),\\
\frac{\mathrm{d}E_r(t)}{\mathrm{d}t} &= \beta_{hr} \frac{\eta_s I_s(t) + \eta_T I_T(t)}{N_h^*} S_r^*(t) + \beta_r \frac{I_r(t)}{N_r^*} S_r^*(t) - (\nu_r + \mu) E_r(t),\\
\frac{\mathrm{d}I_r(t)}{\mathrm{d}t} &= \nu_r E_r(t) - \mu I_r(t).
\end{aligned}$$

Let us introduce the matrix functions $F(t)$ and $V(t)$ of dimension 7×7 as

$$F(t) = \begin{bmatrix}
0 & \beta_m \frac{S_h^*}{N_h^*} & \beta_s \frac{S_h^*}{N_h^*} & \beta_T \frac{S_h^*}{N_h^*} & 0 & \beta_{rh} \frac{S_h^*}{N_h^*} \\
0 & 0 & 0 & 0 & 0 & 0 \\
0 & 0 & 0 & 0 & 0 & 0 \\
0 & 0 & 0 & 0 & 0 & 0 \\
0 & 0 & \beta_{hr} \frac{\eta_s}{N_h^*} S_r^*(t) & \beta_{hr} \frac{\eta_T}{N_h^*} S_r^*(t) & 0 & \beta_r \frac{S_r^*(t)}{N_r^*} \\
0 & 0 & 0 & 0 & 0 & 0
\end{bmatrix},$$

$$V(t) = \begin{bmatrix}
\nu_h + d & 0 & 0 & 0 & 0 & 0 \\
-\theta\nu_h & \gamma_m + d & 0 & 0 & 0 & 0 \\
-(1-\theta)\nu_h & 0 & \gamma_s + d + \delta_s & 0 & 0 & 0 \\
0 & 0 & -\gamma_s & \gamma_T + d + \delta_T & 0 & 0 \\
0 & 0 & 0 & 0 & \nu_r + \mu & 0 \\
0 & 0 & 0 & 0 & -\nu_r & \mu
\end{bmatrix}.$$

Note that $F(t)$ is a non-negative matrix function, while $-V(t)$ is cooperative.

6.4.1 Local stability of the disease-free periodic solution

As per that the above discussion, the following theorem concerns the local stability of the disease-free periodic solution E_0 of (6.1).

Theorem 6.1. *The disease-free periodic solution E_0 of (6.1) is locally asymptotically stable if $\mathcal{R}_0 < 1$, whereas it is unstable if $\mathcal{R}_0 > 1$.*

Proof. The Jacobian matrix of (6.1) calculated at E_0 is given by.

$$J(t) = \begin{bmatrix} F(t) - V(t) & 0 \\ A(t) & M \end{bmatrix},$$

where

$$A(t) = \begin{bmatrix} 0 & \beta_m & \beta_s & \beta_{_T} & 0 & \beta_{rh} \\ 0 & 0 & 0 & 0 & 0 & 0 \\ 0 & 0 & \beta_{hr}\dfrac{\eta_s}{N_h^*}S_r^*(t) & \beta_{hr}\dfrac{\eta_{_T}}{N_h^*}S_r^*(t) & 0 & \beta_r \end{bmatrix} \text{ and } M = \begin{bmatrix} -d & \xi & 0 \\ 0 & -\xi - d & 0 \\ 0 & 0 & -\mu \end{bmatrix}.$$

According to [100], E_0 is L.A.S. if $\rho(\Phi_M(\omega)) < 1$ and $\rho(\Phi_{F-V}(\omega)) < 1$. M is a constant matrix and its eigenvalues are $\lambda_1 = -d < 0$, $\lambda_2 = -\xi - d < 0$ and $\lambda_3 = -\mu < 0$. Since λ_1, λ_2 and λ_3 are negative, we have $\rho(\Phi_M) < 1$. Consequently, the stability of E_0 depends on $\rho(\Phi_{F-V}(\omega))$. Thus, E_0 is locally asymptotically stable if $\rho(\Phi_{F-V}(\omega)) < 1$, and unstable if $\rho(\Phi_{F-V}(\omega)) > 1$. Hence, we complete the proof by applying Theorem B. ■

6.4.2 The time-average basic reproduction number

Using the general method introduced in [37], we calculate the basic reproduction number of the autonomous model obtain from (6.1) by setting the time-varying parameters $\tilde{\Pi}_r(t) \equiv \Pi_r$ and $K(t) \equiv K_r$ to constant.

Substituting the value of $S_r^*(t) \equiv S_r^* = K_r\left(\frac{\Pi_r - \mu}{\Pi_r}\right)$ in the disease-free equilibrium for all $t \geqslant 0$, we obtain the Jacobian F given by

$$F = \begin{bmatrix} 0 & \beta_m & \beta_s & \beta_{_T} & 0 & \beta_{rh} \\ 0 & 0 & 0 & 0 & 0 & 0 \\ 0 & 0 & 0 & 0 & 0 & 0 \\ 0 & 0 & 0 & 0 & 0 & 0 \\ 0 & 0 & \beta_{hr}\dfrac{\eta_s}{N_h^*}S_r^* & \beta_{hr}\dfrac{\eta_{_T}}{N_h^*}S_r^* & 0 & \beta_r \\ 0 & 0 & 0 & 0 & 0 & 0 \end{bmatrix},$$

and the Jacobian V given by

$$V = \begin{bmatrix} \nu_h + d & 0 & 0 & 0 & 0 & 0 \\ -\theta\nu_h & \gamma_m + d & 0 & 0 & 0 & 0 \\ -(1-\theta)\nu_h & 0 & \gamma_s + d + \delta_s & 0 & 0 & 0 \\ 0 & 0 & -\gamma_s & \gamma_T + d + \delta_T & 0 & 0 \\ 0 & 0 & 0 & 0 & \nu_r + \mu & 0 \\ 0 & 0 & 0 & 0 & -\nu_r & \mu \end{bmatrix},$$

thus the characteristic polynomial of FV^{-1} is

$$\lambda^4 \left(\lambda^2 - (\mathcal{R}_{hh} + \mathcal{R}_{rr})\lambda + \mathcal{R}_{hh}\mathcal{R}_{rr} - \mathcal{R}_{hr}\mathcal{R}_{rh}\right) = 0, \tag{6.6}$$

where

$$\begin{aligned} \mathcal{R}_{hh} &= \frac{\nu_h}{d+\nu_h}\left(\frac{\theta\beta_m}{\gamma_m + d} + \frac{(1-\theta)\beta_s}{\gamma_s + d + \delta_s} + \frac{(1-\theta)\gamma_s\beta_T}{(\gamma_s + d + \delta_s)(\gamma_T + d + \delta_T)}\right), \\ \mathcal{R}_{hr} &= \frac{(1-\theta)\nu_h\beta_{hr}S_r^*}{\frac{\Pi_h}{d}(\gamma_s + d + \delta_s)(d+\nu_h)}\left(\eta_s + \frac{\gamma_s\eta_T}{\gamma_T + d + \delta_T}\right), \\ \mathcal{R}_{rh} &= \frac{\beta_{rh}\nu_r}{\mu(\mu+\nu_r)}, \qquad \mathcal{R}_{rr} = \frac{\beta_r\nu_r}{\mu(\mu+\nu_r)}. \end{aligned}$$

The characteristic polynomial therefore is the quadratic equation

$$\lambda^2 - (\mathcal{R}_{hh} + \mathcal{R}_{rr})\lambda + \mathcal{R}_{hh}\mathcal{R}_{rr} - \mathcal{R}_{hr}\mathcal{R}_{rh} = 0. \tag{6.7}$$

According to [37], the basic reproduction number is the largest absolute eigenvalue of FV^{-1} and therefore, it is given by the root of the quadratic equation (6.7),

$$\mathcal{R}_0^A = \rho(FV^{-1}) = \frac{\mathcal{R}_{hh} + \mathcal{R}_{rr} + \sqrt{\left(\mathcal{R}_{hh} - \mathcal{R}_{rr}\right)^2 + 4\mathcal{R}_v^2}}{2}, \tag{6.8}$$

where $\mathcal{R}_{hh}$, $\mathcal{R}_{rr}$ and $\mathcal{R}_v = \sqrt{\mathcal{R}_{hr}\mathcal{R}_{rh}}$ are the basic reproduction numbers of human-to-human transmission, rodent-to-rodent transmission and vectorial transmission, respectively. From (6.8) one can see that $\dfrac{\mathcal{R}_{hh} + \mathcal{R}_{rr} + \mathcal{R}_v^2}{\mathcal{R}_{hh}\mathcal{R}_{rr} + 1} > 1$ is the necessary and sufficient condition for $\mathcal{R}_0^A > 1$.

To calculate the time-average basic reproduction number, $[\mathcal{R}_0]$, of the associated non-autonomous system, we use the Remark 4.1. Then, the time-average basic reproduction number is given by

$$[\mathcal{R}_0] = \frac{\mathcal{R}_{hh} + \mathcal{R}_{rr} + \sqrt{\left(\mathcal{R}_{hh} - \mathcal{R}_{rr}\right)^2 + 4[\mathcal{R}_{hr}]\mathcal{R}_{rh}}}{2}, \tag{6.9}$$

where

$$[\mathcal{R}_{hr}] = \frac{(1-\theta)\nu_h\beta_{hr}[S_r^*]}{\frac{\Pi_h}{d}(\gamma_s+d+\delta_s)(d+\nu_h)}\left(\eta_s + \frac{\gamma_s\eta_{_T}}{\gamma_{_T}+d+\delta_{_T}}\right),$$
$$[S_r^*] = [K]\left(\frac{[\tilde{\Pi}_r]-\mu}{[\tilde{\Pi}_r]}\right).$$

6.5 Threshold dynamics

In this section, we show the dynamics of our model depending on the basic reproduction number. We prove the existence of a positive periodic solution of model (6.1) if the basic reproduction number $\mathcal{R}_0 > 1$. In this case, the disease persists, whereas if the basic reproduction number $\mathcal{R}_0 < 1$, then the unique disease-free equilibrium E_0 is globally asymptotically stable and the disease goes extinct.

6.5.1 Global stability of the disease-free equilibrium

Theorem 6.2. *If $\mathcal{R}_0 < 1$, then the disease-free periodic solution E_0 of (6.1) is globally asymptotically stable and if $\mathcal{R}_0 > 1$, then it is unstable.*

Proof. We realize from Theorem 6.1 that if $\mathcal{R}_0 > 1$, then E_0 is unstable and if $\mathcal{R}_0 < 1$, then E_0 is locally asymptotically stable. Consequently, it remains only to show that for $\mathcal{R}_0 < 1$, E_0 is globally attractive. For any ε_1, from Lemma 6.1 and Equation (6.2), there exists $T_1 > 0$ such that $S_r(t) \leqslant S_r^*(t)+\varepsilon_1$, $N_r(t) \geqslant S_r^*(t)-\varepsilon_1$ and $N_h(t) \geqslant N_h^*-\varepsilon_1$ for $t > T_1$. Thus, we get

$$\frac{S_h(t)}{N_h(t)} \leqslant \frac{S_h^*}{N_h^*-\varepsilon_1}, \quad \frac{S_r(t)}{N_h(t)} \leqslant \frac{S_r^*+\varepsilon_1}{N_h^*-\varepsilon_1} \quad \text{and} \quad \frac{S_r(t)}{N_r(t)} \leqslant \frac{S_r^*+\varepsilon_1}{N_r^*(t)-\varepsilon_1}.$$

From (6.1), we obtain

$$\begin{aligned}
\frac{\mathrm{d}E_h(t)}{\mathrm{d}t} &\leqslant \big(\beta_m I_m(t) + \beta_s I_s(t) + \beta_{_T} I_{_T}(t) - \beta_{rh} I_r(t)\big)\frac{S_h^*}{N_h^*-\varepsilon_1} - (\nu_h+d)E_h(t),\\
\frac{\mathrm{d}I_m(t)}{\mathrm{d}t} &= \theta\nu_h E_h(t) - \gamma_m I_m(t) - dI_m(t),\\
\frac{\mathrm{d}I_s(t)}{\mathrm{d}t} &= (1-\theta)\nu_h E_h(t) - \gamma_s I_s(t) - (d+\delta_s)I_s(t),\\
\frac{\mathrm{d}I_{_T}(t)}{\mathrm{d}t} &= \gamma_s I_s(t) - \gamma_{_T} I_{_T}(t) - (d+\delta_{_T})I_{_T}(t),\\
\frac{\mathrm{d}R(t)}{\mathrm{d}t} &= \gamma_m I_m(t) + \gamma_{_T} I_{_T}(t) - \xi R(t) - dR(t),\\
\frac{\mathrm{d}E_r(t)}{\mathrm{d}t} &\leqslant \beta_{hr}\big(\eta_s I_s(t) + \eta_{_T} I_{_T}(t)\big)\frac{S_r^*(t)+\varepsilon_1}{N_h^*-\varepsilon_1} + \beta_r I_r(t)\frac{S_r^*(t)+\varepsilon_1}{N_r^*-\varepsilon_1} - (\nu_r+\mu)E_r(t),\\
\frac{\mathrm{d}I_r(t)}{\mathrm{d}t} &= \nu_r E_r(t) - \mu I_r(t),
\end{aligned}$$

for $t > T_1$. Let $M_{\varepsilon_1}(t)$ be the 6×6 matrix function defined by

$$\begin{bmatrix} -\nu_h - d & \beta_m \dfrac{S_h^*}{N_h^* - \varepsilon_1} & \beta_s \dfrac{S_h^*}{N_h^* - \varepsilon_1} & \beta_{_T} \dfrac{S_h^*}{N_h^* - \varepsilon_1} & 0 & \beta_{rh} \dfrac{S_h^*}{N_h^* - \varepsilon_1} \\ \theta\nu_h & -\gamma_m - d & 0 & 0 & 0 & 0 \\ (1-\theta)\nu_h & 0 & -\gamma_s - d - \delta_s & 0 & 0 & 0 \\ 0 & 0 & \gamma_s & -\gamma_{_T} - d - \delta_{_T} & 0 & 0 \\ 0 & 0 & \beta_{hr}\eta_s \dfrac{S_r^* + \varepsilon_1}{N_h^* - \varepsilon_1} & \beta_{hr}\eta_{_T} \dfrac{S_r^* + \varepsilon_1}{N_h^* - \varepsilon_1} & -\nu_r - \mu & \beta_r \dfrac{S_r^* + \varepsilon_1}{N_r^*(t) - \varepsilon_1} \\ 0 & 0 & 0 & 0 & \nu_r & -\mu \end{bmatrix}.$$

Consider the following auxiliary system:

$$\frac{\mathrm{d}\tilde{U}(t)}{\mathrm{d}t} = M_{\varepsilon_1}(t)\tilde{U}(t), \tag{6.10}$$

where $\tilde{U}(t) = \big(\tilde{E}_h(t), \tilde{I}_m(t), \tilde{I}_s(t), \tilde{I}_{_T}(t), \tilde{E}_r(t), \tilde{I}_r(t)\big)$.

Applying Theorem B, it flows that $\mathcal{R}_0 < 1$ if and only if $\rho(\Phi_{F-V}(\omega)) < 1$. It is obvious that $\lim_{\varepsilon_1 \to 0} \Phi_{M_{\varepsilon_1}}(\omega) = \Phi_{F-V}(\omega)$. As $\rho(\Phi_{F-V}(\omega))$ is continuous, we can choose $\varepsilon_1 > 0$ small enough such that $\rho(\Phi_{M_{\varepsilon_1}}(\omega)) < 1$.

From Lemma A, there is an ω-periodic positive function $p_1(t)$ such that $p_1(t)e^{\xi_1 t}$ is a solution of (6.10) and $\xi_1 = \frac{1}{\omega}\ln\rho(\Phi_{M_{\varepsilon_1}}(\omega)) < 0$. For any $h(0) \in \mathbb{R}^6_+$, we can choose $n^* > 0$ s.t. $h(0) \leqslant n^* p_1(0)$ where

$$h(t) = (E_h(t), I_m(t), I_s(t), I_{_T}(t), E_r(t), I_r(t))^T.$$

Applying the comparison principle Theorem E, we obtain $h(t) \leqslant p_1(t)e^{\xi_1 t}$ for all $t > 0$. Therefore, we get

$$\lim_{t\to\infty} (E_h(t), I_m(t), I_s(t), I_{_T}(t), E_r(t), I_r(t))^T = (0,0,0,0,0,0)^T.$$

One can easily find that $N_h(t) \to N_h^*$ as $t \to \infty$. Let $\varepsilon_1 > 0$, we can find $t_{\varepsilon_1} > 0$ such that $I_m(t) \leqslant \varepsilon_1$ and $I_{_T}(t) \leqslant \varepsilon_1$ for all $t \geqslant t_{\varepsilon_1}$. Then, the equation for $R'(t)$ of (6.1) gives $\frac{\mathrm{d}R(t)}{\mathrm{d}t} \leqslant (\gamma_m + \gamma_{_T})\varepsilon_1 - \xi R(t) - dR(t)$, for large t. From where $R(t) \to 0$ as $t \to +\infty$. Thus, from (6.5) and the first equation of (6.1), we obtain that

$$\lim_{t\to\infty} S_h(t) = S_h^* \quad \text{and} \quad \lim_{t\to\infty} S_r(t) = S_r^*(t),$$

and the proof is complete. ■

6.5.2 Existence of positive periodic solutions

Define

$$X := \left\{(S_h, E_h, I_m, I_s, I_T, R, S_r, E_r, I_r) \in \mathbb{R}^9_+\right\},$$
$$X_0 := \left\{(S_h, E_h, I_m, I_s, I_T, R, S_r, E_r, I_r) \in X : \begin{array}{l} E_h > 0, I_m > 0, I_s > 0, \\ I_T > 0, E_r > 0, I_r > 0 \end{array}\right\},$$

and

$$\partial X_0 := X \setminus X_0.$$

Let $P\colon \mathbb{R}^9_+ \to \mathbb{R}^9_+$ denote the Poincaré map corresponding to (6.1), then P is given by

$$P(x^0) = u(\omega, x^0), \quad \text{for } x^0 \in \mathbb{R}^9_+,$$

where $u(t, x^0)$ is the unique solution of (6.1) with initial condition $x^0 \in X$. Clearly,

$$P^m(x^0) = u(m\omega, x^0), \qquad \forall m \geqslant 0.$$

Proposition 6.1. *The sets X_0 and ∂X_0 are both positively invariant with respect to the flow defined by* (6.1).

Proof. Let $\phi \in X_0$ be any initial condition. By solving (6.1) for all $t > 0$, we get that

$$S_h(t) = e^{\int_0^t -(a_1(s)+d)\,ds}\left[S_h(0) + \int_0^t \left(\Pi_h + \xi R(t)\right)e^{\int_0^s (a_1(r)+d)\,dr}\,ds\right] > 0, \tag{6.11}$$

$$E_h(t) = e^{-(\nu_h+d)t}\left[E_h(0) + \int_0^t a_1(s)S_h(s)e^{(\nu_n+d)s}\,ds\right] > 0, \tag{6.12}$$

$$I_m(t) = e^{-(\gamma_m+d)t}\left[I_m(0) + \theta\nu_h\int_0^t E_h(s)e^{(\gamma_m+d)s}\,ds\right] > 0, \tag{6.13}$$

$$I_s(t) = e^{-(\gamma_m+d+\delta_s)t}\left[I_m(0) + (1-\theta)\nu_h\int_0^t E_h(s)e^{(\gamma_m+d+\delta_s)s}\,ds\right] > 0, \tag{6.14}$$

$$I_T(t) = e^{-(\gamma_T+d+\delta_T)t}\left[I_T(0) + \gamma_s\int_0^t I_s(r)e^{(\gamma_T+d+\delta_T)r}\,dr\right] > 0, \tag{6.15}$$

$$R_h(t) = e^{-(\xi+d)t}\left[R(0) + \int_0^t \left(\gamma_s I_s(r) + \gamma_T I_T(r)\right)e^{(\xi+d)r}\,dr\right] > 0, \tag{6.16}$$

$$\begin{aligned} S_r(t) &= e^{\int_0^t -(a_2(s)+\mu)\,ds}\left[S_r(0) + \int_0^t \tilde{\Pi}_r(s)\left(1 - \tfrac{N_r(s)}{K(s)}\right)N_r(s)e^{\int_0^s (a_2(r)+\mu)\,dr}\,ds\right] \\ &> 0, \end{aligned} \tag{6.17}$$

$$E_r(t) = e^{-(\nu_r+\mu)t}\left[E_r(0) + \int_0^t a_2(s)S_r(s)e^{(\nu_r+\mu)s}\,ds\right] > 0, \tag{6.18}$$

$$I_r(t) = e^{-\mu t}\left[I_r(0) + \nu_r\int_0^t E_r(s)e^{-\mu s}\,ds\right] > 0, \tag{6.19}$$

where

$$a_1(t) = \frac{\beta_m I_m(t) + \beta_s I_s(t) + \beta_T I_T(t)}{N_h(t)} + \beta_{rh}\frac{I_r(t)}{N_h(t)},$$
$$a_2(t) = \beta_{hr}\frac{\eta_s I_s(t) + \eta_T I_T(t)}{N_h(t)} + \beta_r\frac{I_r(t)}{N_r(t)}.$$

Thus, X_0 is a positively invariant set. Since X is also positively invariant and ∂X_0 is relatively closed in X, it gives ∂X_0 is positively invariant. ■

Lemma 6.2. *If $\mathcal{R}_0 > 1$, then there exists a $\sigma > 0$ such that for any $\phi \in X_0$ with $\|\phi - E_0\| \leqslant \sigma$, we have*

$$\limsup_{m\to\infty} d\left(P^m(\phi), E_0\right) \geqslant \sigma.$$

Proof. We recognize from Theorem B that $\rho(\Phi_{F-V}(\omega)) > 1$ if $\mathcal{R}_0 > 1$. Then, we can select $\kappa > 0$ small enough such that we have $\rho(\Phi_{F-V-M_\kappa}(\omega)) > 1$, where $M_\kappa(t)$ is the 6×6 matrix function defined by

$$\begin{bmatrix} 0 & \beta_m\kappa & \beta_s\kappa & \beta_T\kappa & 0 & \beta_{rh}\kappa \\ 0 & 0 & 0 & 0 & 0 & 0 \\ 0 & 0 & 0 & 0 & 0 & 0 \\ 0 & 0 & 0 & 0 & 0 & 0 \\ 0 & 0 & \beta_{hr}\eta_s\kappa & \beta_{hr}\eta_T\kappa & 0 & \beta_r\kappa \\ 0 & 0 & 0 & 0 & 0 & 0 \end{bmatrix}.$$

Using the continuous dependence of the solutions on initial values, we find a $\sigma = \sigma(\kappa) > 0$ such that for all $\phi \in X_0$ with $\|\phi - E_0\| \leqslant \sigma$, it holds that

$$\|u(t,\phi) - u(t,E_0)\| \leqslant \kappa, \text{ for } 0 \leqslant t \leqslant \omega.$$

We further claim that

$$\limsup_{m\to\infty} d\left(P^m(\phi), E_0\right) \geqslant \sigma. \tag{6.20}$$

By contradiction suppose that (6.20) does not hold. Then

$$\limsup_{m\to\infty} d\left(P^m(\phi), E_0\right) < \sigma, \tag{6.21}$$

for some $\phi \in X_0$. Without loss of generality, we may assume

$$d\left(P^m(\phi), E_0\right) < \sigma, \ \forall m \geq 0.$$

Then, from the above discussion, we have that

$$\|u(t, P^m(\phi) - u(t,E_0)\| < \sigma, \ \forall m \geq 0, \ t \in [0,\omega]\,.$$

For any $t \geqslant 0$, let $t = m\omega + t_1$, where $t_1 \in [0, \omega)$ and $m = [\frac{t}{\omega}]$, which is the largest integer less than or equal to $\frac{t}{\omega}$. Then, we get

$$\|u\,(t, \phi) - u\,(t, E_0)\,\| = \|u\,(t_1, P^m(\phi)) - u(t_1, E_0)\| < \sigma,$$

for all $t \geqslant 0$, which implies that

$$\frac{S_h(t)}{N_h(t)} \geqslant \frac{S_h^*}{N_h^*} - \kappa, \quad \frac{S_r(t)}{N_h(t)} \geqslant \frac{S_r^*}{N_h^*} - \kappa \quad \text{and} \quad \frac{S_r(t)}{N_r(t)} \geqslant \frac{S_r^*(t)}{N_r^*} - \kappa.$$

Then for $\|\phi - E_0\| \leqslant \sigma$, we obtain

$$\begin{aligned}
\frac{\mathrm{d}E_h(t)}{\mathrm{d}t} &\geqslant (\beta_m I_m(t) + \beta_s I_s(t) + \beta_{_T} I_{_T}(t) - \beta_{rh} I_r(t)) \left(\frac{S_h^*}{N_h^*} - \kappa\right) - (\nu_h + d)E_h(t),\\
\frac{\mathrm{d}I_m(t)}{\mathrm{d}t} &= \theta\nu_h E_h(t) - \gamma_m I_m(t) - dI_m(t),\\
\frac{\mathrm{d}I_s(t)}{\mathrm{d}t} &= (1-\theta)\nu_h E_h(t) - \gamma_s I_s(t) - (d + \delta_s)I_s(t),\\
\frac{\mathrm{d}I_{_T}(t)}{\mathrm{d}t} &= \gamma_s I_s(t) - \gamma_{_T} I_{_T}(t) - (d + \delta_{_T})I_{_T}(t),\\
\frac{\mathrm{d}E_r(t)}{\mathrm{d}t} &\geqslant \beta_{hr}\,(\eta_s I_s(t) + \eta_{_T} I_{_T}(t)) \left(\frac{S_r^*}{N_h^*} - \kappa\right) + \beta_r I_r(t) \left(\frac{S_r^*}{N_r^*} - \kappa\right) - \nu_r E_r(t)\\
&\quad - \mu E_r(t),\\
\frac{\mathrm{d}I_r(t)}{\mathrm{d}t} &= \nu_r E_r(t) - \mu I_r(t).
\end{aligned}$$

Next we consider the auxiliary linear system

$$\frac{\mathrm{d}\hat{U}(t)}{\mathrm{d}t} = \big(F(t) - V(t) - M_\kappa(t)\big)\hat{U}(t), \tag{6.22}$$

where $\hat{U}(t) = \big(\hat{E}_h(t), \hat{I_m}(t), \hat{I}_s(t), \hat{I}_{_T}(t), \hat{E}_r(t), \hat{I}_r(t)\big)$.

Now we have that $\rho(\Phi_{F-V-M_\kappa}(\omega)) > 1$. Again, we have from Lemma A that there exists a positive, ω-periodic function $p_2(t)$ such that $h(t) = e^{\xi_2 t}p_2(t)$ is a solution of (6.22) and $\xi_2 = \frac{1}{\omega}\ln\rho(\Phi_{F-V+M_\kappa}(\omega)) > 0$. Let $t = n\omega$ and n be non-negative integer, we obtain

$$h(n\omega) = e^{n\omega\xi_2}p_2(n\omega) \to \big(\infty, \infty, \infty, \infty, \infty, \infty\big)^T.$$

For any $h(0) \in \mathbb{R}^6_+$, we can choose a real number $n_0 > 0$ such that $h(0) \geqslant n_0 p_2(0)$ where

$$h(t) = (E_h(t), I_m(t), I_s(t), I_{_T}(t), E_r(t), I_r(t))^T.$$

Applying the comparison principle Theorem E, we obtain $h(t) \geqslant p_2(t)e^{\xi_2 t}$ for all $t > 0$, which implies that

$$\lim_{t\to\infty}\left(E_h(t), I_m(t), I_s(t), I_{_T}(t), E_r(t), I_r(t)\right)^T = \left(\infty,\infty,\infty,\infty,\infty,\infty\right)^T.$$

This leads to a contradiction that completes the proof. ■

Theorem 6.3. *Assume that $\mathcal{R}_0 > 1$. Then system (6.1) has at least one positive periodic solution and there exists an $\varepsilon > 0$ such that*

$$\liminf_{t\to\infty}\left(E_h(t), I_m(t), I_s(t), I_{_T}(t), R(t), E_r(t), I_r(t)\right)^T \geqslant \left(\varepsilon,\varepsilon,\varepsilon,\varepsilon,\varepsilon,\varepsilon,\varepsilon\right)^T,$$

for all $\phi \in X_0$.

Proof. First, we prove that P is uniformly persistent with respect to $(X_0, \partial X_0)$, as from this, applying Theorem H, it follows that the solution of (6.1) is uniformly persistent with respect to $(X_0, \partial X_0)$.

From Proposition 6.1, we have that both X and X_0 are positively invariant and ∂X_0 is relatively closed in X. Furthermore, from Lemma 6.1 it follows that system (6.1) is point dissipative. Let us introduce

$$M_\partial = \left\{x^0 \in \partial X_0 : P^m(x^0) \in \partial X_0,\ \forall m \geqslant 0\right\}.$$

where $x^0 = \phi$. We will apply the theory developed in [115] (see also [113, Theorem 2.3]). In order to do so, we first show that

$$M_\partial = \left\{(S_h, 0, 0, 0, 0, 0, S_r, 0, 0) : S_h \geqslant 0,\ S_r \geqslant 0\right\}. \tag{6.23}$$

Let us note that $M_\partial \supseteq \{(S_h, 0, 0, 0, 0, 0, S_r, 0, 0) : S_h \geqslant 0,\ S_r \geqslant 0\}$. It suffices to prove that $M_\partial \subset \{(S_h, 0, 0, 0, 0, 0, S_r, 0, 0) : S_h \geqslant 0,\ S_r \geqslant 0\}$, i.e., for arbitrary initial condition $\phi \in \partial X_0$, $E_h(n\omega) = 0$ or $I_m(n\omega) = 0$ or $I_s(n\omega) = 0$ or $I_{_T}(n\omega) = 0$ or $R(n\omega) = 0$ or $E_r(n\omega) = 0$ or $I_r(n\omega) = 0$, for all $n \geqslant 0$.

Assume by contradiction the existence of an integer $n_1 \geqslant 0$ for which $E_h(n_1\omega) > 0$, $I_m(n_1\omega) > 0$, $I_s(n_1\omega) > 0$, $I_{_T}(n_1\omega) > 0$, $R(n_1\omega) > 0$, $E_r(n_1\omega) > 0$ and $I_r(n_1\omega) > 0$. Then, by putting $t = n_1\omega$ into the place of the initial time $t = 0$ in (6.11)–(6.19), we get that $S_h(t) > 0$, $E_h(t) > 0$, $I_m(t) > 0$, $I_s(t) > 0$, $I_{_T}(t) > 0$, $R(t) > 0$, $S_r(t) > 0$, $E_r(t) > 0$, $I_r(t) > 0$. This is in contradiction with the positive invariance of ∂X_0.

By Lemma 6.2, P is weakly uniformly persistent with respect to $(X_0, \partial X_0)$. Lemma 6.1 guarantees the existence of a global attractor of P. Then E_0 is an isolated invariant set in X and $W^s(E_0) \cap X_0 = \emptyset$. Each solution in M_∂ tends to E_0 and E_0 is clearly acyclic in M_∂. By Theorem I and [115, Remark 1.3.1], we can deduce that P is uniformly (strongly) persistent with respect to $(X_0, \partial X_0)$. Hence, there exists an $\varepsilon > 0$ such that

$$\liminf_{t\to\infty}\left(E_h(t), I_m(t), I_s(t), I_{_T}(t), R(t), E_r(t), I_r(t)\right)^T \geqslant \left(\varepsilon,\varepsilon,\varepsilon,\varepsilon,\varepsilon,\varepsilon,\varepsilon\right)^T,$$

for all $\phi \in X_0$. By Theorem J, P has a fixed point $\bar{\phi} \in X_0$, and hence system (6.1) has at least one periodic solution $u(t, \bar{\phi})$ with

$$\bar{\phi} = \big(\bar{S}_h(0), \bar{E}_h(0), \bar{I}_a(0), \bar{I}_a(0), \bar{I}_s(0), \bar{R}_h(0), \bar{S}_r(0), \bar{E}_r(0), \bar{I}_r(0)\big) \in X_0.$$

Now, let us prove that $\bar{S}_h(0)$ and $\bar{S}_r(0)$ are positive. If $\bar{S}_h(0) = 0 = \bar{S}_r(0)$, then we obtain that $\bar{S}_h(0) > 0$ and $\bar{S}_r(0) > 0$ for all $t > 0$. However, using the periodicity of solution, we have $\bar{S}_h(0) = \bar{S}_h(n\omega) = 0$, and $\bar{S}_r(0) = \bar{S}_r(n\omega) = 0$, that is a contradiction. ■

6.6 A case study – Lassa fever in Nigeria 2017–2020

In this section, we use our model to study the spread of Lassa fever in Nigeria during the epidemic in November 2017 to May 2020. From Section 6.5, we see that $\mathcal{R}_0$ is a threshold parameter for the persistence of the disease in the population (see Theorems 6.2 and 6.3). Simulation results are provided to demonstrate that our model with periodic parameters is well aligned with seasonal fluctuation data.

The functions $\tilde{\Pi}_r(t)$ and $K(t)$ are assumed to be time-periodic with one year as a period and, following e.g. [12, 32], they are supposed to be of the form

$$\tilde{\Pi}_r(t) = \Pi_r \cdot \left(a + \sin\left(\tfrac{2\pi(t+b)}{p}\right)\right) \quad \text{and} \quad K(t) = K_r \cdot \left(1 - \Lambda \cos\left(\tfrac{2\pi(t+b)}{p}\right)\right),$$

where p is period length, a is free adjustment parameter, Λ is the amplitude of seasonality, b is phase angle and (Π_r, K_r) are the (constant) baseline values of the corresponding time-dependent parameters.

Figure 6.3 shows the weekly confirmed cases of 2017–2020 Lassa outbreak in Nigeria ([28]).

6.6.1 Parameter estimation for Nigeria

We used Latin Hypercube Sampling, a sampling tool applied in statistics to quantify simultaneous variation of many parameter values (see, e.g., [70]), as a way to estimate the parameters providing the best fit. The method consists of generating a representative sample set for all parameters shown in Table 6.2 from parameter ranges obtained from literature and the World Bank website [99] as shown in Table 6.2. Then the solutions of model (6.1) with the specified parameters value are determined numerically for all elements of this representative sample set. Finally, the least squares method is used to get the best fit.

Figure 6.4 shows model (6.1) fitted to data from Nigeria [28]. Our model provides a reasonably good fit, generating the three peaks of Lassa fever happened in

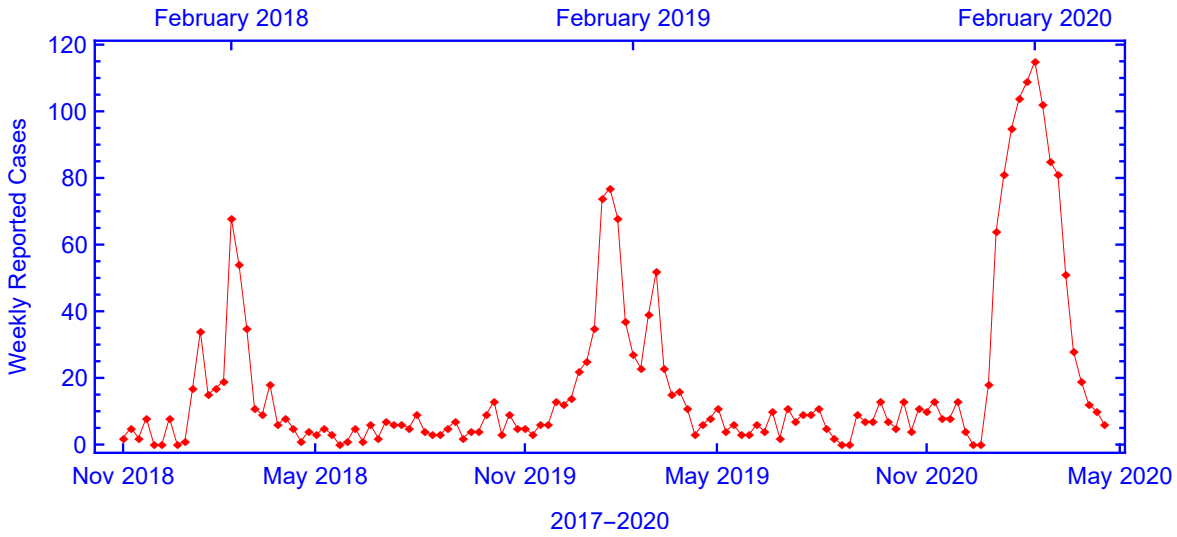

Figure 6.3: *Confirmed number of cases reported of the November* 2017*–May* 2020 *Lassa fever epidemic in Nigeria ([28]).*

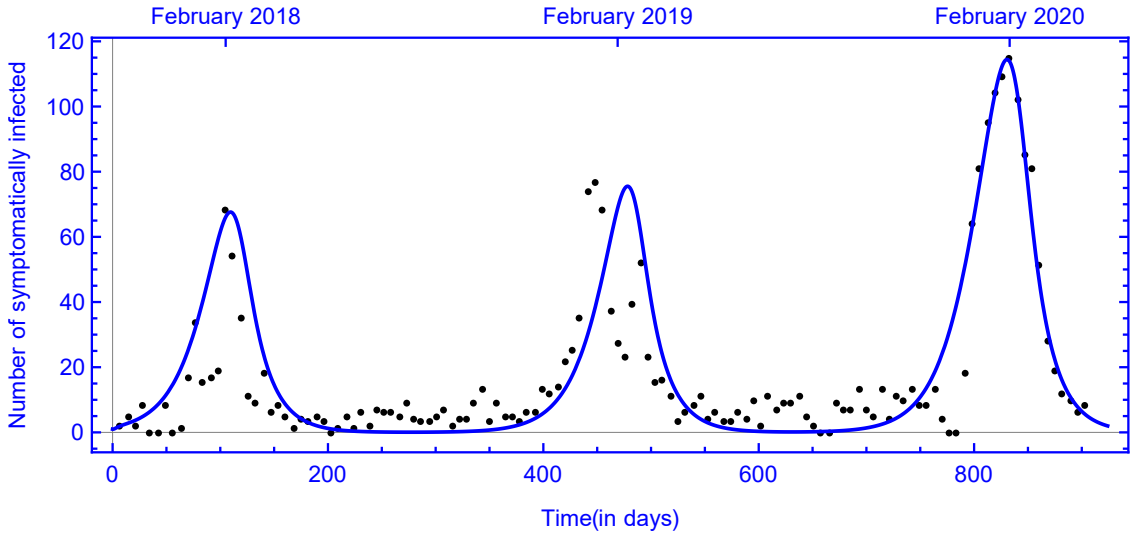

Figure 6.4: *Fitting the model to the data for the 2017-2020 Lassa outbreaks in Nigeria with parameter values in Table 6.2 and initial condition* $(S_h, E_h, I_m, I_s, I_T, R, S_r, E_r, I_r)(0) = (2 \times 10^8, 40, 49, 2, 20, 14 \times 10^3, 5 \times 10^8, 10^6, 10^3)$.

the last three seasons in Nigeria.

Figure 6.5 shows the long-term behaviour of infectious humans and rodents with the best fit parameters given in Table 6.2 (see baseline). The results indicate that Lassa fever in Nigeria will persist and show periodic fluctuations in the coming years

unless additional measures are taken.

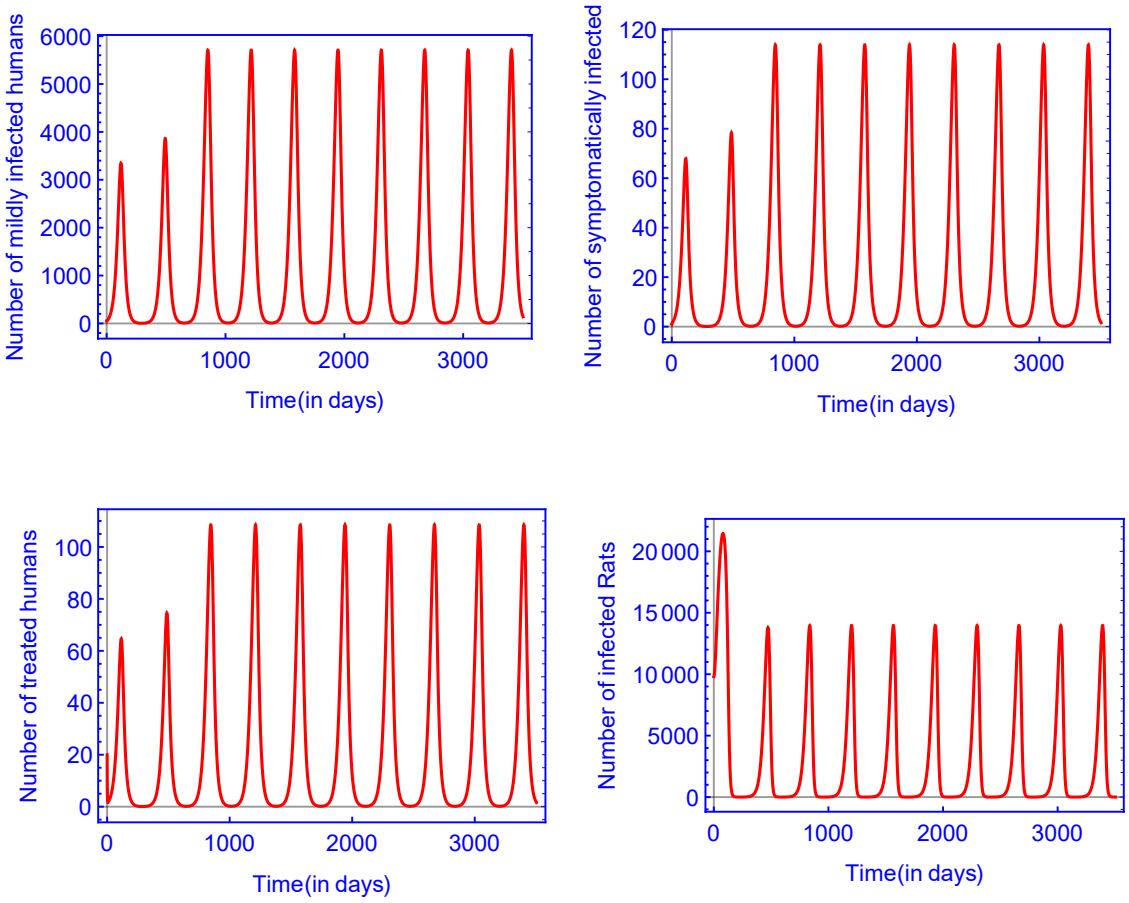

Figure 6.5: *The long-term dynamic behaviour of the model* (6.1) *variables with parameter values in Table 6.2 (see baseline).*

6.6.2 Long-term behaviour

We compute the basic reproduction $\mathcal{R}_0$ numerically by using the method developed in [72, Section 2]. By Theorem 6.2, we know that the disease will die out if $\mathcal{R}_0 < 1$. We obtain $\mathcal{R}_0 = 0.7165 < 1$ with the set of parameter values in Table 6.2 (see Extinction). In this case, the long-term behaviours of the infectious humans and rodents are shown in Figure 6.6, which implies that the unique disease-free equilibrium E_0 is globally asymptotically stable when $\mathcal{R}_0 < 1$.

By Theorem 6.3, system (6.1) has a positive ω-periodic solution if $\mathcal{R}_0 > 1$. Figure 6.7 illustrates the uniform persistence of the disease when $\mathcal{R}_0 = 3.2678 > 1$ with the set of parameter values in Table 6.2 (see Persistent). These simulations correspond to our theoretical results.

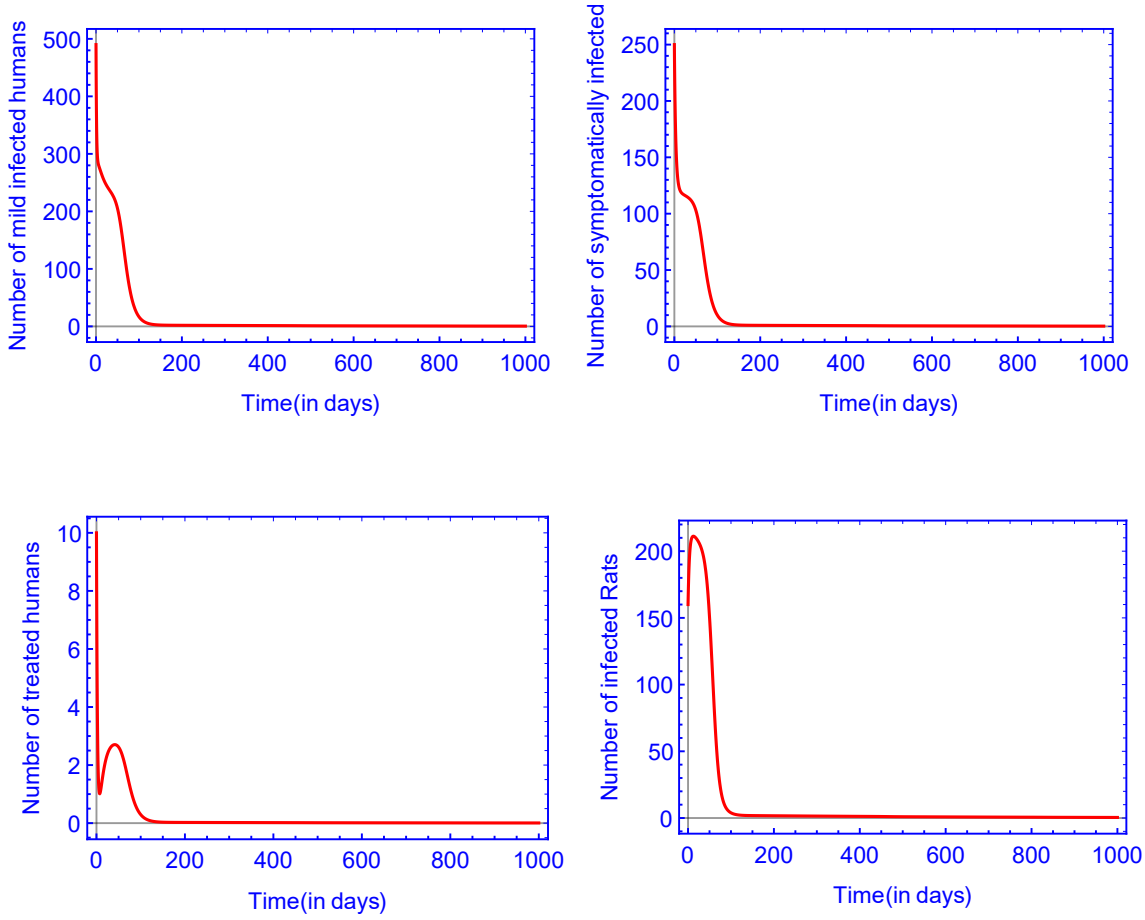

Figure 6.6: *Extinction of Lassa fever for* $\mathcal{R}_0 = 0.7165 < 1$ *with parameters given in Table 6.2 (see Extinction).*

6.6.3 Parameter changes for Nigeria

In this study, one of our core concerns was to see what changes in the parameters might trigger a periodic reappearance of the epidemic. Since we have a large number of parameters, it is not easy to rigorously determine which of the parameters play the most important role in the variation of the dynamics, so we are just attempting to explain the possible changes through a few examples.

Numerically, with the same set of parameter values used in the extinction case (see Figure 6.6) except human-to-human transmission (β_s) and the rodent-related parameters ($\beta_{rh}, \beta_r, \Pi_r, \mu, K_r$), we calculated the value of the basic reproduction number $\mathcal{R}_0 = 3.2678 > 1$, i.e. we increased human-to-human, rodent-to-human and rodent-to-rodent transmission rates, rodent death rate and maximal carrying capacity of rodents, while rodent birth rate was decreased. Accordingly, it can be seen that the disease compartments are persistent with these parameters, and the epidemic

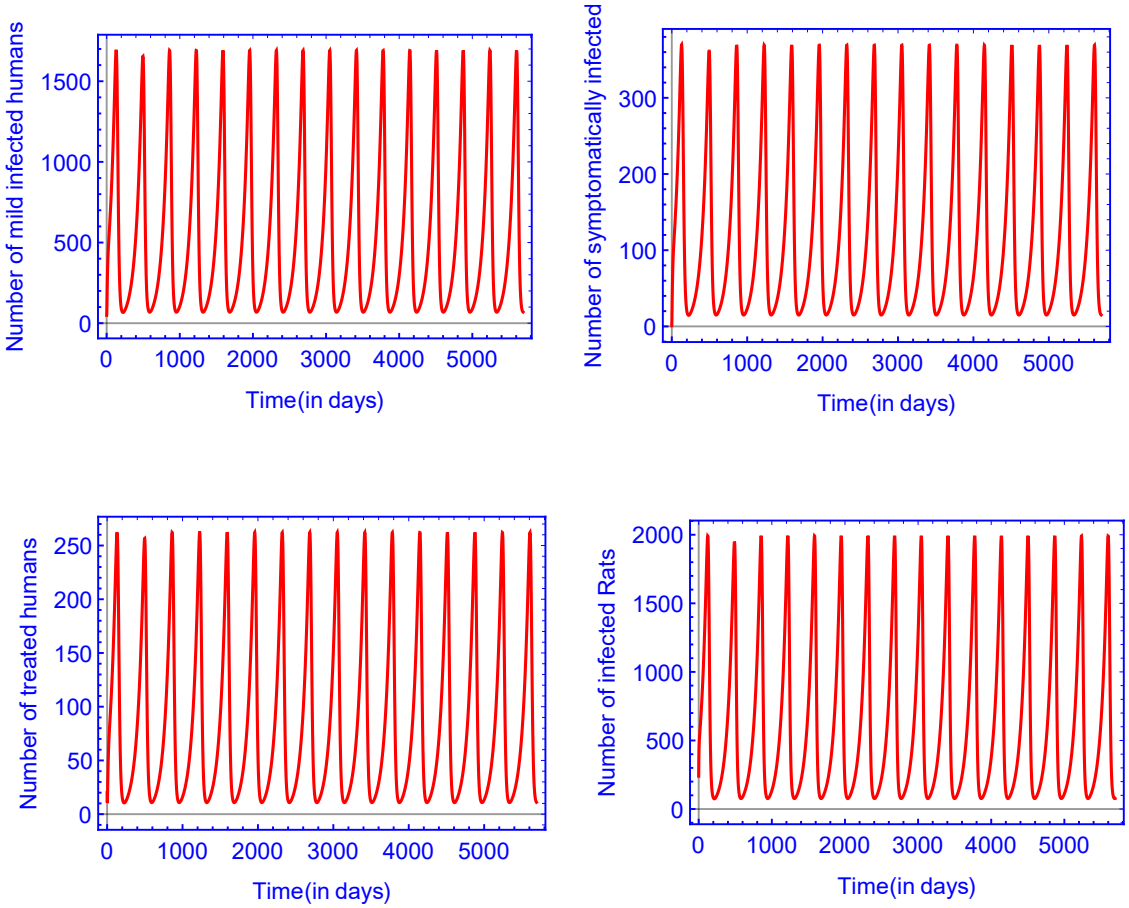

Figure 6.7: *Uniform persistence of Lassa fever for* $\mathcal{R}_0 = 3.2678 > 1$ *with parameters given in Table 6.2 (see Persistence).*

becomes endemic in the population periodically recurring annually (see Figure 6.7).

For a further illustration to explain the impact of parameter changes on the spread of Lassa fever, we plotted the solution of our model with three different values for a rodent birth rate (Π_r), human-to-human transmission rate (β_s) and rodent-to-rodent transmission rate(β_r) in Figure 6.8. As is observed, the number of symptomatically infected people increases by raising any term of Π_r or β_s or β_r, and the disease becomes recurring periodically every year.

6.6.4 Sensitivity analysis of $\mathcal{R}_0$

In any given time, formula (6.8) gives us with the basic reproduction number, $\mathcal{R}_0^A$, of the associated autonomous system by substituting the parameter values in it, along with the value of the time-dependent parameters at that time. Moreover, for-

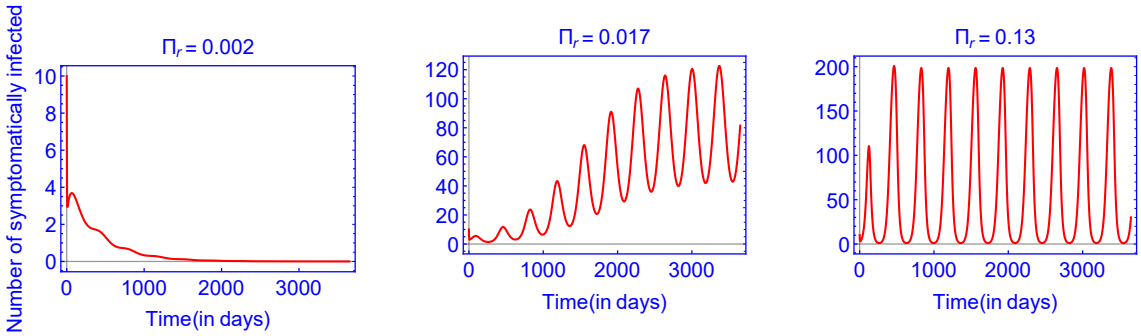

(a) *Model* (6.1) *solution with distinct* Π_r*–values.*

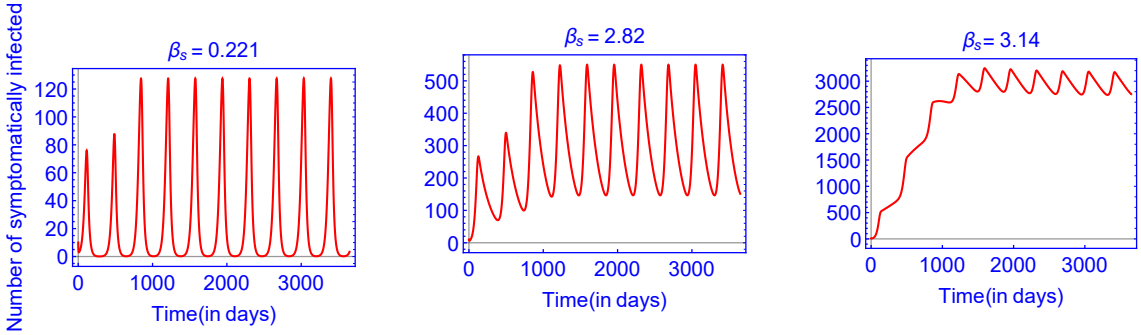

(b) *Model* (6.1) *solution with distinct* β_s*–values.*

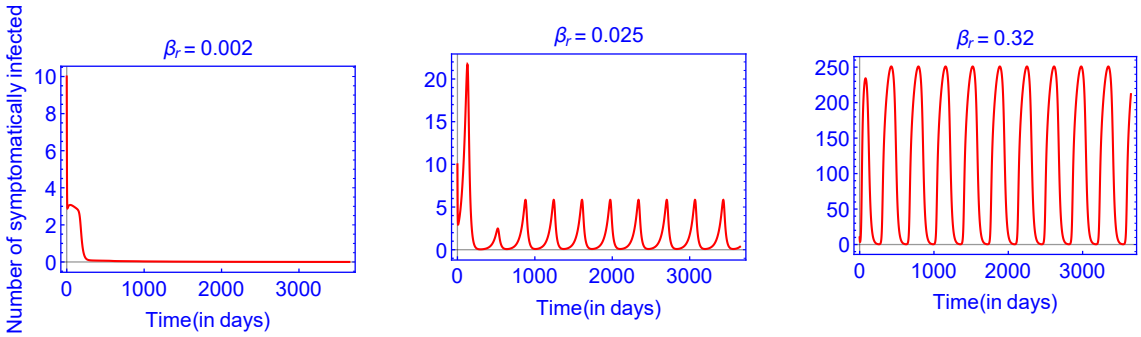

(c) *Model* (6.1) *solution with distinct* β_r*–values.*

Figure 6.8: *The number sympatrically infected humans with three different values of in (a) rodent birth rate* (Π_r)*, in (b) human-to-human transmission rate(* β_s*) and in (c) rodent-to-rodent transmission rate(* β_r*) with parameter values are given in Table 6.2.*

mula (6.9) provides us the time-average basic reproduction number, $[\mathcal{R}_0]$, of the associated non autonomous system which can be calculated using the notation in Remark 4.1.

In Figure 6.9, we plot the time-average basic reproduction number $[\mathcal{R}_0]$ (see Figure 6.9a) and the basic reproduction number $\mathcal{R}_0^A$ (see Figure 6.9b), as a function of maximal carrying capacity of the rodents (K_r), and human-to-human transmis-

sion rate (β_s), rodent-to-human transmission rate (β_{rh}) and human-to-rodent transmission rate (β_{hr}). The rest of the parameters are set as obtained in the fitting of symptomatically infected cases in Table 6.2 (see baseline). As can be observed, both reproduction numbers increase by increasing the transmission rates β_s, β_{rh} and β_{hr}. Increasing rodent birth rates also increase reproduction numbers. Although human-to-human and human-to-rodent transmission rates have a notable impact on the increase in both reproduction numbers, the figure indicates that rodent control is a significant factor in Lassa's spread and that vector control might be necessary to suppress the disease.

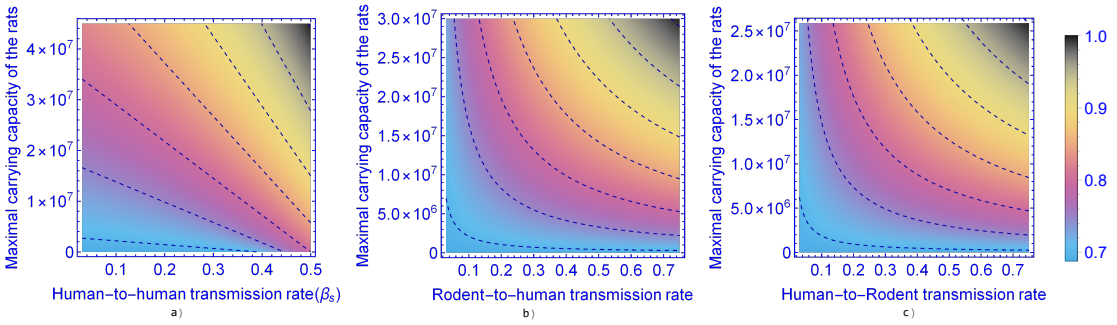

(a) *The contour plot of the time-average reproduction number,* $[\mathcal{R}_0]$.

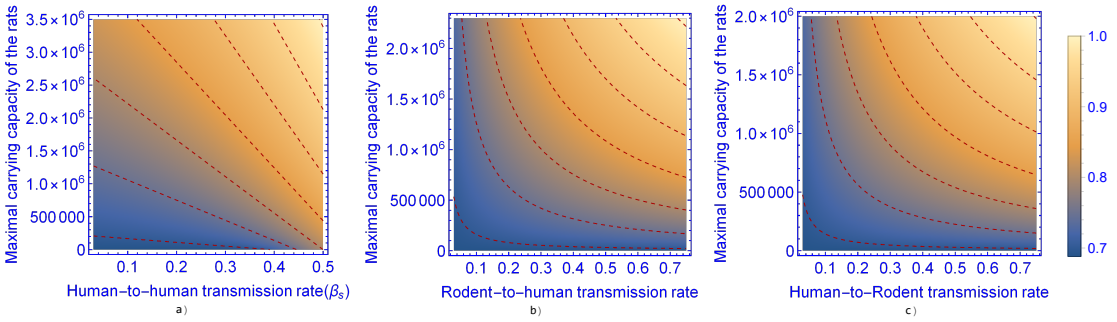

(b) *The contour plot of the basic reproduction number,* $\mathcal{R}_0^A$.

Figure 6.9: *The contour plot of the time-average basic reproduction number,* $[\mathcal{R}_0]$ *in (a) and the basic reproduction number,* $\mathcal{R}_0^A$ *of the autonomous model in (b), as a function of maximal carrying capacity of the rats* (K_r) *and in a) human-to-human transmission rate* (β_s)*, b) rodent-to-human transmission rate* (β_{rh}) *and c) human-to-rodent transmission rate* (β_{hr})*.*

In Figure 6.10, we plot the curves of the time-average basic reproduction number $[\mathcal{R}_0]$, and the basic reproduction number $\mathcal{R}_0^A$ with respect to maximal carrying capacity of rodents (K_r), rodents birth rate (Π_r), human-to-human transmission rate (β_s), human-to-rodent transmission rate (β_{hr}), rodent-to-human transmission rate (β_{rh}) and rodent-to-rodent transmission rate (β_r), respectively. The calculations show that

$[\mathcal{R}_0] \geqslant \mathcal{R}_0^A$, suggesting that $\mathcal{R}_0^A$ provides an underestimation of the risk of disease transmission.

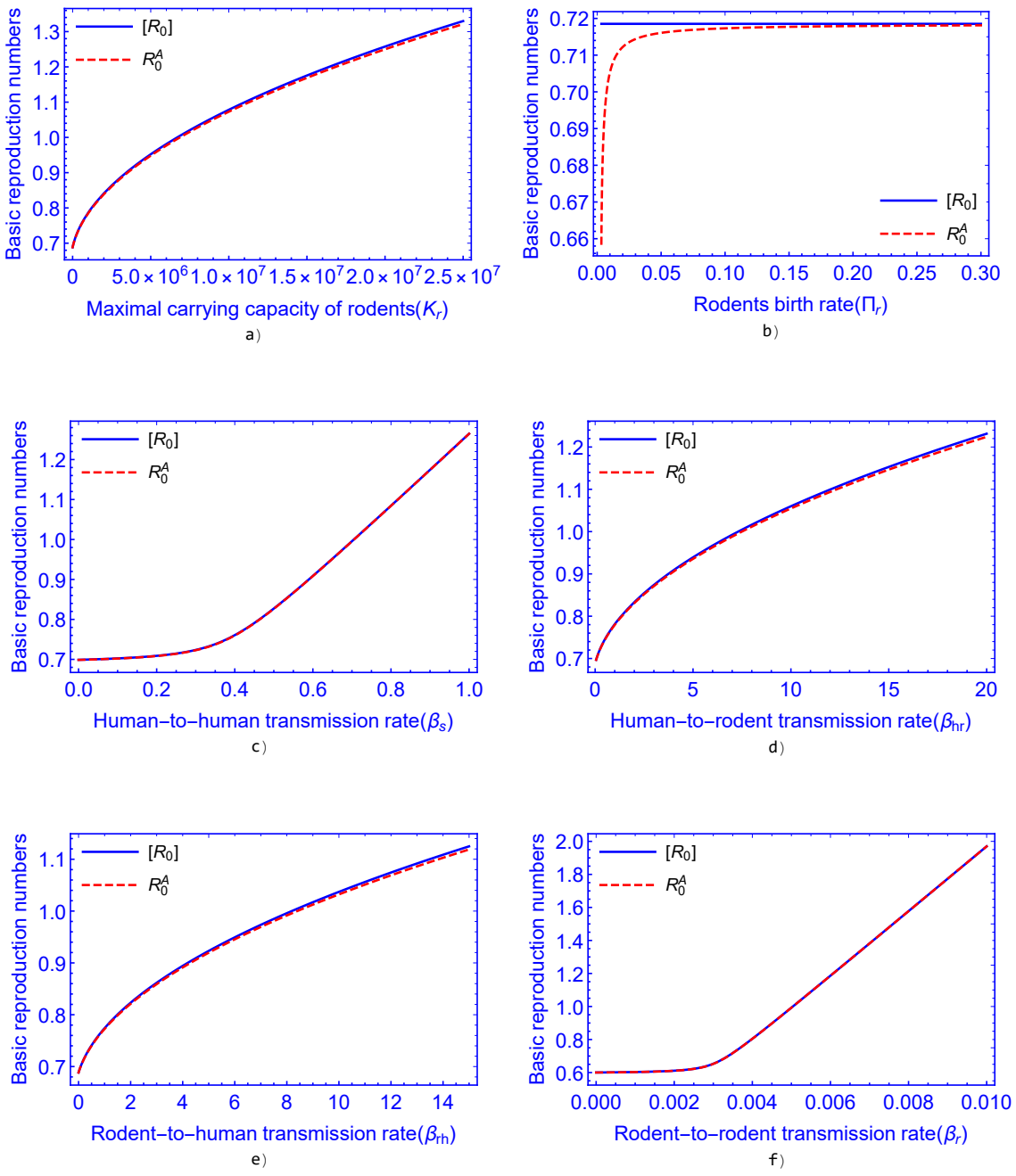

Figure 6.10: *The curves of the time-average basic reproduction number* $[\mathcal{R}_0]$ *and the basic reproduction number of the autonomous model* $\mathcal{R}_0^A$ *versus in a) maximal carrying capacity of rodents* (K_r)*, b) rodents birth rate* (Π_r)*, c) human-to-human transmission rate* (β_s)*, d) human-to-rodent transmission rate* (β_{hr})*, e) rodent-to-human transmission rate* (β_{rh}) *and f) rodent-to-rodent transmission rate* (β_r).

We mention that numerous papers have results on under-and overestimation of the average basic reproduction number. For instance, it was shown in [103] that $\mathcal{R}_0 > [\mathcal{R}_0]$, while in [62] the authors gave an example with $\mathcal{R}_0 < [\mathcal{R}_0]$. In general, $\mathcal{R}_0 \neq [\mathcal{R}_0]$ and more details can also be found in [9, 103].

Table 6.2: *Baseline values, ranges, units and values for extinction and persistence of model* (6.1) *parameters.*

Parameter	Baseline	Range	Units	Value for		Source
				Extinction	Persistence	
N_h	2×10^8	–	Persons	2×10^8	2×10^8	[99]
Π_h	$10,000$	–	Persons day^{-1}	$10,000$	$10,000$	[99]
d	0.00005	–	Day^{-1}	0.00005	0.00005	[99]
δ_s	0.485	$0.1 - 0.5$	Day^{-1}	0.201	0.201	[75]
δ_T	0.269	$0.1 - 0.5$	Day^{-1}	0.224	0.224	[75]
β_m	0.0637	$0.03 - 0.5$	Day^{-1}	0.181	0.181	[34, 75]
β_s	0.221	$0.03 - 0.5$	Day^{-1}	0.275	0.367	[34, 75]
β_T	0.206	$0.03 - 0.5$	Day^{-1}	0.259	0.259	[34, 75]
β_{hr}	0.259	$0.03 - 0.5$	Day^{-1}	0.242	0.242	[75]
β_{rh}	0.0296	$0.1 - 0.8$	Day^{-1}	0.216	0.373	[75]
β_r	0.052	$0.005 - 0.4$	Day^{-1}	0.007	0.02	[32, 75]
η_s	0.238	$0.1 - 0.5$	Day^{-1}	0.392	0.392	Assumed
η_T	0.319	$0.1 - 0.5$	Day^{-1}	0.344	0.344	Assumed
θ	0.815	$0.7 - 0.9$	Day^{-1}	0.802	0.802	[99]
γ_m	0.108	$0 - 1$	Day^{-1}	0.433	0.433	[75]
γ_s	0.024	$0.001 - 0.025$	Day^{-1}	0.0123	0.0123	[75]
γ_T	0.446	$0 - 1$	Day^{-1}	0.256	0.256	[75]
ν_h	0.528	$0.1 - 1$	Day^{-1}	0.515	0.515	[32, 75]
ν_r	0.32	$0.1 - 1$	Day^{-1}	0.299	0.299	[32, 75]
ξ	0.00578	$0.0035 - 0.03$	Day^{-1}	0.00578	0.00578	[75]
Π_r	0.172	–	–	0.2	0.146	Assumed
μ	0.003	$0.001 - 0.006$	Day^{-1}	0.005	0.006	[32, 75]
K_r	$20,000$	–	–	$198,000$	$342,000$	Assumed
a	0.31	$0 - 1$	–	0.31	0.31	Assumed
Λ	0.31	$0 - 1$	–	0.31	0.31	[32]
b	134.8	$0 - 365$	–	249	163.5	[32]

6.7 Discussion

We formulated and analyzed a periodic LHF transmission model between humans and rodents that involves the seasonal effects (by including periodic coefficients), human-to-human transmission and the vertical transmission of the virus in rodents.

By using the theory presented in [103], we derived and numerically computed the basic reproduction number $\mathcal{R}_0$. It is demonstrated that the global dynamics is determined by the basic reproduction number $\mathcal{R}_0$. If $\mathcal{R}_0 > 1$, then the disease is uniformly persistent and there exists at least one positive periodic solution, while the disease-free periodic solution E_0 is globally asymptotically stable and the disease dies out if $\mathcal{R}_0 < 1$. Our numerical simulations show that there is only one positive periodic solution which is globally asymptotically stable in the case where $\mathcal{R}_0 > 1$ (see Figure 6.7) and the disease dies out if $\mathcal{R}_0 < 1$ (see Figure 6.6).

Numerically, we have computed all constant and periodic parameters by using some published data and studied LHF in Nigeria. The fitted curve based on our model reflects the seasonal fluctuation and coincide in quite well with the reported data (see Figure 6.4). The reproduction numbers were estimated as a function of the parameters $K_r, \Pi_r, \beta_s, \beta_{hr}, \beta_{rh}$ and β_r. The calculations show that the basic reproduction number $\mathcal{R}_0^A$ underestimates the disease transmission risk (see Figure 6.10).

Our model enables us to evaluate what kind of parameter changes might trigger a periodic recurrence of LHF. Using numerical simulations, we observed that the human-to-human transmission rate has a substantial impact on the prevalence of the disease, but the most significant factors in Lassa's periodic recurrence are the rodent related parameters.

The simulation results indicate that, if no additional intervention is taken, Lassa will persist and exhibit periodic fluctuation in the next few years in Nigeria. These simulations are compatible with our analytic results, and the model can be also used to study the Lassa fever transmission in other countries of West Africa such as Benin, Ghana, Guinea, Liberia, Mali, Sierra Leone, and Togo so long as the data are accessible.

Summary

The Ph.D. thesis investigates the impact of the periodicity of weather on the spread of malaria, Zika fever, and Lassa fever by applying non-autonomous compartmental population models with time-dependent (periodic) parameters. The dynamics of the system is characterized by the basic reproduction number ($\mathcal{R}_0$) of periodic compartmental models, defined as the spectral radius of an integral operator acting on the space of continuous periodic functions, and it has also been shown that the reproduction number is a threshold parameter with respect to disease extinction or persistence. Our aim is to show that the disease-free periodic solution of our newly established models is globally asymptotically stable if $\mathcal{R}_0 < 1$, while for $\mathcal{R}_0 > 1$, there exists at least one positive ω-periodic solution. We provide numerical studies and give examples to describe what kind of parameter changes might trigger the periodic recurrence of the disease.

Chapter 2 begins with a short introduction to mosquito-borne and rodent-borne diseases, then we discuss the effects of periodicity of weather on malaria, Zika fever and Lassa fever.

In Chapter 3, we briefly discuss the general form of non-autonomous epidemic systems and the most important definitions, conditions, theorems and methods relevant to the topic of the thesis.

Malaria is an acute febrile illness caused by *Plasmodium* microorganisms spread to humans by female *Anopheles* mosquitoes. Malaria is the deadliest vector-borne disease, causing an estimated 409,000 deaths in 2019. Periodicity of weather and climate change are very important factors in the life cycle of the parasites and the mosquitoes transmitting them. Hence, it is of crucial importance to understand how changes in weather affect the spread of malaria.

In Chapter 4, we set up and study a periodic compartmental population model for the spread of malaria, dividing the human population into two types based on their immunity level: the non-immune, i.e. those who have not developed any immunity against malaria, and the semi-immune, that is those who have some partial immunity due to their genetics or by contracting the disease earlier in their life. Semi-immune human, non-immune human and mosquito compartments are denoted by the lower indices m, n and v. Susceptible humans (S_m and S_n) can be infected by malaria. Following the infectious mosquito bite, susceptibles proceed to the exposed compart-

ment (E_m, E_n). Individuals in these compartments have no symptoms yet. After the incubation time, exposed individuals proceed to the infectious class (I_m, I_n). For semi-immune, there is an additional immune compartment (R_m). Humans in the class R_m are partially immune to the disease, but their blood stream still has a low level of parasites and they are still able to infect susceptible mosquitoes. We have three compartments for the mosquitoes: susceptibles (S_v), exposed (E_v) and infected (I_v). Following the annual change of weather, we consider periodic vital dynamics of mosquitoes by setting the mosquito birth rates and mosquito death rates as well as the biting rates to be periodic with one year as period. We determine the basic reproduction number $\mathcal{R}_0$ to characterize the dynamics of our model, and we show the global stability of the disease-free periodic solution or the endemicity of malaria as well as the existence of a positive ω-periodic solution, depending on the basic reproduction number. Numerical simulations consistent with the analytical results suggest that mosquito control is an important factor in malaria transmission. Finally, we show that the time-average reproduction rate yields an underestimate of malaria transmission risk.

Zika fever is a mosquito-borne disease caused by the Zika virus. Zika virus is spread primarily in tropical and subtropical regions through the bite of infected female mosquitoes of the *Aedes* genus, the same species responsible for transmitting dengue, chikungunya, and yellow fever. The Zika virus is also transmitted through sexual contact, mainly from men to women. Mothers infected with Zika virus can transmit the disease to their fetus during pregnancy or during delivery. This transmission can lead to microcephaly and other congenital malformations that can cause lifelong disabilities. Although a regular periodic recurrence of Zika has not been observed so far, it is expected that this might be altered by weather seasonality.

In Chapter 5, we develop a nine-compartment model that describes the spread of Zika virus disease, including sexual and vectorial transmission, in a periodically changing environment. We apply a non-autonomous model with periodic mosquito birth, death and biting rates to integrate the impact of the periodicity of weather on the spread of Zika. We divide the total human population into six compartments: susceptible $S_h(t)$, exposed $E_h(t)$, symptomatically infected $I_s(t)$, asymptomatically infected $I_a(t)$, convalescent $I_r(t)$, and recovered $R(t)$ at time $t > 0$, while the vector population is divided into three classes: susceptible $S_v(t)$, exposed $E_v(t)$ and infectious $I_v(t)$ individuals. Our aim is to determine the basic reproduction number for our newly established periodic model which serves as a threshold parameter regarding the persistence of the disease. In the analysis we follow the methods established in Rebelo et al. [90] to show the global stability of the disease-free solution and the persistence of the infectious compartments. Using our model and taking Ecuador and Colombia as two examples, the fitted curves match the data very well. We show some seasonal measures of Zika virus disease control in both Ecuador and Colombia. The

results suggest that even mosquito control limited to the peak period of mosquito abundance could have a significant impact on disease control. Based on the sensitivity analysis, we can assess that the most effective measures to reduce transmission are control of mosquito populations and protection against their bites. Our model allows us to estimate what kind of parameter changes might lead to a periodic recurrence of Zika. Using numerical simulations, we found that mosquito birth and death rates are the most significant factors in a possible periodic recurrence of Zika, however, sexual transmission also has a significant effect on the prevalence of the disease.

Lassa haemorrhagic fever (LHF) is a zoonotic, acute viral hemorrhagic fever caused by the Lassa virus from the *Arenaviridae* family. LHF is usually transmitted to humans via direct or indirect exposure to food or other items contaminated with urine or feces of infected multimammate rats (*Mastomys natalensis*), through the respiratory or gastrointestinal tracts. Person-to-person transmission has also been observed. The virus remains in body fluids even after recovery. Lassa fever is endemic among rats in parts of West Africa, while it is endemic in humans in several countries of the region. In these regions, the number of infections per year is estimated between 100,000 and 300,000, with around 5,000 deaths. Lassa fever appears in WHO's Blueprint list of diseases to be prioritized for research and development. Although rodent populations are affected by weather conditions, so far, no compartmental model with time-dependent parameters has been established.

In Chapter 6, we formulate and study a seasonal compartmental model for Lassa fever transmission dynamics considering human-to-human, rodent-to-human transmission and the vertical transmission of the virus in rodents as well as time-dependent parameters. We divide the human population into six compartments: susceptible S_h, exposed E_h, symptomatically infected $I_s(t)$, mildly infected I_m, treated I_T, and recovered individuals with temporary immunity R. An individual may proceed from susceptible (S_h) to exposed (E_h) upon contracting the disease. Individuals in the exposed compartment have no symptoms yet. After the incubation time, an exposed individual moves either to the symptomatically infected class (I_s) or to the mildly infected class (I_m), depending on whether that person shows symptoms or not. Infected people from I_s may move to the treated compartment (I_T), including those who need hospital treatment. After the infection period, recovered persons move to the class R. The vector population (*Mastomys natalensis* rat) is divided into three compartments: susceptible S_r, exposed E_r and infectious I_r, respectively. To incorporate the impact of periodicity of weather on the spread of Lassa, we introduce a non-autonomous model with time-dependent parameters for rodent birth rate and carrying capacity of the environment with respect to rodents. To study the dynamics of our time-periodic model, we will apply the theory initiated in [90, 103]. Here we adapt these methods to our system with human-to-human and rodent-to-human

transmission with a logistic growth of rodents. We derived and numerically computed the basic reproduction number, it is also demonstrated that the global dynamics is determined by the basic reproduction number. Numerically, we have computed all constant and periodic parameters by using some published data and studied Lassa fever in Nigeria. The fitted curve based on our model reflects the seasonal fluctuation and coincide in quite well with the reported data in Nigeria. The reproduction numbers were estimated as a function of the parameters $K_r, \Pi_r, \beta_s, \beta_{hr}, \beta_{rh}$ and β_r. The calculations show that the basic reproduction number $\mathcal{R}_0^A$ underestimates the disease transmission risk. Our model enables us to evaluate what kind of parameter changes might trigger a periodic recurrence of LHF. Using numerical simulations, we observed that the human-to-human transmission rate has a substantial impact on the prevalence of the disease, but the most significant factors in Lassa's periodic recurrence are the rodent related parameters.

The dissertation is based on three articles of the author. These publications are the following:

- M. A. Ibrahim and A. Dénes. A mathematical model for Lassa fever transmission dynamics in a seasonal environment with a view to the 2017–20 epidemic in Nigeria. *Nonlinear Analysis: Real World Applications*, 60:103310, 2021. https://doi.org/10.1016/j.nonrwa.2021.103310.

- M. A. Ibrahim and A. Dénes. Threshold and stability results in a periodic model for malaria transmission with partial immunity in humans. *Applied Mathematics and Computation*, 392:125711, 2021. https://doi.org/10.1016/j.amc.2020.125711

- M. A. Ibrahim and A. Dénes. Threshold dynamics in a model for Zika virus disease with seasonality. *Bulletin of Mathematical Biology*, 83:27, 2021. https://doi.org/10.1007/s11538-020-00844-6

Összefoglalás

A doktori értekezés az időjárás periodicitásának a malária, a Zika-láz és a Lassa-láz terjedésére gyakorolt hatását vizsgálja nemautonóm, időfüggő (periodikus) paraméterekkel rendelkező kompartmentmodellek alkalmazásával. A rendszerek dinamikáját a periodikus kompartmentmodellek elemi reprodukciós számával ($\mathcal{R}_0$) jellemezzük, amelyet egy, a folytonos periodikus függvények terén ható integráloperátor spektrálsugaraként definiálunk, és azt is megmutattuk, hogy a reprodukciós szám küszöbparaméter a betegség kihalása vagy perzisztenciája szempontjából. Célunk megmutatni, hogy újonnan felállított modelljeink betegségmentes periodikus megoldása globálisan aszimptotikusan stabil, ha $\mathcal{R}_0 < 1$, míg $\mathcal{R}_0 > 1$ esetén legalább egy pozitív ω-periodikus megoldás létezik. Numerikus vizsgálatokkal és példákkal mutatjuk be, hogy a paraméterek mely változásai idézhetik elő a periodikus a betegség periodikus visszatérését.

A 2. fejezet a szúnyogok, illetve rágcsálók által terjesztett betegségek rövid bemutatásával kezdődik, majd az időjárás periodicitásának a maláriára, a Zika-lázra és a Lassa-lázra gyakorolt hatásait tárgyaljuk.

A 3. fejezetben röviden tárgyaljuk a nemautonóm járványtani modellek általános alakját, valamint a dolgozat témája szempontjából releváns legfontosabb definíciókat, feltételeket, tételeket és módszereket.

A malária *Plasmodium* mikroorganizmusok által okozott akut lázas betegség, amelyet nőstény *Anopheles* szúnyogok terjesztenek az emberre. A malária a vektorok által terjesztett betegségek közül a leghalálosabb, 2019-ben becslések szerint 409 000 halálesetet okozott. Az időjárás periodicitása és az éghajlatváltozás nagyon fontos tényezők a paraziták és az azokat terjesztő szúnyogok életciklusában. Ezért döntő fontosságú annak megértése, hogy az időjárás változásai hogyan befolyásolják a malária terjedését.

A 4. fejezetben egy, a malária terjedését leíró periodikus kompartmentmodellt állítunk fel és vizsgálunk, amelyben az emberi populációt immunitási szint alapján két típusra osztjuk: a nem immunisakra, vagyis azokra, akiknek nem alakult ki immunitásuk a malária ellen, és a félig immunisakra, vagyis azokra, akiknek genetikai adottságaik miatt vagy korábbi fertőzésből adódóan van valamilyen szintű részleges immunitásuk. A félig immunis emberi, nem immunis emberi és szúnyogkompartmenteket az m, n és v alsó indexek jelölik. A fogékony emberek (S_m és S_n) megfer-

tőződhetnek maláriával. A fertőző szúnyogcsípést követően a fogékonyak átkerülnek a látens osztályba (E_m, E_n). Az ezekben a kompartmentekben lévőknek még nincsenek tüneteik. A lappangási idő után a látens egyedek a fertőző osztályba (I_m, I_n) kerülnek. A félig immunisak esetében van egy további immunis kompartment (R_m). A R_m osztályba tartozó emberek részben immunisak a betegségre, de vérükban még mindig alacsony a paraziták szintje, és még mindig képesek megfertőzni a fogékony szúnyogokat. A szúnyogok esetében három kompartmentünk van: fogékonyak (S_v), látensek (E_v) és fertőzöttek (I_v). Az időjárás éves változását követve a szúnyogpopuláció periodikus dinamikáját úgy foglaljuk bele modellünkbe, hogy a szúnyogok születési és halálozási rátáját, valamint a csípési rátákat periodikusnak tekintjük, egy év periódussal. Modellünk dinamikájának jellemzésére meghatározzuk az $\mathcal{R}_0$ reprodukciós számot, és megmutatjuk a betegségmentes periodikus megoldás globális stabilitását, illetve a malária endemicitását, valamint a reprodukciós számtól függően egy pozitív ω-periodikus megoldás létezését. Az analitikus eredményekkel konzisztens numerikus szimulációk arra utalnak, hogy a szúnyogok populációjának szabályozása fontos tényező a malária terjedésében. Végül megmutatjuk, hogy az időben átlagolt reprodukciós szám alulbecsüli a malária terjedésének kockázatát.

A Zika-láz egy szúnyogok által terjesztett betegség, amelyet a Zika-vírus okoz. A Zika-vírus elsősorban a trópusi és szubtrópusi régiókban terjed a fertőzött nőstény szúnyogok csípése révén, amelyek az Aedes nemzetséghez tartoznak, amely faj a dengue, a chikungunya és a sárgaláz terjesztéséért is felelős. A Zika-vírus szexuális érintkezés útján is terjed, főként férfiakról nőkre. A Zika-vírussal fertőzött anyák a terhesség alatt vagy a szülés során átadhatják a betegséget magzatuknak. Ez az átvitel mikrokefáliához és más veleszületett rendellenességekhez vezethet, amelyek élethosszig tartó fogyatékosságot okozhatnak. Bár a Zika rendszeres, periodikus visszatérését eddig nem figyelték meg, várhatóan az időjárás szezonalitása ezt megváltoztathatja.

A 5. fejezetben egy kilenc kompartmentből álló modellt dolgozunk ki, amely periodikusan változó környezetben írja le a Zika-vírus terjedését, beleértve a szexuális és vektoriális terjedést is. Nemautonóm modellt alkalmazunk, amelyben a szúnyogok születési, halálozási és csípési rátája periodikus, hogy figyelembe vegyük az időjárás periodicitásának hatását a Zika terjedésére. A teljes emberi populációt hat részre osztjuk: fogékonyak ($S_h(t)$), látensek ($E_h(t)$), tünetesen fertőzöttek ($I_s(t)$), tünetmentes fertőzöttek ($I_a(t)$), lábadozók ($I_r(t)$), felgyógyultak ($R(t)$), míg a vektorpopulációt három osztályra osztjuk: fogékony ($S_v(t)$), látens ($E_v(t)$) és fertőző ($I_v(t)$) egyedek. Célunk, hogy az újonnan létrehozott periodikus modellünkre meghatározzuk az elemi reprodukciós számot, amely küszöbparaméterként szolgál a betegség perzisztenciájára vonatkozóan. A modell vizsgálata során a Rebelo et al. [90] által bevezetett módszereket követve igazoljuk a betegségmentes megoldás globális stabilitását és a fertőző kompartmentek perzisztenciáját. A modellünket alkalmazva,

Ecuadort és Kolumbiát példaként tekintve az adatokra illesztett görbék nagyon jól illeszkednek a valós esetszámokhoz. Bemutatjuk bizonyos szezonális intézkedéseknek a Zika-vírus okozta megbetegedésekre gyakorolt hatását Ecuadorban és Kolumbiában. Az eredmények azt sugallják, hogy még a szúnyogpopulációk csúcsidőszakára korlátozott szúnyogirtás is jelentős hatással lehet a betegség elleni védekezésre. A szenzitivitásvizsgálat alapján úgy értékelhetjük, hogy a fertőzés terjedésének csökkentésére a leghatékonyabb intézkedések a szúnyogpopulációk szabályozása és a szúnyogcsípések elleni védelem. Modellünk segítségével megbecsülhetjük, milyen paraméterváltozások vezethetnek a Zika periodikus visszatéréséhez. Numerikus szimulációk segítségével azt találtuk, hogy a szúnyogok születési és halálozási rátája a legjelentősebb tényező a Zika esetleges periodikus visszatérésében, azonban a szexuális átvitel is jelentős hatással van a betegség prevalenciájára.

A Lassa vérzéses láz (LHF) egy zoonotikus, akut vírusos vérzéses láz, amelyet az *Arenaviridae* vírusok családjába tartozó Lassa-vírus okoz. Az LHF általában fertőzött *Mastomys natalensis* patkányok vizeletével vagy ürülékével szennyezett élelmiszerrel vagy más tárgyakkal való közvetlen vagy közvetett érintkezés útján, a légző- vagy gyomor-bélrendszeri traktusokon keresztül terjed az emberre. Megfigyelték az emberről emberre történő átvitelt is. A vírus a gyógyulás után is megmarad a testnedvekben. A Lassa-láz Nyugat-Afrika egyes részein a patkányok között, míg a régió több országában az emberekben is endémiás. Ezekben a régiókban a fertőzések száma évente 100 000 és 300 000 közé tehető, és körülbelül 5000 haláleset történik. A Lassa-láz szerepel a WHO kutatási és fejlesztési prioritást élvező betegségek listáján. Bár a rágcsálópopulációkat befolyásolják az időjárási viszonyok, eddig még nem állítottak fel időfüggő paraméterekkel rendelkező kompartmentmodellt.

A 6. fejezetben a Lassa-láz terjedési dinamikájára vonatkozó periodikus kompartmentmodellt állítunk fel és vizsgálunk, amely figyelembe veszi az emberről emberre, rágcsálóról emberre történő terjedést és a vírus vertikális terjedését rágcsálókban, valamint a paraméterek időbeli változását. Az emberi populációt hat kompartmentre osztjuk: fogékonyak (S_h), látensek (E_h), tünetesen fertőzöttek ($I_s(t)$), enyhén fertőzöttek (I_m), kezeltek (I_T) és ideiglenes immunitással rendelkező gyógyult egyének (R). Egy egyén a megbetegedést követően a fogékony állapotból (S_h) a látens osztályba (E_h) jut. A látens egyéneknek még nincsenek tüneteik. A lappangási idő letelte után a látens egyén vagy a tünetesen fertőzött osztályba (I_s), vagy az enyhén fertőzött osztályba (I_m) kerül, attól függően, hogy az illető mutat-e tüneteket vagy sem. Az I_s-ből a fertőzöttek átkerülhetnek a kezelt osztályba (I_T), beleértve azokat is, akik kórházi kezelésre szorulnak. A fertőző időszak után a gyógyult személyek az R osztályba kerülnek. A vektorpopuláció (*Mastomys natalensis* patkány) három kompartmentre oszlik: fogékonyak (S_r), látensek (E_r) és fertőzöttek (I_r).

Ahhoz, hogy figyelembe vegyük az időjárás periodicitásának a Lassa terjedésére gyakorolt hatását, nemautonóm modellt vezetünk be, amelyben a rágcsálók születési

rátája és a környezet rágcsálókra vonatkozó eltartóképessége időfüggő paraméter. Periodikus modellünk dinamikájának vizsgálatához a [90, 103] munkákban megalkotott elméletet alkalmazzuk. Munkánkban ezeket a módszereket alkalmazzuk az emberről emberre és rágcsálóról emberre történő átvitelt tartalmazó rendszerünkre, melyben a rágcsálópopuláció mérete a logisztikus modellnek megfelelően változik. Levezettük és numerikusan kiszámítottuk a reprodukciós számot, azt is megmutattuk, hogy a reprodukciós szám meghatározza a rendszer globális dinamikáját. Numerikusan meghatároztuk a konstans és periodikus paramétereket a betegség nigériai terjedéséről publikált adatok felhasználásával. A modellünkön alapuló illesztett görbe tükrözi a szezonális ingadozást, és meglehetősen jól egybeesik a nigériai jelentett adatokkal. A reprodukciós számokat a $K_r, \Pi_r, \beta_s, \beta_{hr}, \beta_{rh}$ és β_r paraméterek függvényében becsültük. A számítások azt mutatják, hogy az $\mathcal{R}_0^A$ reprodukciós szám alábecsüli a betegség átvitelének kockázatát. Modellünk lehetővé teszi annak vizsgálatát, hogy milyen paraméterváltozások válthatják ki a Lassa-láz periodikus visszatérését. Numerikus szimulációk segítségével megfigyeltük, hogy az emberről emberre történő átviteli sebességnek jelentős hatása van a betegség gyakoriságára, de a Lassa-járványok periodikus ismétlődésének legjelentősebb tényezői a rágcsálókkal kapcsolatos paraméterek.

A disszertáció a szerző három cikkén alapul. Ezek a publikációk a következők:

- M. A. Ibrahim és Dénes A. A mathematical model for Lassa fever transmission dynamics in a seasonal environment with a view to the 2017–20 epidemic in Nigeria. *Nonlinear Analysis: Real World Applications*, 60:103310, 2021. https://doi.org/10.1016/j.nonrwa.2021.103310.

- M. A. Ibrahim és Dénes A. Threshold and stability results in a periodic model for malaria transmission with partial immunity in humans. *Applied Mathematics and Computation*, 392:125711, 2021. https://doi.org/10.1016/j.amc.2020.125711

- M. A. Ibrahim és Dénes A. Threshold dynamics in a model for Zika virus disease with seasonality. *Bulletin of Mathematical Biology*, 83:27, 2021. https://doi.org/10.1007/s11538-020-00844-6

Bibliography

[1] A. Abdelrazec and A. B. Gumel. Mathematical assessment of the role of temperature and rainfall on mosquito population dynamics. *Journal of Mathematical Biology*, 74(6):1351–1395, 2017.

[2] G. J. Abiodun, R. Maharaj, P. Witbooi, and K. O. Okosun. Modelling the influence of temperature and rainfall on the population dynamics of Anopheles arabiensis. *Malaria Journal*, 15(1):364, 2016.

[3] G. J. Abiodun, P. J. Witbooi, and O. O. Okosun. Mathematical modelling and analysis of mosquito-human malaria model. *International Journal of Ecological Economics & Statistics*, 38(3):1–22, 2017.

[4] K. F. Ahmed, G. Wang, L. You, and M. Yu. Potential impact of climate and socioeconomic changes on future agricultural land use in West Africa. *Earth System Dynamics*, 7(1):151–165, 2016.

[5] A. R. Akhmetzhanov, Y. Asai, and H. Nishiura. Quantifying the seasonal drivers of transmission for Lassa fever in Nigeria. *Philosophical Transactions of the Royal Society B*, 374(1775):20180268, 2019.

[6] M. Andraud, N. Hens, C. Marais, and P. Beutels. Dynamic epidemiological models for dengue transmission: A systematic review of structural approaches. *PLoS ONE*, 7(11):e49085, 2012.

[7] H. Asad and D. O. Carpenter. Effects of climate change on the spread of Zika virus: a public health threat. *Reviews on Environmental Health*, 33(1):31–42, 2018.

[8] D. Baca-Carrasco and J. X. Velasco-Hernández. Sex, mosquitoes and epidemics: An evaluation of Zika disease dynamics. *Bulletin of Mathematical Biology*, 78(11):2228–2242, 2016.

[9] N. Bacaër. Approximation of the basic reproduction number R_0 for vector-borne diseases with a periodic vector population. *Bulletin of Mathematical Biology*, 69(3):1067–1091, 2007.

[10] N. Bacaër and E. Ait Dads. On the biological interpretation of a definition for the parameter R_0 in periodic population models. *Journal of Mathematical Biology*, 65(4):601–621, 2012.

[11] N. Bacaër and S. Guernaoui. The epidemic threshold of vector-borne diseases with seasonality. *Journal of Mathematical Biology*, 53(3):421–436, 2006.

[12] E. Bakare, E. Are, O. Abolarin, S. Osanyinlusi, B. Ngwu, and O. N. Ubaka. Mathematical modelling and analysis of transmission dynamics of Lassa fever. *Journal of Applied Mathematics*, 2020, 2020.

[13] T. Bakary, S. Boureima, and T. Sado. A mathematical model of malaria transmission in a periodic environment. *Journal of Biological Dynamics*, 12(1): 400–432, 2018.

[14] M. Baldari, A. Tamburro, G. Sabatinelli, R. Romi, C. Severini, G. Cuccagna, G. Fiorilli, M. P. Allegri, C. Buriani, and M. Toti. Malaria in Maremma, Italy. *The Lancet*, 351(9111):1246–1247, 1998.

[15] W. Bearcroft. Zika virus infection experimentally induced in a human volunteer. *Transactions of the Royal Society of Tropical Medicine and Hygiene*, 50(5): 438–441, 1956.

[16] L. M. Beck-Johnson, W. A. Nelson, K. P. Paaijmans, A. F. Read, M. B. Thomas, and O. N. Bjørnstad. The effect of temperature on Anopheles mosquito population dynamics and the potential for malaria transmission. *PLOS One*, 8(11), 2013.

[17] S. M. Blower and H. Dowlatabadi. Sensitivity and uncertainty analysis of complex models of disease transmission: An HIV model, as an example. *International Statistical Review/Revue Internationale de Statistique*, 62(2):229, 1994.

[18] J. Boorman and J. Porterfield. A simple technique for infection of mosquitoes with viruses transmission of Zika virus. *Transactions of the Royal Society of Tropical Medicine and Hygiene*, 50(3):238–242, 1956.

[19] F. Bordes, K. Blasdell, and S. Morand. Transmission ecology of rodent-borne diseases: new frontiers. *Integrative Zoology*, 10(5):424–435, 2015.

[20] F. Brauer, C. Castillo-Chavez, A. Mubayi, and S. Towers. Some models for epidemics of vector-transmitted diseases. *Infectious Disease Modelling*, 1(1): 79–87, 2016.

[21] S. M. Buckley, J. Casals, and W. G. Downs. Isolation and antigenic characterization of Lassa virus. *Nature*, 227(5254):174–174, 1970.

[22] C. Caminade, J. Turner, S. Metelmann, J. C. Hesson, M. S. C. Blagrove, T. Solomon, A. P. Morse, and M. Baylis. Global risk model for vector-borne transmission of Zika virus reveals the role of El Niño 2015. *Proceedings of the National Academy of Sciences*, 114(1):119–124, 2016.

[23] Centers for Disease Control and Prevention. *Lassa fever*. URL https://www.cdc.gov/vhf/lassa/index.html.

[24] Centers for Disease Control and Prevention. *Mosquito-Borne Diseases*, 2016. URL https://www.cdc.gov/niosh/topics/outdoor/mosquito-borne/.

[25] Centers for Disease Control and Prevention. *Zika Virus*, 2016. URL https://www.cdc.gov/niosh/topics/outdoor/mosquito-borne/zika.

[26] Centers for Disease Control and Prevention. *Lassa fever*, 2019. URL https://www.cdc.gov/vhf/lassa/.

[27] Centers for Disease Control and Prevention. *Malaria*, 2021. URL https://www.cdc.gov/parasites/malaria/.

[28] N. Centre for Disease Control. *Disease situation report: an update of Lassa fever outbreak in Nigeria*, 2020. URL https://www.ncdc.gov.ng/diseases/sitreps.

[29] E. Chikaki and H. Ishikawa. A dengue transmission model in Thailand considering sequential infections with all four serotypes. *The Journal of Infection in Developing Countries*, 3(9), 2009.

[30] N. Chitnis, J. M. Cushing, and J. Hyman. Bifurcation analysis of a mathematical model for malaria transmission. *SIAM Journal on Applied Mathematics*, 67 (1):24–45, 2006.

[31] M. H. Craig, R. Snow, and D. le Sueur. A climate-based distribution model of malaria transmission in sub-Saharan Africa. *Parasitology Today*, 15(3):105–111, 1999.

[32] J. Davies, K. Lokuge, and K. Glass. Routine and pulse vaccination for Lassa virus could reduce high levels of endemic disease: A mathematical modelling study. *Vaccine*, 37(26):3451–3456, 2019.

[33] B. Dembele, A. Friedman, and A.-A. Yakubu. Malaria model with periodic mosquito birth and death rates. *Journal of Biological Dynamics*, 3(4):430–445, 2009.

[34] A. Dénes and A. B. Gumel. Modeling the impact of quarantine during an outbreak of Ebola virus disease. *Infectious Disease Modelling*, 4:12–27, 2019.

[35] A. Dénes, M. A. Ibrahim, L. Oluoch, M. Tekeli, and T. Tekeli. Impact of weather seasonality and sexual transmission on the spread of Zika fever. *Scientific Reports*, 9(1):1–10, 2019.

[36] G. Dick, S. Kitchen, and A. Haddow. Zika virus (i). Isolations and serological specificity. *Transactions of the Royal Society of Tropical Medicine and Hygiene*, 46(5):509–520, 1952.

[37] O. Diekmann, J. Heesterbeek, and M. G. Roberts. The construction of next-generation matrices for compartmental epidemic models. *Journal of the Royal Society Interface*, 7(47):873–885, 2010.

[38] R. Djidjou-Demasse, G. J. Abiodun, A. M. Adeola, and J. O. Botai. Development and analysis of a malaria transmission mathematical model with seasonal mosquito life-history traits. *Studies in Applied Mathematics*, 144:389–411, 2020.

[39] A. Ducrot, S. Sirima, B. Some, and P. Zongo. A mathematical model for malaria involving differential susceptibility, exposedness and infectivity of human host. *Journal of Biological Dynamics*, 3(6):574–598, 2009.

[40] M. R. Duffy, T.-H. Chen, W. T. Hancock, A. M. Powers, J. L. Kool, R. S. Lanciotti, M. Pretrick, M. Marfel, S. Holzbauer, C. Dubray, et al. Zika virus outbreak on Yap Island, Federated States of Micronesia. *New England Journal of Medicine*, 360(24):2536–2543, 2009.

[41] S. E. Eikenberry and A. B. Gumel. Mathematical modeling of climate change and malaria transmission dynamics: a historical review. *Journal of Mathematical Biology*, 77(4):857–933, 2018.

[42] European Centers for Disease Control and Prevention. *Rodent-borne diseases*, 2019. URL https://www.ecdc.europa.eu/en/climate-change/climate-change-europe/rodent-borne-diseases.

[43] Z. Feng and J. X. Velasco-Hernández. Competitive exclusion in a vector-host model for the dengue fever. *Journal of Mathematical Biology*, 35(5):523–544, 1997.

[44] F. Forouzannia and A. B. Gumel. Mathematical analysis of an age-structured model for malaria transmission dynamics. *Mathematical Biosciences*, 247:80–94, 2014.

[45] G. Fulford, M. Roberts, and J. Heesterbeek. The metapopulation dynamics of an infectious disease: Tuberculosis in possums. *Theoretical Population Biology*, 61(1):15–29, 2002.

[46] D. Gao, Y. Lou, D. He, T. C. Porco, Y. Kuang, G. Chowell, and S. Ruan. Prevention and control of Zika as a mosquito-borne and sexually transmitted disease: A mathematical modeling analysis. *Scientific Reports*, 6(1), 2016.

[47] A.-C. Gourinat, O. O'Connor, E. Calvez, C. Goarant, and M. Dupont-Rouzeyrol. Detection of Zika virus in urine. *Emerging Infectious Diseases*, 21(1):84–86, 2015.

[48] D. J. Gubler, P. Reiter, K. L. Ebi, W. Yap, R. Nasci, and J. A. Patz. Climate variability and change in the United States: potential impacts on vector-and rodent-borne diseases. *Environmental Health Perspectives*, 109(suppl 2):223–233, 2001.

[49] M. B. Hoshen and A. P. Morse. A weather-driven model of malaria transmission. *Malaria Journal*, 3(1):1–14, 2004.

[50] J. M. Hyman, J. Li, and E. A. Stanley. The differential infectivity and staged progression models for the transmission of HIV. *Mathematical Biosciences*, 155 (2):77–109, 1999.

[51] M. A. Ibrahim and A. Dénes. Assessment of microcephaly risk due to Zika virus infection via a mathematical model with vertical transmission. under review.

[52] M. A. Ibrahim and A. Dénes. A mathematical model for Lassa fever transmission dynamics in a seasonal environment with a view to the 2017–20 epidemic in Nigeria. *Nonlinear Analysis: Real World Applications*, 60:103310, 2021. ISSN 1468-1218.

[53] M. A. Ibrahim and A. Dénes. Threshold and stability results in a periodic model for malaria transmission with partial immunity in humans. *Applied Mathematics and Computation*, 392:125711, 2021.

[54] M. A. Ibrahim and A. Dénes. Threshold dynamics in a model for Zika virus disease with seasonality. *Bulletin of Mathematical Biology*, 83(4):27, 2021.

[55] P. Jia, X. Chen, J. Chen, L. Lu, Q. Liu, and X. Tan. How does the dengue vector mosquito Aedes albopictus respond to global warming? *Parasites & Vectors*, 10(1):1–12, 2017.

[56] F. Keesing, L. K. Belden, P. Daszak, A. Dobson, C. D. Harvell, R. D. Holt, P. Hudson, A. Jolles, K. E. Jones, C. E. Mitchell, et al. Impacts of biodiversity on the emergence and transmission of infectious diseases. *Nature*, 468(7324):647–652, 2010.

[57] O. Koutou, B. Traoré, and B. Sangaré. Mathematical modeling of malaria transmission global dynamics: taking into account the immature stages of the vectors. *Advances in Difference Equations*, 2018(1):220, 2018.

[58] A. Krüger, A. Rech, X.-Z. Su, and E. Tannich. Two cases of autochthonous Plasmodium falciparum malaria in Germany with evidence for local transmission by indigenous Anopheles plumbeus. *Tropical Medicine & International Health*, 6(12):983–985, 2001.

[59] K. Laneri, R. E. Paul, A. Tall, J. Faye, F. Diene-Sarr, C. Sokhna, J.-F. Trape, and X. Rodó. Dynamical malaria models reveal how immunity buffers effect of climate variability. *Proceedings of the National Academy of Sciences*, 112(28): 8786–8791, 2015.

[60] S. H. Lee, K. W. Nam, J. Y. Jeong, S. J. Yoo, Y.-S. Koh, S. Lee, S. T. Heo, S.-Y. Seong, and K. H. Lee. The effects of climate change and globalization on mosquito vectors: evidence from Jeju Island, South Korea on the potential for Asian tiger mosquito (Aedes albopictus) influxes and survival from Vietnam rather than Japan. *PloS One*, 8(7):e68512, 2013.

[61] J. Liu. Threshold dynamics of a time-delayed hantavirus infection model in periodic environments. *Mathematical Biosciences and Engineering*, 16(5):4758–4776, 2019.

[62] L. Liu, X.-Q. Zhao, and Y. Zhou. A tuberculosis model with seasonality. *Bulletin of Mathematical Biology*, 72(4):931–952, 2010.

[63] X. Liu, Y. Wang, and X.-Q. Zhao. Dynamics of a climate-based periodic chikungunya model with incubation period. *Applied Mathematical Modelling*, 80: 151–168, 2020.

[64] G. Lo Iacono, A. A. Cunningham, E. Fichet-Calvet, R. F. Garry, D. S. Grant, M. Leach, L. M. Moses, G. Nichols, J. S. Schieffelin, J. G. Shaffer, et al. A unified framework for the infection dynamics of zoonotic spillover and spread. *PLoS Neglected Tropical Diseases*, 10(9):e0004957, 2016.

[65] L. Luzzatto. Sickle cell anaemia and malaria. *Mediterranean Journal of Hematology and Infectious Diseases*, 4(1), 2012.

[66] G. Macdonald. *The epidemiology and control of malaria*. Oxford University Press, 1957.

[67] T. Magalhaes, B. D. Foy, E. T. Marques, G. D. Ebel, and J. Weger-Lucarelli. Mosquito-borne and sexual transmission of Zika virus: Recent developments and future directions. *Virus Research*, 254:1–9, 2018.

[68] A. Matysiak and A. Roess. Interrelationship between climatic, ecologic, social, and cultural determinants affecting dengue emergence and transmission in Puerto Rico and their implications for Zika response. *Journal of Tropical Medicine*, 2017, 2017.

[69] J. J. McCarthy, O. F. Canziani, N. A. Leary, D. J. Dokken, K. S. White, et al. *Climate change 2001: impacts, adaptation, and vulnerability: contribution of Working Group II to the third assessment report of the Intergovernmental Panel on Climate Change*, volume 2. Cambridge University Press, 2001.

[70] M. D. McKay, R. J. Beckman, and W. J. Conover. A comparison of three methods for selecting values of input variables in the analysis of output from a computer code. *Technometrics. A Journal of Statistics for the Physical, Chemical and Engineering Sciences*, 21(2):239–245, 1979.

[71] P. S. Mead, N. K. Duggal, S. A. Hook, M. Delorey, M. Fischer, D. Olzenak McGuire, H. Becksted, R. J. Max, M. Anishchenko, A. M. Schwartz, et al. Zika virus shedding in semen of symptomatic infected men. *New England Journal of Medicine*, 378(15):1377–1385, 2018.

[72] C. Mitchell and C. Kribs. A comparison of methods for calculating the basic reproductive number for periodic epidemic systems. *Bulletin of Mathematical Biology*, 79(8):1846–1869, 2017.

[73] E. A. Mordecai, K. P. Paaijmans, L. R. Johnson, C. Balzer, T. Ben-Horin, E. de Moor, A. McNally, S. Pawar, S. J. Ryan, T. C. Smith, et al. Optimal temperature for malaria transmission is dramatically lower than previously predicted. *Ecology Letters*, 16(1):22–30, 2013.

[74] E. A. Mordecai, J. M. Cohen, M. V. Evans, P. Gudapati, L. R. Johnson, C. A. Lippi, K. Miazgowicz, C. C. Murdock, J. R. Rohr, S. J. Ryan, et al. Detecting the impact of temperature on transmission of Zika, dengue, and chikungunya using mechanistic models. *PLoS Neglected Tropical Diseases*, 11(4):e0005568, 2017.

[75] S. S. Musa, S. Zhao, D. Gao, Q. Lin, G. Chowell, and D. He. Mechanistic modelling of the large-scale Lassa fever epidemics in Nigeria from 2016 to 2019. *Journal of Theoretical Biology*, page 110209, 2020.

[76] D. Musso, C. Roche, E. Robin, T. Nhan, A. Teissier, and V.-M. Cao-Lormeau. Potential sexual transmission of Zika virus. *Emerging Infectious Diseases*, 21 (2):359–361, 2015.

[77] Y. Nakata and T. Kuniya. Global dynamics of a class of SEIRS epidemic models in a periodic environment. *Journal of Mathematical Analysis and Applications*, 363(1):230–237, 2010.

[78] A. Nguyen, J. Mahaffy, and N. K. Vaidya. Modeling transmission dynamics of Lyme disease: Multiple vectors, seasonality, and vector mobility. *Infectious Disease Modelling*, 4:28–43, 2019.

[79] A. Nwankwo and D. Okuonghae. Mathematical assessment of the impact of different microclimate conditions on malaria transmission dynamics. *Mathematical Biosciences and Engineering*, 16:1414–1444, 2019.

[80] K. Okuneye and A. B. Gumel. Analysis of a temperature-and rainfall-dependent model for malaria transmission dynamics. *Mathematical Biosciences*, 287:72–92, 2017.

[81] I. S. Onah, O. C. Collins, P.-G. U. Madueme, and G. C. E. Mbah. Dynamical system analysis and optimal control measures of Lassa fever disease model. *International Journal of Mathematics and Mathematical Sciences*, 2020:Art. ID 7923125, 2020.

[82] K. P. Paaijmans, A. F. Read, and M. B. Thomas. Understanding the link between malaria risk and climate. *Proceedings of the National Academy of Sciences*, 106(33):13844–13849, 2009.

[83] P. Padmanabhan, P. Seshaiyer, and C. Castillo-Chavez. Mathematical modeling, analysis and simulation of the spread of Zika with influence of sexual transmission and preventive measures. *Letters in Biomathematics*, 4(1), 2017.

[84] Pan American Health Organization. *Countries and territories with autochthonous transmission of Zika virus in the Americas reported in 2015–2017*, 2015. URL https://www.paho.org/hq/index.php?option=com_content&view=article&id=11603:countries-and-territories-with-autochthonous-transmission-of-zika-virus-in-the-americas-reported-in-2015-2017&Itemid=41696&lang=en.

[85] Pan American Health Organization. *Zika–Epidemiological Report Colombia*, 2017. URL https://www.paho.org/hq/dmdocuments/2017/2017-phe-zika-situation-report-col.pdf.

[86] M. Pascual, J. A. Ahumada, L. F. Chaves, X. Rodo, and M. Bouma. Malaria resurgence in the East African highlands: temperature trends revisited. *Proceedings of the National Academy of Sciences*, 103(15):5829–5834, 2006.

[87] L. R. Petersen, D. J. Jamieson, A. M. Powers, and M. A. Honein. Zika Virus. *New England Journal of Medicine*, 374(16):1552–1563, 2016.

[88] M. E. Price, S. P. Fisher-Hoch, R. B. Craven, and J. B. McCormick. A prospective study of maternal and fetal outcome in acute Lassa fever infection during pregnancy. *British Medical Journal*, 297(6648):584–587, 1988.

[89] Q. Qu, C. Fang, L. Zhang, W. Jia, J. Weng, and Y. Li. A mumps model with seasonality in China. *Infectious Disease Modelling*, 2(1):1–11, 2017.

[90] C. Rebelo, A. Margheri, and N. Bacaër. Persistence in seasonally forced epidemiological models. *Journal of Mathematical Biology*, 64(6):933–949, 2012.

[91] D. W. Redding, L. M. Moses, A. A. Cunningham, J. Wood, and K. E. Jones. Environmental-mechanistic modelling of the impact of global change on human zoonotic disease emergence: A case study of Lassa fever. *Methods in Ecology and Evolution*, 7(6):646–655, 2016.

[92] J. K. Richmond and D. J. Baglole. Lassa fever: epidemiology, clinical features, and social consequences. *British Medical Journal*, 327(7426):1271–1275, 2003.

[93] R. Ross. *The prevention of malaria*. Murray, London, 1911.

[94] M. Roy, M. Bouma, R. C. Dhiman, and M. Pascual. Predictability of epidemic malaria under non-stationary conditions with process-based models combining epidemiological updates and climate variability. *Malaria Journal*, 14(1): 419, 2015.

[95] S. K. Sasmal, I. Ghosh, A. Huppert, and J. Chattopadhyay. Modeling the spread of Zika virus in a stage-structured population: Effect of sexual transmission. *Bulletin of Mathematical Biology*, 80(11):3038–3067, 2018.

[96] J. C. Semenza and B. Menne. Climate change and infectious diseases in Europe. *The Lancet Infectious Diseases*, 9(6):365–375, 2009.

[97] H. L. Smith and P. Waltman. *The theory of the chemostat: dynamics of microbial competition*. Cambridge University Press, 1995.

[98] K. C. Smithburne. Neutralizing antibodies against certain recently isolated viruses in the sera of human beings residing in East Africa. *The Journal of Immunology*, 69(2):223–234, 1952.

[99] The World Bank. *The World Bank demography, 2019. Nigeria*, 2019. URL https://data.worldbank.org/country/nigeria.

[100] J. P. Tian and J. Wang. Some results in Floquet theory, with application to periodic epidemic models. *Applicable Analysis*, 94(6):1128–1152, 2015.

[101] P. van den Driessche and J. Watmough. Reproduction numbers and subthreshold endemic equilibria for compartmental models of disease transmission. *Mathematical Biosciences*, 180(1-2):29–48, 2002.

[102] L. Wang, Z. Teng, and T. Zhang. Threshold dynamics of a malaria transmission model in periodic environment. *Communications in Nonlinear Science and Numerical Simulation*, 18(5):1288–1303, 2013.

[103] W. Wang and X.-Q. Zhao. Threshold dynamics for compartmental epidemic models in periodic environments. *Journal of Dynamics and Differential Equations*, 20(3):699–717, 2008.

[104] X. Wang and X.-Q. Zhao. A periodic vector-bias malaria model with incubation period. *SIAM Journal on Applied Mathematics*, 77(1):181–201, 2017.

[105] A. Wilkinson. Beyond biosecurity: The politics of Lassa fever in Sierra Leone. *One health: Science, Politics and Zoonotic Disease in Africa*, pages 117–138, 2016.

[106] World Health Organization. *WHO Global Health Observatory data repository. Crude birth and death rate. Data by country*, 2015. URL http://apps.who.int/gho/data/node.main.CBDR107?lang=en.

[107] World Health Organization. *WHO list of blueprint priority diseases*, 2018. URL https://www.who.int/blueprint/priority-diseases/en/.

[108] World Health Organization. *Zika virus*, 2018. URL https://www.who.int/en/news-room/fact-sheets/detail/zika-virus.

[109] World Health Organization. *World Malaria Report*, 2019. URL https://www.who.int/publications-detail/world-malaria-report-2019.

[110] World Health Organization. *Lassa fever*, 2019. URL https://www.who.int/health-topics/lassa-fever/.

[111] World Health Organization. *Vector-borne diseases*, 2020. URL https://www.who.int/news-room/fact-sheets/detail/vector-borne-diseases/.

[112] X. Wu, Y. Lu, S. Zhou, L. Chen, and B. Xu. Impact of climate change on human infectious diseases: Empirical evidence and human adaptation. *Environment International*, 86:14–23, 2016.

[113] F. Zhang and X.-Q. Zhao. A periodic epidemic model in a patchy environment. *Journal of Mathematical Analysis and Applications*, 325(1):496–516, 2007.

[114] S. Zhao, S. S. Musa, H. Fu, D. He, and J. Qin. Large-scale Lassa fever outbreaks in Nigeria: quantifying the association between disease reproduction number and local rainfall. *Epidemiology & Infection*, 148, 2020.

[115] X.-Q. Zhao. *Dynamical systems in population biology*. Springer, 2003.

[116] G. Zhou, N. Minakawa, A. K. Githeko, and G. Yan. Climate variability and malaria epidemics in the highlands of East Africa. *Trends in Parasitology*, 21 (2):54–56, 2005.

Publications

Hungarian Scientific Bibliography identifier: 10067429– MTMT Publications.

Journal publications

[1] **M. A. Ibrahim** and A. Dénes, Threshold and stability results in a periodic model for malaria transmission with partial immunity in humans. *Applied Mathematics and Computation*, 392:125711, **2021**.
https://doi.org/10.1016/j.amc.2020.125711

[2] **M. A. Ibrahim** and A. Dénes, Threshold dynamics in a model for Zika virus disease with seasonality. *Bulletin of Mathematical Biology*, 83:27, **2021**.
https://doi.org/10.1007/s11538-020-00844-6

[3] **M. A. Ibrahim** and A. Dénes, A mathematical model for Lassa fever transmission dynamics in a seasonal environment with a view to the 2017–20 epidemic in Nigeria. *Nonlinear Analysis: Real World Applications*, 60:103310, **2021**.
https://doi.org/10.1016/j.nonrwa.2021.103310.

[4] **M. A. Ibrahim**, A. AL-Najafi and A. Dénes, Predicting the COVID-19 Spread Using Compartmental Model and Extreme Value Theory with Application to Egypt and Iraq. *In: R. P. Mondaini (Ed.), Trends in Biomathematics: Chaos and Control in Epidemics, Ecosystems, and Cells*, Springer, **2021**.
https://doi.org/10.1007/978-3-030-73241-7_4

[5] **M. A. Ibrahim** and A. AL-Najafi, Modeling, Control, and Prediction of the Spread of COVID-19 Using Compartmental, Logistic, and Gauss Models: A Case Study in Iraq and Egypt. *Processes*, 8:1400, **2020**.
https://doi.org/10.3390/pr8111400

[6] S. Barua, A. Dénes and **M. A. Ibrahim**, A seasonal model to assess intervention strategies for preventing periodic recurrence of Lassa fever. *Heliyon*, e07760,

2021. https://doi.org/10.1016/j.heliyon.2021.e07760

[7] A. Dénes, **M. A. Ibrahim**, Global dynamics of a mathematical model for a honeybee colony infested by virus-carrying Varroa mites. *Journal of Applied Mathematics and Computing*, 61:349–371, **2019**. https://doi.org/10.1007/s12190-019-01250-5

[8] A. Dénes, **M. A. Ibrahim**, L. Oluoch, M. Tekeli, T. Tekeli, Impact of weather seasonality and sexual transmission on the spread of Zika fever. *Scientific Reports*, 9:1–10, **2019**. https://doi.org/10.1038/s41598-019-53062-z

Abstracts in conference books

[9] **M. A. Ibrahim** and A. Dénes, A mathematical model for Lassa fever transmission dynamics in a seasonal environment with a view to the 2017–20 epidemic in Nigeria . In *12th Dynamical Systems Applied to Biology and Natural Sciences, BCAM, Bilbao, Spain, ISBN: 978-989-98750-8-1*, **2021**.

[10] A. Dénes, **M. A. Ibrahim** and G. Röst, Malaria dynamics with bimodality of incubation period in hosts in a seasonal environment. In *12th Dynamical Systems Applied to Biology and Natural Sciences, BCAM, Bilbao, Spain, ISBN: 978-989-98750-8-1*, **2021**.

[11] **M. A. Ibrahim** and A. Dénes, Threshold dynamics in a model for Zika virus disease with seasonality. In *11th Dynamical Systems Applied to Biology and Natural Sciences, Trento, Italy, ISBN: 78-989-98750-7-4*, **2020**.

[12] **M. A. Ibrahim** and A. Dénes, L. Oluoch, M. Tekeli and T. Tekeli, The effect of weather changes and sexual transmission on the spread of ZIKA fever. In *10th Dynamical Systems Applied to Biology and Natural Sciences, Napoli, Italy, ISBN: 978-989-98750-6-7*, **2019**.

Conference Lectures and Posters

Lectures:

[1] **M. A. Ibrahim** and A. Dénes, BioMATEmatics international biomathematics and biostatistics conference, Augustus 31, 2021, Online.

[2] **M. A. Ibrahim** and A. Dénes, BIOMAT 2020–20th International Symposium on Mathematical and Computational Biology, November 1–6, 2020, Online.

[3] **M. A. Ibrahim** and A. Dénes, 11th Conference on Dynamical Systems Applied to Biology and Natural Sciences, February 4–7, 2020, Trento, Italy.

[4] **M. A. Ibrahim** and A. Dénes, BIOMAT 2019–19th International Symposium on Mathematical and Computational Biology, October 20–26, 2019, Szeged, Hungary.

[5] **M. A. Ibrahim** and A. Dénes, 11th Colloquium on the Qualitative Theory of Differential Equations, June 17–21, 2019, Szeged, Hungary.

[6] **M. A. Ibrahim** and A. Dénes, The 5th Conference of PhD Students in Mathematics, June 25–27, 2018, Szeged, Hungary.

Posters:

[1] **M. A. Ibrahim**, A. Dénes, 12th Conference on Dynamical Systems Applied to Biology and Natural Sciences, February 2–5, 2021, DSABNS 2021-Virtual.

[2] A. Dénes, **M. A. Ibrahim**, and G. Röst, 12th Conference on Dynamical Systems Applied to Biology and Natural Sciences, February 2–5, 2021, DSABNS 2021-Virtual.

[3] **M. A. Ibrahim**, A. Dénes, L. Oluoch, M. Tekeli and T. Tekeli, 10th Conference on Dynamical Systems Applied to Biology and Natural Sciences, February 3–6, 2019, Naples, Italy.